Dissertation

submitted to the

Combined Faculties for the Natural Sciences and for Mathematics

of the Ruperto-Carola University of Heidelberg, Germany

for the degree of

Doctor of Natural Sciences

presented by

Jan Brod, Dipl.-Ing. (FH)

born in Fulda

Date of oral examination: July 24, 2018

Reconstitution of clathrin coated vesicles

Referees: Prof. Dr. Felix Wieland

Prof. Dr. Thomas Söllner

Abstract

Receptor-mediated endocytosis by clathrin coated vesicles (CCVs) is a well investigated process, in which clathrin, the adaptor AP-2 and the large GTPase dynamin play crucial roles. However, the minimal machinery for the formation of CCVs has not been defined in vitro. Specifically, scission of clathrin coated endocytic buds (CCBs), the last step in this process that results in the release of free vesicles, is not clearly defined mechanistically. Actually, five AP-complexes are described and except AP-2, all are recruited in an Arf-dependent manner to their donor membrane. Here, Arf is likely to play a distinct and GTPase activity-independent role in the scission mechanism via its myristoylated amphipathic helix, as has been shown for Arf's role in COPI vesicle scission. In case of AP-2 no Arf is known to be involved, but it has been shown that epsin-1 with its N-terminal amphiphilic helix (ENTH-domain) is an endocytic accessory protein involved in the biogenesis of endocytic clathrin coated vesicles and was suggested to be implicated in scission. To identify the minimal machinery required for CCV formation and to investigate the molecular roles of dynamin and epsin-1 in this process, an in vitro reconstitution system for the biogenesis of CCVs was established using defined components in the form of synthetic membranes and recombinant, purified proteins.

I observed that a combination of AP-2 and epsin-1 recruits clathrin to synthetic liposomes more efficiently than each single adaptor, indicating cooperativity between AP-2 and epsin-1. CCV-reconstitution experiments with giant unilamellar vesicles showed that clathrin coated vesicles can be reconstituted dependent on clathrin adaptors, clathrin, dynamin and GTP. Moreover, blocking GTP-hydrolysis abolished the formation of CCVs, supporting the widely accepted hypothesis that hydrolysis of GTP by dynamin is mandatory for vesicle release. However, as hydrolysis of GTP was an absolute requirement of vesicle release, epsin-1 alone does not have the propensity for scission, but is required for bud formation, as AP-2 and clathrin alone are not sufficient. A role of the endocytic protein epsin-1 for the progression of endocytosis to CCBs would also be structurally supported as epsin-1 contains a membrane bending ENTH-domain that would facilitate such a function by introducing curvature to the membrane.

In summary this work comprises the first in vitro reconstitution system of endocytic CCVs that uses full length proteins in a chemically defined environment. Using this system, I confirmed and refined the roles of known constituents of the minimal endocytic CCV biogenesis machinery, which is comprised of AP-2, epsin-1, clathrin, dynamin, and by GTP-hydrolysis in dynamin.

Zusammenfassung

Die Rezeptor-vermittelte Endozytose durch Clathrin Vesikel (CCV) ist ein umfassend untersuchter Prozess, bei dem Clathrin, der Adapterkomplex 2 (AP-2) und die große GTPase Dynamin zentrale Rollen spielen. Die minimale Maschinerie zur Bildung endozytotischer Clathrin Vesikel wurde in vitro jedoch noch nicht definiert, wobei insbesondere die Abschnürung endozytotischer Clathrin Knospen (CCB) zu freien Vesikeln mechanistisch nicht eindeutig geklärt ist. In der Literatur werden fünf AP-Komplexe beschrieben, die mit Ausnahme von AP-2 durch direkte Interaktion mit kleinen GTPasen der Arf-Familie an die Membran rekrutiert werden. Hierbei könnten Proteine der Arf-Familie, vermittelt durch ihre myristoylierte amphipathische Helix, eine wichtige Funktion in der Abspaltung zu freien CCV haben, ähnlich wie es für die Abschnürung von COPI-Vesikeln durch Arf gezeigt wurde. Bei der Biogenese von endozytotischen Clathrin Vesikeln ist eine direkte Beteiligung von Proteinen der Arf-Familie nicht bekannt. Allerdings könnte hierbei das Protein Epsin, welches ebenfalls eine amphiphile Helix am Ende der sogenannten ENTH-Domäne besitzt, alternativ zu Arf an der Abschnürung von CCVs beteiligt sein. Um die Frage nach den notwendigen Komponenten zur Bildung endozytotischer CCV und eines generellen Abspaltungsmechanismus zu beantworten wurde in dieser Arbeit ein in vitro Rekonstitutionssystem mit chemisch definierten Komponenten etabliert.

Experimente zur Charakterisierung der rekombinant exprimierten Proteine zeigten einen kooperativen Effekt zwischen AP-2 und Epsin-1, sowohl in der Rekrutierung von Clathrin an synthetische Liposomen, als auch in der Menge an membrangebundenem Adaptor. Experimente zur Rekonstitution von CCV mit großen unilamellaren Vesikeln (GUVs) als Donor-Membranen zeigten eine deutliche Abhängigkeit der Vesikelbildung von Clathrin, einem Clathrinadaptor, Dynamin und GTP. Darüber hinaus war die Hydrolyse von GTP durch Dynamin für die Vesikelfreisetzung zwingend erforderlich. Eine Freisetzung von CCV konnte jedoch nur in Anwesenheit von Epsin beobachtet werden, das allerdings nicht die Abspaltung von CCVs direkt bewirken kann. Elektronenmikroskopische Aufnahmen negativ kontrastierter Proben haben gezeigt, dass AP-2 allein nicht in der Lage ist CCBs zu bilden. Dies legt nahe, dass das endozytotische Protein Epsin mit seiner Membrankurvatur induzierenden ENTH-Domäne einen wichtigen Faktor in frühen Stadien der Biogenese von CCVs ist sowie für deren Reifung darstellt.

Unter Verwendung des hier etablierten Rekonstitutionssystems haben ich die Rolle bekannter Komponenten der minimalen Maschinerie bestätigt und ergänzt, welche aus AP-2, Epsin-1, Clathrin, Dynamin und der Hydrolyse von GTP durch Dynamin besteht.

AAK1	adaptor-associated kinase 1
AP	adaptor protein complex
AP180	clathrin coat assembly protein AP180
APS	ammonium persulfate
Arf	ADP-ribosylation factor
ATP	adenosine 5′-triphosphate
BAR	Bin/Amphiphysin/Rvs
BARS	brefeldin A ADP-ribosylated substrate
BFA	brefeldin A
BIIC	baculovirus infected insect cell
BSA	bovine serum albumin
BSE	bundle signaling element
CCB	clathrin coated bud
CCP	clathrin coated pit
CCV	clathrin coated vesicle
CHC	clathrin heavy chain
CI-MPR	cation-dependent manose-6-phosphate receptor
CLASP	clathrin associated sorting proteins
CLC	clathrin light chain
CLIC	clathrin-independent carrier
COPI	coat protein complex I
COPII	coat protein complex II
DAG	diacylglycerols
DMSO	dimethyl sulfoxide
DNA	deoxyribonucleic acid
DTT	dithiothreitol
EDTA	ethylenediaminetetraacetic acid
EM	electron microscopy
ENTH	epsin N-terminal homology domain
Eps15	epidermal growth factor receptor substrate 15
ER	endoplasmic reticulum
ERGIC	ER-Golgi intermediate compartment
ESCRT	endosomal sorting complexes required for transport
FCH	Fes/CIP4 homology

FCHo	FCH domain only
FEME	fast endophilin mediated endocytosis
g	times gravity
GAP	GTPase-activating protein
GEEC	glycosyl phosphatidylinositol-anchored protein enriched early endosomal compartment
GEF	guanine nucleotide exchange factor
GGA	ADP-ribosylation factor-binding protein GGA1
GPI-AP	glycosylphosphatidylinositol anchored proteins
GST	glutathione-S-transferase GTP Guanosine-5′-triphosphate
GTP	guanosine-5′-triphosphate
GTPγS	guanosine-5′-O-[γ-thio]-triphosphate
HEPES	4-(2-hydroxyethyl)-1-piperazin-ethansulfonic acid
IPTG	isopropyl-1-thio-β-D-galactopyranoside
K_d	dissociation constant
KDEL	ER-retrieval sequence composed of Lysine (K), Aspartate (D), Glutamate (E) and Leucine (L)
kDa	kilo Dalton
LB	Luria-Bertani broth
MHC II	major histocompatibility complex class II
N-WASP	Neural Wiskott-Aldrich syndrome protein
OD	optical density
p24	transmembrane emp24 domain-containing protein
PA	phosphatidic acid
PBS	phosphate buffer saline
PBS-T	phosphate buffer saline + Tween 20
PCR	polymerase chain reaction
PH	plextrin homology
Pi	inorganic phosphate
PIPKIγ	type Iγ phosphatidylinositol 4-phosphate 5-kinase
PLD2	phospholipase D2
PRD	proline-rich domain
PVDF	polyvinylidene difluoride
rpm	revolutions per minute
Sar1	secretion-associated and Ras-related protein 1

SDS-PAGE	sodium dodecyl sulfate-polyacrylamide gel electrophoresis
Sf9	insect cell line derived from Sf21 (spodoptera frugiperda) ovary cells
SH3	Src-homology 3
SNARE	N-ethylmaleimide sensitive-factor attachment receptors
SNX	sorting nexin
TGN	trans-Golgi network
TEMED	N, N, N', N'-Tetramethylethylenediamine
Tris	2-Amino-2-(hydroxymethyl)propane-1,3-diol
VSV-G	vesicular stomatitis virus glycoprotein
w/w	weight per weight
w/v	weight per volume

1 Introduction

1.1 Vesicular transport

Membrane trafficking is a major task of cells in which processes are encompassed to mediate the transport of proteins, lipids, pathogens or macromolecules to maintain cell homeostasis, signaling or the crosstalk with the environment. The transported molecules are referred to as cargo and transferred within vesicular or tubular carriers from one organelle to another, or across the cell membrane to and from the extracellular space. A proper regulation of all these processes, to have a required molecule at the right place and time, is essential for all living beings. Based on the transport direction, either to or from the extracellular space, membrane trafficking is divided into exocytosis and endocytosis (Figure 1-1). With exceptions, each pathway in exo- and endocytosis selects specific cargo and targets them to their correct compartment while maintaining the homeostasis of participating organelles.

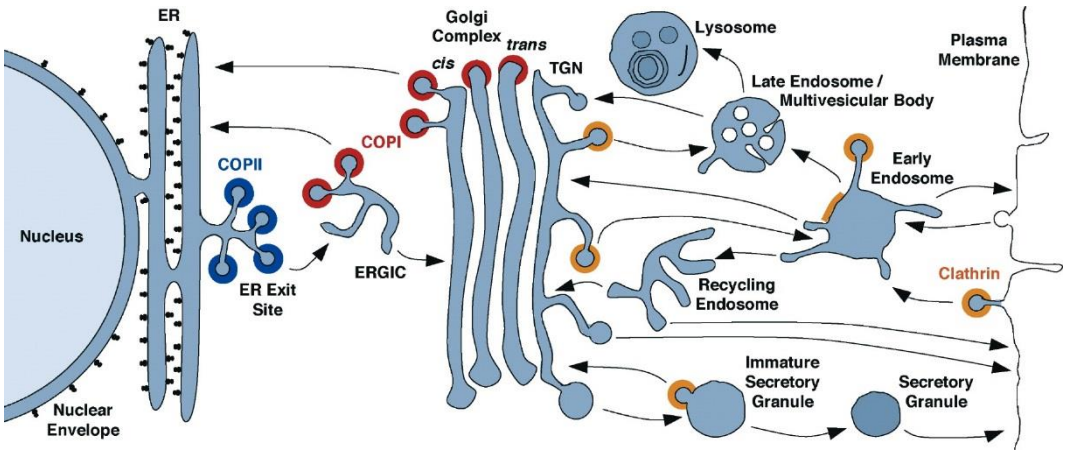

Figure 1-1 Intracellular transport pathways. Depicted are compartments of the secretory and endocytic pathway. Arrows indicate the transport routes. The main classes of membrane trafficking are colored: COPII (blue), COPI (red), clathrin (yellow). Secretory cargos are synthesized in the ER and transported towards the ERGIC from specialized ER-exit sites via COPII coated vesicles. At the ERGIC cargos are sorted for anterograde transport to the Golgi apparatus. After passaging through the Golgi, cargos are sorted and delivered to their final destination, in which clathrin coated carriers are implicated. clathrin vesicles are also important carriers for the uptake of extracellular material. A recycling pathway for the retrieval of ER-resident proteins from the ERGIC and the Golgi apparatus is mediated by COPI coated vesicles. Not depicted are additional carriers in the endosomal system (retromer, ESCRT) and the various types of endocytic processes at the plasma membrane. Picture taken from (Bonifacino and Glick, 2004).

As part of exocytosis, the secretory pathway transports newly synthesized proteins from the endoplasmic reticulum (ER) to the Golgi apparatus and finally to the plasma membrane or the extracellular space. After translocation into the ER, secretory cargos are sorted into vesicles encapsulated by a specialized coat known as coat protein II (COPII) (Barlowe et al., 1994).

Then, COPII vesicles are transported to and fuse with the ER-Golgi intermediate compartment (ERGIC) (Schweizer et al., 1988). At the ERGIC, proteins are distinguished between secretory proteins and those who are ER-resident that need to be transported back to the ER (retrograde transport). The latter one's harbor sorting signals to pack them into a second class of vesicles, the COPI vesicles. Secretory proteins are further transported within the ERGICs towards the *cis*-Golgi site, were they fuse and assemble the *cis*-Golgi network (Lippincott-Schwartz et al., 2000). The mechanism of transport within the Golgi are still controversial. In one model, the individual Golgi cisternae are believed to be static and the anterograde transport is mediated by COPI vesicles, budding from one cisternae and fusing with the next. Another model predicts a more dynamic Golgi apparatus. Here, cargo is transported from the *cis*-Golgi to the *trans*-Golgi stacks within cisternae as they progress towards the *trans*-Golgi site. Although these models are quite different, they are not mutually exclusive (Pelham and Rothman, 2000). Detailed information on the various Golgi trafficking models can be found in (Glick and Luini, 2011). The so-far mentioned pre-Golgi membrane trafficking mechanisms constitute the early secretory pathway. Upon arrival at the *trans*-Golgi network (TGN), proteins are sorted into transport carriers and targeted to their final cellular destination, such as the plasma membrane, endosomal compartments or, in case of specialized cells, to secretory granules. In these processes a third class of vesicles are implicated and termed, according to their scaffolding protein, clathrin coated vesicles. In addition to the transport from the TGN, clathrin coated vesicles are also important for the trafficking within the endosomal system and the uptake of extracellular material into the cell. Detailed information about the sorting and transport from the TGN towards the plasma membrane and the endosomal system and trafficking within the endosomal system can be found in (Lemmon and Traub, 2000, De Matteis and Luini, 2008, Guo et al., 2014).

The following sections will give an overview of basic mechanisms about the biogenesis of the three well established vesicle classes COPII, COPI, and clathrin, with a more detailed view on the latter vesicle type and endocytosis.

1.1.1 COPII vesicles

Secretory proteins are synthesized at the rough endoplasmic reticulum (ER), a process that couples translocation into the ER lumen with translation. Prior secretion, they undergo several processes requiring for their maturation: folding and assembly with the help of chaperons, and post-translational modifications. Thereafter, proteins designated for secretion enter a vesicular transport system, called COPII, for their journey towards the Golgi apparatus. In eukaryotic cells, COPII vesicles bud from specialized regions, termed ER exit sites (ER) or translational ER (tER) (Orci et al., 1991, Bannykh et al., 1996, Budnik and Stephens, 2009). The following chapter briefly describes how a set of cytosolic proteins facilitates the formation of COPII vesicles (Barlowe et al., 1994) and how cargo is sorted into these vesicles (Figure 1-2).

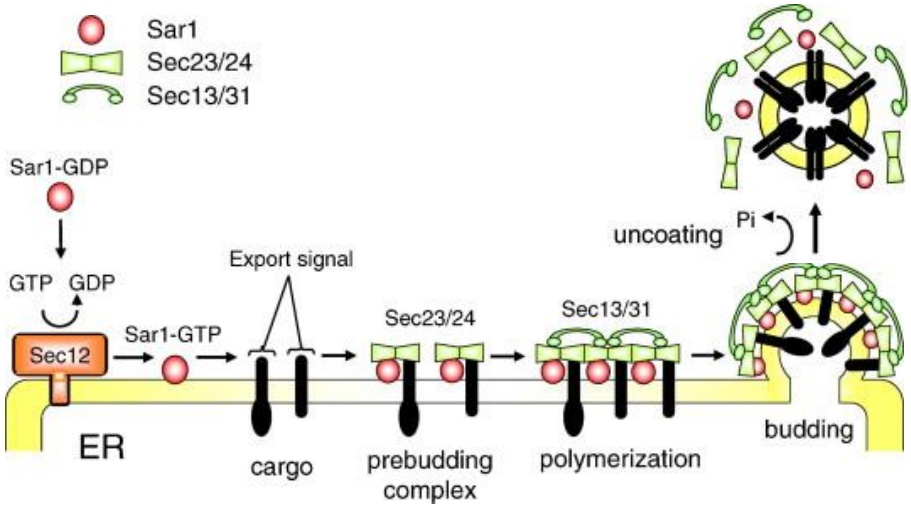

Figure 1-2 Individual steps in COPII vesicle biogenesis. The formation of COPII vesicles is initiated by the exchange of GDP to GTP on Sar1 by the transmembrane guanine exchange factor (GEF) Sec12. GTP loaded Sar1 is anchored to the ER-membrane via its N-terminal amphipathic helix. Subsequently, the inner coat layer (Sec23/Sec24 dimer) is recruited by activated Sar1, to form a pre-budding complex. Cargo proteins are sorted into vesicles via direct interaction with Sec24. Finally, the pre-budding complex is clustered by the Sec13/Sec31 subcomplex to polymerize to a bud. Generated buds are separated from the donor membrane by activated Sar1. To release the coat proteins, hydrolysis of GTP is activated by the coat component Sec23, the GTPase activating protein (GAP) of Sar1. Picture taken and modified from (Sato and Nakano, 2007).

The first step of COPII vesicle biogenesis is initiated by the activation of the small Ras-like GTPase Sar1 via GDP to GTP exchange through Sec12 (Nakano and Muramatsu, 1989, Barlowe and Schekman, 1993), a transmembrane guanine nucleotide exchange factor (GEF). Sec12 is strictly localized to the ER, thus Sar1 activation can exclusively occur at this organelle (Sato et al., 1996). The transition of the nucleotide state to GTP triggers a conformational change in Sar1 to expose a N-terminal amphipathic helix that is inserted into the ER membrane; thereby, Sar1 becomes tightly bound to the membrane (Barlowe, 1995). In contrast to almost all other members of the Arf-family, the amphipathic helix of Sar1 is neither myristoylated nor

acetylated (Huang et al., 2001, Donaldson and Jackson, 2011). Successively, two large complexes are recruited to membrane bound Sar1, first the heterodimer Sec23/Sec24 followed by the heterotetramer Sec13/Sec31. Both subunits of Sec23/Sec24-complex, assembling the inner layer of the coat (Matsuoka et al., 2001), exhibit distinct functions. Sec23 interacts with Sar1, whereas Sec24 is the major cargo recognition component. Together, this trimeric complex is referred as to the "pre-budding complex" (Kuehn et al., 1998, Bi et al., 2002). Although, the pre-budding complex does not provide the force for vesicle formation, it influences the rather uniformly size of COPII vesicles by its concave shaped inner surface (Barlowe et al., 1994, Bi et al., 2002). Notably, Sec23 is also the GTPase activating protein (GAP) for Sar1 (Yoshihisa et al., 1993). Finally, the pre-budding complex is clustered by the heterotetrameric Sec13/Sec31 complex, assembling the outer layer of the coat, deforming the membrane, and generating COPII buds. The interaction between both layers occurs between Sec31 and Sec23/Sar1, additionally important to trigger GTP hydrolysis by Sar1 (Antonny et al., 2001, Bi et al., 2007). In vitro data clearly demonstrate a GTP hydrolysis-independent scission mechanism, in which Sar1 seems to play a major role (Barlowe et al., 1994, Adolf et al., 2013). Thus, Sar1 functions not only in the very first step of COPII vesicle biogenesis as initiator of vesicle formation, but also in the very last step of COPII vesicle biogenesis, the separation of COPII coated buds from the ER membrane. First hints for this hypothesis came from the observation that activated Sar1 at high concentrations is able to deform and tubulate artificial liposomes, suggesting an involvement of the N-terminal helix in scission (Lee et al., 2005).

Proteins can exit the ER either by bulk-flow, a non-specific process, or as most secreted proteins, are selectively incorporated into vesicles with the help of short cytosolic export signals (Malkus et al., 2002, Barlowe, 2003). Whereas transmembrane proteins can directly interact with COPII coat proteins, soluble proteins require receptors to be sorted into vesicles. As mentioned earlier, the major cargo sorting hub is Sec24. Structural and biochemical approaches revealed distinct cargo binding sites: A-site, B-site and C-site (Mossessova et al., 2003, Miller et al., 2003). The first cargo recognition motif identified was within the cytoplasmic tail of the vesicular stomatitis virus glycoprotein (VSV-G). Together with other proteins like Kir2.1 or the yeast proteins Sys1p and GAP-2, VSV-G harbors a di-acidic motif with the consensus sequence (D/E)x(D/E), (where x represents any amino acid), binding to the B-site (Nishimura and Balch, 1997, Votsmeier and Gallwitz, 2001). A second cargo signal within transmembrane proteins comprises two hydrophobic amino acids adjacent to each other (FF, LL, YY, FY), also binding to the B-site. Examples are members of the p24 family, the Erv41/46 complex, or the

cargo receptor ERGIC53 and its yeast homologues Emp46p and Emp47p (Kappeler et al., 1997, Dominguez et al., 1998, Otte and Barlowe, 2002, Sato and Nakano, 2002). A third cargo signal (consensus motif: Lxx(L/M)E) that interacts with the B-site of Sec24 was found in the yeast SNARE proteins Sed5p and Bet1p. In the same study, Sed5p was found to bind additionally to the A-site of Sec24 via the cytoplasmic peptide YNNSNPF (Mossessova et al., 2003). Different to the above cargo signals is the interaction of Sec22 with the C-site of Sec24. Rather than a defined peptide sequence, a folded epitope is important for the sorting of the SNARE into vesicles, suggesting a mechanism in which cargo sorting discriminates between the folded state of a protein and/or its assembly into an oligomeric complex (Mossessova et al., 2003, Mancias and Goldberg, 2007).

The aforementioned cargo motifs sort transmembrane cargo into vesicles. The sorting of soluble cargo on the other hand is less investigated. ERGIC53 seems to be essential for the transport of blood coagulation factors, cathepsin C, cathepsin Z and other glycoproteins (Nichols 1998; Appenzeller 1999; Appenzeller-Herzog 2004). In yeast, the transmembrane protein Erv29 is required to sort the glycosylated α factor pheromone precursor (gpαf) into vesicles (Belden and Barlowe, 2001). Mutational analysis revealed three hydrophobic residues (I-L-V) within the N-terminal domain necessary for the uptake of gpαf. Moreover, an ER-resident protein fused with this domain (residue 1 – 86) was packed into vesicles more efficiently than a fusion protein with mutations of the hydrophobic residues. Therefore, an I-L-V containing ER-export motif for soluble cargo proteins was suggested (Otte and Barlowe, 2004).

Additional specificity arises from the four Sec24 isoforms (A – D) identified in mammals. Several studies identified specific interactors for the different Sec24 isoforms (Wendeler et al., 2007, Mancias and Goldberg, 2008, Adolf et al., 2016). In yeast, the two Sec24 homologues Iss1p and Lst1p can substitute Sec24 to assemble a dimer with Sec23 and incorporate a different set of cargo into vesicles (Roberg et al., 1999, Pagano et al., 1999, Kurihara et al., 2000).

1.1.2 COPI vesicles

How newly synthesized proteins are transported in the early secretory pathway from the ER to the Golgi via COPII vesicles is described in the previous chapter. During this process, also ER-resident proteins can reach the Golgi, either accidentally by default, or because they are to be post-translationally modified. The retrieval of these proteins back to the ER is the main task of a second vesicular transport system, termed COPI (Orci et al., 1986, Waters et al., 1991). This chapter briefly describes molecular mechanisms underlying COPI vesicle biogenesis and cargo recognition (Figure 1-3).

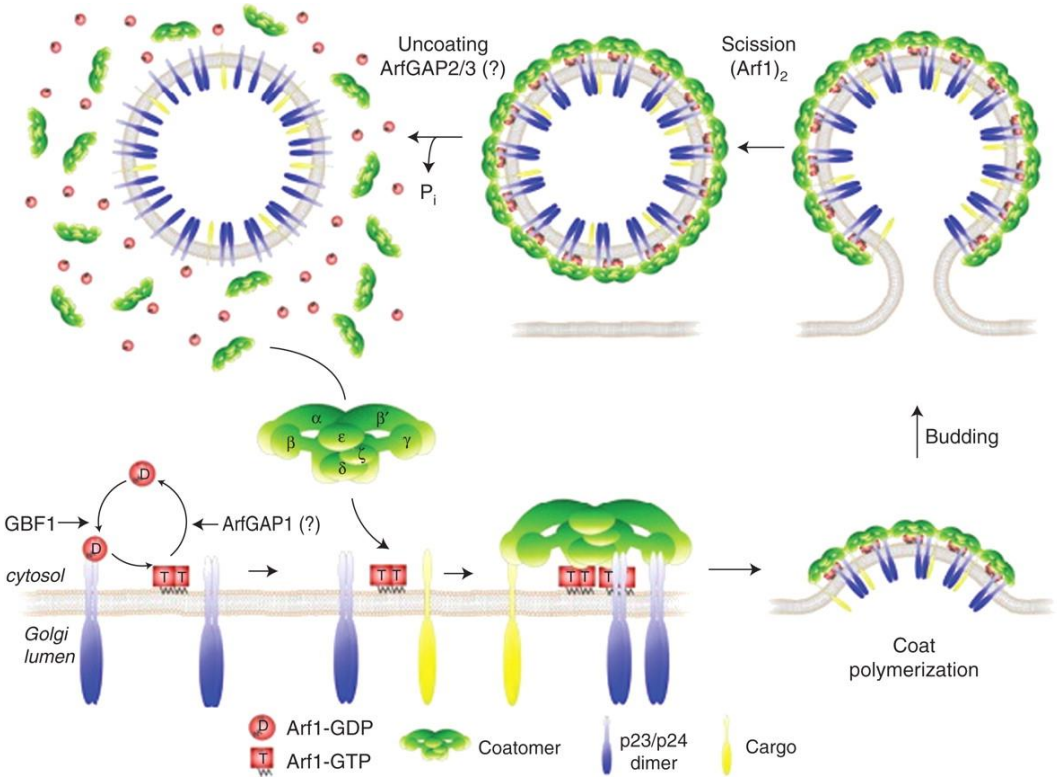

Figure 1-3 Individual steps in COPI vesicle biogenesis. Initially, the small GTP binding protein ADP-ribosylation factor (Arf) is recruited to the Golgi membrane by dimerized proteins of the p24 family, and activated by exchange of GDP with GTP with the help of the guanine nucleotide exchange factor GBF1, resulting in a stable membrane anchoring. Subsequently, the coat complex coatomer is recruited to membrane bound Arf via several interactions. Potential cargo proteins are sorted into vesicles via interactions with coatomer. Coat polymerization is supported by binding of coatomer to dimeric p24 family members, known to cause a structural rearrangement of coatomer, the source of energy for bud formation. Last, scission is mediated by activated and dimerized Arf as suggested from in vitro studies. Prior fusion to the acceptor membrane, the coat has to be shed off via the activation of GTP hydrolysis by GTPase activating proteins of the Arfgap family. The picture was taken from (Popoff et al., 2011).

The primary step of COPI vesicle biogenesis is the recruitment of a small GTPase from the ADP-ribosylation factor-family (Arf) by dimerized p23 protein, a member of the p24-protein family, close to the membrane (Gommel et al., 2001). Then, activation can occur by a brefeldin A (BFA) sensitive nucleotide exchange factor (GEF) (Donaldson et al., 1992). To date, 15 Arf

GEFs were identified in humans, divided into six subfamilies. Due to their different subcellular localization and specificity, they contribute to the localization of the six mammalian Arfs known (Arf2 is not expressed in humans) (Donaldson and Honda, 2005). Most likely, the relevant GEF for the biogenesis of COPI vesicles is GBF1, as it is localized to the Golgi apparatus (Zhao et al., 2002). Upon the exchange of GDP to GTP, Arf1 undergoes a structural rearrangement to expose its N-terminal myristoylated amphipathic helix for a stable association with the membrane (Franco et al., 1996, Antonny et al., 1997). This activation leads to the subsequent recruitment of coatomer, a heteroheptameric ~550 kDa complex consisting of the subunits α-, β-, γ- and δ-, β´-, ε-, ζ-COP (Serafini et al., 1991, Waters et al., 1991, Stenbeck et al., 1993, Kuge et al., 1993, Duden et al., 1991). The Coatomer complex can be divided into two stable sub-complexes, a tetrameric complex including the β-, γ-, δ- and ζ-COP, and a trimeric complex including the subunits α, β´and ε. Both sub-complexes share structural aspects, but no sequence similarity, with the clathrin system: the tetrameric sub-complex with the adaptor protein complexes and the trimeric sub-complex with clathrin. Thus, cargo recognition and scaffolding are combined within one complex (Hara-Kuge et al., 1994). Diversity arises from an additional isoform for the γ-COP and ζ-COP subunit termed γ2 and ζ2 (Blagitko et al., 1999, Futatsumori et al., 2000), suggesting for the incorporation of different cargo into vesicles. Thus, four different coatomer combinations are theoretically possible, which were indeed shown to be localized at different sites of the Golgi complex. The combinations including γ1ζ1, γ1ζ2 are localized to early Golgi compartments and γ2ζ1 to late Golgi compartments (Moelleken et al., 2007). Although there are four possible combinations, the γ2ζ2-complex is present in only minor amounts (Wegmann et al., 2004). Biochemical analysis mapped the interaction between Arf and coatomer to the β´-, β-, δ- and γ-COP subunit (Zhao et al., 1999, Sun et al., 2007), which was also confirmed by structural data (Dodonova et al., 2015, Dodonova et al., 2017). However, to sufficiently recruit coatomer to the membrane further interaction with dimerized members of the p24-family with the γ-COP subunit is prerequisite, which induces a conformational change of coatomer, providing energy to drive vesicle formation (Reinhard et al., 1999, Bremser et al., 1999, Bethune et al., 2006).

Finally, scission of COPI vesicles was demonstrated to depend only on the cytosolic proteins coatomer and Arf1, as described (Bremser et al., 1999). This step is, similar to the COPII system, but unlike the clathrin system, independent on the hydrolysis of GTP, as use of non-hydrolyzable GTP analogs results in amounts of vesicles similar to those obtained with GTP (Adolf et al., 2013). A pivotal feature of Arf in scission is its ability to dimerize. Like GTP-loaded Sar1 in the COPII system, GTP-loaded Arf exhibits a strong membrane bending activity

which is potentiated upon dimerization and was shown at high concentrations to tubulate liposomes in vitro (Beck et al., 2008, Krauss et al., 2008). In contrast, the dimerization-deficient Arf mutant Y35A cannot induce scission, as confirmed by electron microscopy analysis, but scission can be rescued upon its chemical crosslinking (Beck et al., 2011). In spite of these findings, a second model suggests that the brefeldin A ADP-ribosylated substrate (BARS) together with other COPI components constricts the vesicle neck in the first place, leading to the subsequent scission step, in which phosphatidic acid (PA) generated by phospholipase D2 (PLD2) and diacylglycerols (DAG) seems to play a certain role (Yang et al., 2005, Yang et al., 2008), most likely due their potential to induce a negative membrane curvature as they are cone-shaped lipids (Shemesh et al., 2003). Although, in vitro BARS and PA are not necessary to generate free COPI vesicle, they could assist the scission process in vivo.
In order to fuse with the acceptor membrane, the COPI coat needs to be shed off. Uncoating is initiated by GTP hydrolysis, disrupting the interaction of Arf with the membrane. Arf proteins do not show any or a measurable GTPase activity themselves, but have a high affinity to GTP. Thus, the GTPase needs to be activated by GTPase-activating proteins (GAPs) (Randazzo and Kahn, 1994). From the identified 31 mammalian Arf GAPs, Arfgap1, 2, and 3 are implicated in this process (Donaldson and Jackson, 2011).

As mentioned earlier, the COPI system facilitates the retrograde transport from the Golgi to the endoplasmatic reticulum as well as intra-Golgi transport. A motif within the amino acid sequence of soluble proteins was identified to distinguishing between ER-resident proteins and those designated for secretion, the C-terminal KDEL sequence (HDEL in yeast) (Munro and Pelham, 1987). As KDEL sequence containing proteins become post-translationally modified by non-ER located proteins, they must traffic from the Golgi back to the ER (Pelham, 1988, Dean and Pelham, 1990). To actively sort these proteins into COPI vesicles the help of receptors is needed. The first kind of such K/HDEL receptors was the yeast protein ERD2, an integral seven transmembrane spanning protein (Semenza et al., 1990). Nowadays further receptors were identified including three orthologues in mammals (Lewis and Pelham, 1990, Lewis and Pelham, 1992, Raykhel et al., 2007). Directionality of this transport is believed to be caused by a shift of pH between the *cis*-Golgi and the ER, where the higher pH of the ER lumen leads to dissociation of the KDEL sequence from the KDEL receptor. The empty receptor is then recycled back to the Golgi (Wilson et al., 1993). The KDEL receptor itself was shown to directly interact with coatomer upon phosphorylation of serine 209 at the C-terminus (Cabrera et al., 2003).

Additional motifs for the sorting of transmembrane proteins were identified. The best characterized ones are the dilysine-motifs KKXX and KXKXX, directly recognized by the coatomer subunits α- and β´-COP, respectively (Nilsson et al., 1989, Jackson et al., 1990, Eugster et al., 2004). As mentioned earlier, members of the p24 family interact with the γ-COP subunit of coatomer. Although their binding signal looks similar, the consensus sequence FFXX(KR)(KR)X_n ($n \geq 2$) found in these proteins is not conform with the canonical KKKXX motif. Furthermore, their interaction with coatomer requires dimerization of these p24 family members (Bethune et al., 2006).

Another retrieval motif is based on the presence of arginine, first identified in the invariant chain of the major histocompatibility complex class II (MHC II), following the consensus sequence [ΦΨR]RXR (Φ and Ψ correspond to an aromatic or bulky hydrophobic residue) (Lotteau et al., 1990, Schutze et al., 1994, Michelsen et al., 2005). Yeast two-hybrid screens mapped the interaction of such motifs with coatomer to the β- and δ-COP subunits (Michelsen et al., 2007). Although the function of this motif is to retrieve proteins back to the ER, their actual purpose is to keep subunits of some multimeric proteins in the ER as long as they are completely assembled. This will inactivate the motif allowing secretion of correctly assembled complexes (Zerangue et al., 1999, Margeta-Mitrovic et al., 2000, O'Kelly et al., 2002).

1.1.3 Clathrin vesicles

Clathrin structures were first observed already in 1964 during the studies of uptake of yolk-protein by mosquito oocytes (Roth and Porter, 1964). Thomas Roth and Keith Porter observed "bristle-coated" pits and vesicles at the cell surface containing yolk and also naked vesicles fusing to storage granules in the cell interior. However, it lasted until 1976 when Barbara Pearse observed these "bristle-coated" structures in a vesicle fraction. She subsequently characterized the coat protein and named it clathrin after its cage-like assembly character (Pearse, 1975, Pearse, 1976). During Pearse's characterization studies of clathrin she already observed additional bands at about 100 – 110 kDa in SDS-gels. Four years later the same proteins were found to promote clathrin assembly (Keen et al., 1979). Finally, Emil Unanue, Ernst Ungewickel and Daniel Branton linked these proteins to the attachment of clathrin to membranes in 1981 (Unanue et al., 1981). Some years later, these bands were identified to be part of two distinct complexes termed assembly polypeptide 1 and 2, nowadays called adaptor proteins 1 and 2 (Pearse and Robinson, 1984, Keen, 1987). Up to now, five of these complexes are known, plus a number of additional monomeric clathrin adaptors, increasing the repertoire of incorporated cargo (Traub, 2009).

1.1.3.1 The assembly polypeptide complexes

In the late secretory and endocytic pathways, the so-called assembly polypeptide complexes or adaptor protein complexes (AP-complexes) select cargo for incorporation into coated vesicles and recruit, with exceptions, the scaffolding protein clathrin. Up to now five AP-complexes were identified, AP-1 to AP-5, all involved in post-Golgi trafficking pathways. Due to their highly enriched appearance in clathrin coated vesicles (CCV), the first two clathrin adaptors that were identified are AP-1 and AP-2 (Keen et al., 1987, Pearse, 1975, Pearse and Robinson, 1984). By searching sequence databases for homologs of AP-1 and AP-2, three other AP-complexes were discovered, AP-3 to AP-5. All complexes are heterotetrameric oligomers with a related set of subunits, but they have distinct localizations and functions. AP-1 can be found at the *trans*-Golgi network as well as at tubular endosomes. AP-2, as the main endocytic clathrin adaptor and by far the most characterized complex, is localized to the plasma membrane (Jackson et al., 2010). The third AP-complex mediates transport of cargo from tubular endosomes to late endosomes and lysosomes and AP-4 traffics cargo form the *trans*-Golgi network to endosomes (Burgos et al., 2010). The fifth AP-complex was recently discovered in 2011 in the lab of Margaret Robinson (Cambridge, UK) and seems to be localized to late endosomes. Whereas AP-1, AP-2 and AP-3 are colocalized with clathrin, AP-4 and AP-5 seem to work in an clathrin-independent pathway (Dell'Angelica et al., 1999, Hirst et al., 2011). Recently, two proteins with a high affinity to AP-5 were identified, SPG11 and SPG15, having predicted α-solenoid structures similar to that of the clathrin heavy chain and subunits of the COPI-coat. Thus, they are good candidates to substitute clathrin as the scaffolding protein (Hirst et al., 2013). Each of the five complexes are composed of four subunits, two large subunits with a molecular weight of 90 – 130 kDa (γ/α/δ/ε/ζ and β1-5, respectively), one medium-sized subunit of about 50 kDa (μ1–5) and one small-sized subunit of about 20 kDa (σ1–5). In addition, some of the subunits occur as isoforms encoded from different genes. For AP-1 two γ (γ1 and γ2), two μ1 (μ1A and μ1B) and three σ1 (σ1A, σ1B and σ1C) are known; for AP-2 two α (α1 and α2) are known; for AP-3 two β3 (β3A and β3B), two μ3 (μ3A and μ3B) and two σ3 (σ3A and σ3B) are known (Boehm and Bonifacino, 2001, Park and Guo, 2014). To date, no isoforms for AP-4 and AP-5 are described. All heterotetrameric AP-complexes are structured as a so called “core” comprised of the N-terminal “trunk” part from the two large subunits and the full-length medium and small subunit. The C-terminal parts of both large subunits are called “appendage” or “ear” domains which are connected to the “core” by a largely unstructured part, called “hinge” (Figure 1-4). Whereas the core domain is responsible

for membrane binding and cargo recognition, the appendage- and hinge-domain interact with accessory or regulatory proteins and clathrin, respectively.

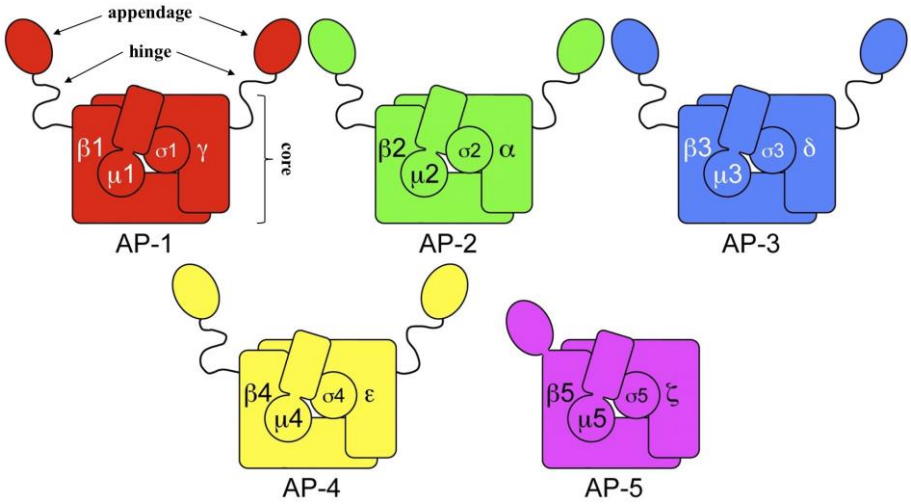

Figure 1-4 Subunit assembly of the AP-complexes. The adaptor protein complexes are heterotetramers, each are composed of four subunits, two large subunits with a molecular weight of 90 – 130 kDa (γ/α/δ/ε/ζ and β1-5, respectively), one medium-sized subunit of about 50 kDa (μ1–5) and one small-sized subunit of about 20 kDa (σ1–5). The N-terminal part of the two large subunits together with the medium and small subunit constitute the core. Except of AP-5, both C-terminal appendage domains are connected to the core by a largely unstructured linker, the hinge. Whereas the core is responsible for the interaction with membranes and sorting of cargo, the appendage- and hinge-domain interact with accessory or regulatory proteins as well as with clathrin. Picture taken and modified from (Hirst et al., 2014).

Although many AP variants are theoretically possible, little is known about special functions for a single isoform or their combinations. AP-1 is ubiquitously expressed in all mammalian tissues, except the μ1B isoform, which is exclusively expressed in polarized epithelial and exocrine cells and targets cargo to the basolateral plasma membrane (Folsch et al., 1999, Ohno et al., 1999). In contrast to the AP1-complex harboring γ1 the recruitment to membranes with γ2 in the complex is not sensitive to brefeldin A (BFA), a drug stabilizing the Arf(GDP)-GEF-complex, thus preventing the activation of Arf by GDP to GTP exchange important for AP-1 recruitment (Lewin et al., 1998, Peyroche et al., 1999). An isoform-specific function is not known for AP-2, however, diversity arises from splice variants. The AP-2α1 subunit is alternatively spliced in brain and skeletal muscle cells, resulting in an elongation of the hinge region by 21 amino acids (Ball et al., 1995). For AP-2μ the alternative splicing of exon 5 leads to the presence or absence of histidine 142 and glutamine 143 in the protein primary structure (Ohno et al., 1998b). A splice variant for AP-2σ lacking 38 amino acids was also identified in human blood cells, however, its function is unknown (Holzmann et al., 1998). Interestingly, β1 can partially substitutes the missing β2-subunit of AP-2 in embryonic fibroblasts from homozygous mutant mice. This results in a reduced AP-2 expression level with β1 instead of

β2 in the AP-2-complex. However, this AP-2-variant maintains viability of homozygous mutant embryos only until birth (Li et al., 2010). Two of the AP-3 subunits, β3B and μ3B, are expressed exclusively in neurons and neuroendocrine cells (Newman et al., 1995, Pevsner et al., 1994), whereas all other subunits are expressed ubiquitously. Besides these known tissue specific expression levels there is a broad list of observed diseases and disorders linked to mutations of specific AP-isoforms (Boehm and Bonifacino, 2001).

The localization of all AP-complexes and therefor the specificity in membrane trafficking is orchestrated by the diversity of phosphatidylinositol phosphates, small GTPases, and sorting signals in the cytoplasmic tail of transmembrane receptors. Cytoplasmic sorting signals contain short, linear amino acid sequences. Two well characterized ones are the tyrosine-based (YxxΦ) and the dileucine-based ([DE]xxxL[LI]) sorting-signal recognized by the complexes AP-1, AP-2 and AP-3. The interaction between the YxxΦ-motif and the APs occurs with the μ-subunit of each AP-complex, whereas the dileucine-motif interacts with the heterodimers γ-σ1, α-σ2, δ-σ3 of the respective AP-complex (Dell'Angelica et al., 1997, Doray et al., 2007, Janvier et al., 2003, Ohno et al., 1995). Both binding sites are occluded in the cytosolic "closed" conformation of the AP-complexes 1 and 2 and become accessible only upon membrane binding ("open" conformation), caused by a conformational rearrangement of the subunits (Jackson et al., 2010, Ren et al., 2013). Structural data for a conformational rearrangement of AP-3 upon membrane binding is missing, but structural homology suggests that its binding sites become accessible in an "open" conformation, similar to AP-1 and AP-2 (Mardones et al., 2013). Structural analysis of AP-2 in complex with the dileucine-motif of CD4 illustrate that most residues important for the interaction with dileucine signals are on the σ2 subunit and highly conserved in σ1 and σ3. However, mutational analysis of these amino acids in combination with yeast three-hybrid screens revealed a signal- and adaptor-dependent specificity. Further specificity was observed for the hemicomplexes γ2-σ1A and γ2-σ1B, which bound to the tyrosine-signal, but not to the other two dileucine-signals, from Nef and LIMP-II, tested. The respective AP-4 hemicomplex bound to none of them (Collins et al., 2002, Mattera et al., 2011).

During the studies of sorting of the Alzheimer´s disease amyloid precursor protein (APP), a specific interaction between the μ4-subunit and the YKFFE-sequence was reported, whilst μ1, μ2 and μ3 do not bind to this sequence, fitting very well to a YxxΦ-motif (Burgos et al., 2010). Another study identified some non-canonical signals (the di-aromatic residue FXF, phenylalanine-based motif FGSV and FR motifs) important for the interaction with the μ4-

subunit (Yap et al., 2003). Mutational analysis of the APPs YKFFE-sequence defined the novel sorting signal YX[FYL][FL]E exclusively interacting with AP-4 at a site distinct from the interaction of the YxxΦ-motif with µ1-µ3 (Burgos et al., 2010, Ross et al., 2014). Sorting-signals recognized by AP-5 were not identified so far. Analysis of the AP-5 sequence revealed that key residues in the µ5-subunits important for the recognition of YxxΦ-signal are missing, this might implicate that AP-5 does not bind to this type of cargo-signal at all or that it probably interacts with another type of cargo-signal (Hirst et al., 2011). Although all tyrosine-based signals fit to the consensus sequence YxxΦ, each µ-subunit prefers a different set of amino acids at the two x-positions (Y+1 and Y+2) and the Φ-position (Y+3). At the Φ-position the subunits µ1, µ2 and µ3B prefer a leucine, whereas µ4 prefers a phenylalanine. Only the µ3A-subnit did show a preference for two amino acids at the Φ-position, with a slightly higher preference for isoleucine as compared to leucine. In addition to the commonly preferred proline at position Y+2, each subunit prefers a distinct set of amino acids at the Y+2-position. The preference for amino acids at position Y+1 seems to be more diverse then for the other two positions, except for the µ4-subunit, which seems to prefer aspartic acid at this position (Aguilar et al., 2001, Ohno et al., 1998a).

Another factor for localization specificity is the diversity of phosphoinositides in the cell. Seven different phosphorylated phosphoinositides can be found in eukaryotic cells, comprising less than 1 % of the cell lipids. Nevertheless, they play important roles in trafficking, signal transducing pathways or serve as precursors of secondary messengers (Kutateladze, 2010, Polo et al., 2002). At the plasma membrane, the major phosphoinositide is phosphatidylinositol 4,5-bisphosphate (hereafter PI(4,5)P_2) (Falkenburger et al., 2010). PI(4,5)P_2 is primarily synthesized from phosphatidylinositol (PI) first by PI 4-kinase to produce PI(4)P, which is delivered to the plasma membrane from the Golgi complex or recycling organelles. Only a minor portion of PI(4)P is directly synthesized at the plasma membrane. Subsequently, PI(4)P is further phosphorylated by PI(4)-5-kinase at the plasma membrane to generate PI(4,5)P_2 (Odorizzi et al., 2000). The second important phosphoinositide at the plasma membrane is phosphatidylinositol (3,4,5)-trisphosphate (hereafter PI(3,4,5)P_3). PI(3,4,5)P_3 is generated from PIP_2 upon the activation of the PI(3)-kinase by growth factor receptors at the plasma membrane. Even though PI(3,4,5)P_3 is present in minor amounts at the plasma membrane, it is very important for the physiology of the cell as it effects for example cell proliferation, migration, chemotaxis, differentiation or metabolic changes (Cantley, 2002, Czech, 2003, Katso et al., 2001). PI(4)P, PI(3)P and PI(3,5)P_2 can predominantly be found on the Golgi, early endosomes

and late endocytic organelles, respectively (Di Paolo and De Camilli, 2006). PI(3,4)P_2 has been implicated in late stages of endocytosis by recruiting the BAR-domain containing protein SNX9 to clathrin-coated pits at the plasma membrane (Posor et al., 2013). Two other PI(3,4)P_2 pools were identified at the endoplasmic reticulum and multivesicular endosomes by use of the PH-domain of tandem-PH-domain-containing protein 1 (TAPP1), tagged to glutathione S-transferase, (Watt et al., 2004). The majority of the least investigated phosphatidylinositide PI(5)P can be found at the plasma membrane, but it is also enriched at the smooth endoplasmic reticulum and the Golgi (Sarkes and Rameh, 2010). From the five known AP-complexes, AP-1, AP-2 and AP-5 bind to a phosphoinositide at their specific target membrane. Similar specificities of AP-3 and AP-4 are still unknown. AP-2 is selectively recruited to the plasma membrane via the interaction with PI(4,5)P_2, and only then AP-2 can bind to a cargo protein. AP-2 does not show any significant binding to one of the other phosphoinositides in a surface-plasmon-resonance-(SPR)-based approach (Gaidarov and Keen, 1999, Honing et al., 2005, Jackson et al., 2010, Rohde et al., 2002). In a solid phase lipid binding assay, the phosphoinositides AP-1 can bind to have been shown to be predominantly the Golgi-enriched PI(4)P, slightly less to PI(5)P and to a minor extend PI(3,5)P_2. Interestingly, no binding was observed to the plasma membrane phosphoinositides PI(4,5)P_2 and PI(3,4,5)P_3, which is most likely caused by the lack of basic amino acids important for the interaction of AP-2 with PI(4,5)P_2 (Wang et al., 2003, Collins et al., 2002). The third AP-complex whose localization is connected to a phosphoinositide is AP-5. However, AP-5 did not bind directly to the lipid. Furthermore, it is suggested that AP-5 together with the two known interactors SPG11 and SPG15 can form a coat-like structure. In this structure SPG15 facilitates docking to PI(3)P-enriched membranes via its FYVE-domain whereas AP-5 is responsible for protein sorting (Hirst et al., 2013).

Last, small GTPases of the Arf-family, namely Arf1 and Arf6, play a role in the recruitment of various AP-complexes to membranes. The recruitment of AP-1 to its target membrane strongly depends on GTP-bound, and therefore membrane bound, Arf1. Structural and biochemical analysis revealed that AP-1 can bind to cargo only in the Arf1 bound state, which causes a structural rearrangement similar to AP-2. In this open conformation two Arf1 molecules are bridging two copies of AP-1 at different sites, one Arf1 binds to the trunk portion of β1 and the second Arf1 to the trunk portion of γ from another AP-1 complex. However, only the Arf1 interaction with the β1 subunit is important to induce the open conformation, which is different to AP-2, where PI(4,5)P_2 induces the open conformation, which needs to be further stabilized

by interactions with cargos (Honing et al., 2005, Jackson et al., 2010). In addition, a third Arf1 molecule important for recruitment, but not activation, binds to another side of γ (Ren et al., 2013, Stamnes and Rothman, 1993, Traub et al., 1993). In vivo and in vitro data have shown that GTP-bound Arf1 is mandatory for the recruitment of AP-3 and AP-4 to membranes, however more systematic data and structural analysis are missing (Ooi et al., 1998, Boehm et al., 2001). For AP-4 the binding site for Arf1 has been narrowed down in a yeast two-hybrid system to the ε subunit of AP-4 and to the μ4-subunit, but without Arf1-GTP dependency for μ4 (Boehm et al., 2001). The second Arf-family member which has been connected to the AP-complexes, Arf6, can stimulate the recruitment of AP-2 to the synaptic membrane by the activation of a synaptically enriched type Iγ phosphatidylinositol 4-phosphate 5-kinase (PIPKIγ), locally elevating the amount of $PI(4,5)P_2$ (Honda et al., 1999, Krauss et al., 2003). The direct interaction of Arf6 with AP-2 is contradictory. Whereas Arf6 was shown to directly interact with AP-2 in a liposomal pull-down experiment (Paleotti et al., 2005), another report excluded the interaction of Arf6 with clathrin, all subunits of AP-2, AP180, amphyphysin 1, dynamin-1 and auxilin in a GST Pull-down experiment (Krauss et al., 2003). Another link of Arf6 to endocytosis is the interaction of dynamin-2 with EFA6A, EFA6B and EFA6D, three Arf6-specific guanine nucleotide exchange factors (GEF). Arf6 activation by GTP exchange was further shown to be dependent on the GTPase activity of dynamin-2 and critical for the uptake of transferrin (Okada et al., 2015).

So far, AP-5 was not found to bind to any of the Arf-family members, moreover its localization seems to be insensitive to brefeldin A. This finding suggests that AP-5 recruitment to membranes is at least not dependent on Arfs whose activation is dependent on a BFA-sensitive GEF (Hirst et al., 2011).

1.1.3.2 Clathrin – a scaffolding complex

Clathrin was the first component of the kind of vesicles observed in 1964 and finally characterized in 1976 (Roth and Porter, 1964, Pearse, 1976). Itself, it is not able to bind to membranes; hence, it must be recruited to the membrane bilayer by adaptors. After the first observations of clathrin coated vesicles by Roth and Porter, they described the structure of the coat as a layer of bristles, comparable to hairs on a sphere. However, in 1969, Toku Kanasaki and Ken Kadota analyzed electron micrographs of thin sections of isolated clathrin vesicles from guinea pig brain and liver using the same method but they fixed the structures with glutaraldehyde in addition to osmium tetroxide, to preserve the protein structures, and compared their results with negative stained electron micrographs. Their findings revealed a

highly ordered basket-like clathrin structure composed of hexagons and pentagons enclosing a vesicle (Kanaseki and Kadota, 1969). It lasted until 1981 as Ernst Ungewickel and Daniel Branton used a rotary shadowing technique for electron microscopy to identify the building block of the clathrin basket, the triskelion. This building block is a trimer of dimers comprised of three clathrin heavy chains (CHC) and three clathrin light chains (CLC), each bound to one CHC. Actually, two isoforms of the heavy chain and light chain are known. The two CHC isoforms are named according to the encoding chromosome, CHC17 and CHC22. Whereas the ubiquitously expressed CHC17 is involved in endocytosis, intracellular traffic pathways, lysosome biogenesis and endosomal sorting, the CHC22 isoform mediates retrograde transport from endosomes to the *trans*-Golgi network. Although the sequence identity of both isoforms is 85 %, CHC22 does not bind to any of the two light chain isoforms (CLCa and CLCb) and interacts with AP-1 and AP-3, but not with AP-2. Indeed, the sequence differences are predominantly found in regions responsible for adaptor and light chain binding (Liu et al., 2001, Wakeham et al., 2005). In a yeast two-hybrid screen, SNX5 was identified to interact with CHC22 at a site equivalent to the site on CHC17 interacting with CLCs (Towler et al., 2004).

Over several years, the structure of clathrin and also of an assembled coat was solved by X-ray crystallography and cryo-electron microscopy, which gave an understanding of how the triskelion is assembled and how the light chain interacts with the heavy chain. CHC comprises two structural elements, a long α-solenoid region and a single seven-bladed β-propeller domain at its N-terminus. The α-solenoid part consists of eight repeats of a structural motif of 10 helices, designated as clathrin heavy chain repeats (CHCR0 to CHCR7), forming the ankle, distal leg, knee and proximal leg segment of CHC. The β-propeller forms the terminal domain, connected to the ankle segment (CHCR0) by a linker, which is the main interaction site for clathrin-binding proteins (Figure 1-5). So far, four adaptor interaction sites within the terminal domain were identified, the clathrin-binding box (adaptor motif: LΦXΦ[DE]), W-box (adaptor motif: PWXXW), β-arrestin 1L-site (adaptor motif: [LI][LI]GXL), and a more recently identified fourth interaction site (Willox and Royle, 2012). Although specific adaptor motifs are necessary to bind to one of these interaction sites, mutational analysis gave rise to the assumption that the four interaction sites exhibit functional redundancy, as only the quadruple interaction site mutant remarkably reduces endocytosis. Another adaptor binding site, which GGA1 binds to, is located between CHCR1 and CHCR2 in the ankle segment (Lemmon and Traub, 2012, Willox and Royle, 2012). At the opposite side, the very C-terminal end of CHC, 45 poorly structured amino acids protrude to the center of an assembled cage, harboring a

sequence (QLMLT) recognized by Hsc70 (Figure 1-5), which is, in cooperation with auxilin/GAK, responsible for vesicle uncoating, most likely by destabilizing the clathrin assembly (Fotin et al., 2004, Rapoport et al., 2008).

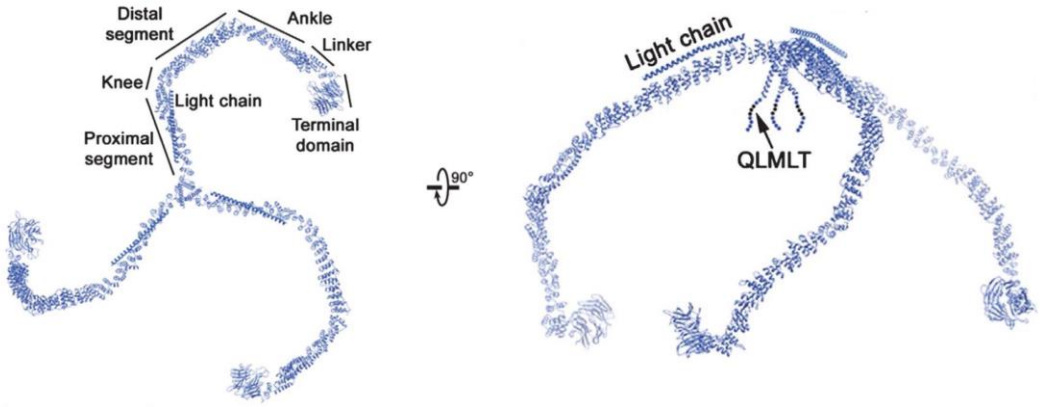

Figure 1-5 Structure of a clathrin triskelion. Each CCV is surrounded by a clathrin assembly composed of hexagons and pentagons. The building block of such a cage is the heterohexameric clathrin triskelion, composed of three clathrin heavy chains (CHC) and three clathrin light chains (CLC). Structurally, the CHC is divided into a long α-solenoid part (subdivided into five segments) and the adaptor interacting terminal domain, structured as a β-propeller (left, top view). The CLC is unstructured until binding to the proximal segment (C-terminus). This interaction stabilizes the CHC-trimerization and attenuates clathrin assembly. As can be seen from the side view (right), each leg of a triskelion protrudes towards the center of the cage to interact with adaptors at the membrane. Also depicted are poorly structured amino acids protruding from the trimerization-region towards the membrane harboring QLMLT-sequences recognized by HSC70. Together with auxilin/GAK, Hsc70 mediates uncoating of CCV. Picture taken and modified from (Xing et al., 2010)

CLCa and CLCb are unstructured until binding to the proximal leg segment (C-terminus) of CHC17. Mutagenesis and cryo-EM studies revealed three tryptophan residues in the binding interface critical for the interaction between the chains. This interaction is disrupted upon mutation of the tryptophan residues. The light chains stabilize trimerization due to their C-terminal interaction with the heavy chain and attenuate clathrin lattice formation at physiological pH. CLC occurs in two conformations. In one conformation the interaction of CLC with CHC extends from the trimerization domain to the knee segment, resulting in a knee conformation not compatible with lattice formation. Only when the CLC is retracted from the knee segment of CHC (second conformation), either by downregulating the pH (< 6.5), or by interacting with adaptors at physiological pH, the clathrin lattice can assemble. When assembled, each leg of a triskelion protrudes towards the center of the cage or vesicle to interact with adaptors via the terminal domain (Vigers et al., 1986, Kirchhausen et al., 1987, ter Haar et al., 1998, Ybe et al., 1999, Fotin et al., 2004, Knuehl et al., 2006, Ybe et al., 2007, Wilbur et al., 2010).

1.1.3.3 Dynamin – the scission factor in CCV biogenesis

In the very last step of clathrin vesicle biogenesis the large GTPase dynamin comes into play for separating the matured bud from the donor membrane. In 1989, Howard Shpetner and Richard Vallee found, in addition to kinesin and dynein, a protein of 100 kDa in their nucleotide free microtubule preparations from calf brain and named it dynamin. Although, this protein was falsely identified to be a microtubule-binding protein two years before, the same authors identified GTP to be a regulatory factor for dynamin as they extracted it from microtubules in the presence of GTP (Paschal et al., 1987, Shpetner and Vallee, 1989). A possible role of dynamin in the biogenesis of clathrin coated vesicles was already identified in the early 80s. Toshio Kosaka and Kazuo Ikeda investigated a temperature-sensitive Drosophila shibire-mutant, which is paralyzed at the non–permissive temperature (Grigliatti et al., 1973). This phenotype was shown to be based on a block of endocytosis as this mutant lacks synaptic vesicles and accumulates clathrin coated pits (CCP) at the plasma membrane (Kosaka and Ikeda, 1983). Finally, sequence analysis identified the shibire gene to be a homologue of the mammalian dynamin (van der Bliek and Meyerowitz, 1991, Chen et al., 1991) and indeed, overexpressing negative dynamin mutants inhibit endocytosis in cells (Herskovits et al., 1993, Damke et al., 1994). Electron-microscope studies showed that recombinant expressed dynamin self-assembles into rings and spirals and is able to form helical tubes on a lipid bilayer (Hinshaw and Schmid, 1995), resembling the structures which have been observed at the base of CCP in the shibire mutant. This, together with the finding that dynamin applies forces to the membrane, caused by a constriction and elongation of the dynamin spiral upon GTP hydrolysis (Sweitzer and Hinshaw, 1998, Stowell et al., 1999, Roux et al., 2006), led to the hypothesis that dynamin acts as a GTP-dependent mechanochemical enzyme that pinches off endocytic clathrin coated buds after assembling around their neck. Nowadays, its role as a scission factor in endocytosis is well established. However, little is known about intracellular functions of dynamin. At least, dynamin-2 was found to be localized to the *trans*-Golgi network and contributes to the formation of transport vesicles (Maier et al., 1996, Jones et al., 1998) and also plays a certain role in the recycling of the cation-dependent manose-6-phosphate receptor (CI-MPR) from late endosomes to the *trans*-Golgi network (Nicoziani et al., 2000).

In mammals three dynamin isoforms with additional splice variants were identified that oligomerize to a tetramer of two dynamin-dimers (Cao et al., 1998, Reubold et al., 2015): neuronal dynamin-1 with 8 splice variants (Scaife and Margolis, 1990), ubiquitously expressed dynamin-2 with 4 splice variants (Cook et al., 1994), and dynamin-3 with 13 splice variants

expressed predominantly in testis but also in neuronal and lung cells (Nakata et al., 1993, Cook et al., 1996). The members of the dynamin family have a five-domain architecture composed of the GTPase-(G) domain mediating GTP binding and hydrolysis, the bundle signaling element (BSE) transmitting the conformational change from the G-domain to the stalk domain upon GTP hydrolysis, the stalk is important for oligomerization and assembly around the neck of CCB, the plextrin homology-(PH) domain responsible for membrane binding ($PI(4,5)P_2$) and the proline-rich domain (PRD) involved in the interaction with proteins containing BAR- and SH3-domains to recruit dynamin to necks of CCB (Daumke et al., 2014). To assemble in a right-handed helical structure around the neck of a CCB, dynamins are interacting via the stalk with each other. Only in this assembly, the GTPase activity is triggered upon dimerization of GTP-bound G-domains from adjacent rungs. The subsequent conformational change is transmitted via the BSE to the stalk, resulting in the helix constriction mentioned above (Hinshaw and Schmid, 1995, Takei et al., 1995, Chappie et al., 2010, Faelber et al., 2012). Although much is known about the function of dynamin and its domains, it is still unclear how dynamin uses these functions to mediate the scission of invaginated clathrin coated buds to release clathrin coated vesicles. According to the findings that dynamin (1) oligomerizes into a helical structure at the neck of CCB, (2) these structures constrict in the presence of GTP (Sweitzer and Hinshaw, 1998, Sundborger et al., 2014) and (3) dynamin catalyzes scission upon GTP-hydrolysis, several scission models were forwarded. The following part describes two currents models (Antonny et al., 2016) that differ in the way how Dynamin uses the GTP-hydrolysis energy for scission: (I) the disassembly model and (II) the constriction model.

The first model, also known as the disassembly model, suggests two temporally distinct stages, first the assembly of the dynamin helix and second the subsequent disassembly upon GTP hydrolysis causing the separation of a bud form the membrane. In the primary assembly-stage, dynamin constricts the membrane at the neck (7 nm in diameter) and potentially stabilize it until the transition to the disassembly-stage, initiated by GTP hydrolysis (Antonny et al., 2016). Right after the hydrolysis of GTP to GDP+Pi, the neck is in a super-constricted state (3.7 nm in diameter) allowing the formation of a hemi-scission intermediate. This transition state requires the interaction of G-domains between adjacent rungs (Shnyrova et al., 2013). Finally, the release of Pi will loosen and disassemble the dynamin scaffold to complete the scission process due to viscoelastic stress of the membrane (Sundborger et al., 2014, Mattila et al., 2015). To achieve the transient hemi-scission stage, it is important that all dynamin dimers are in the same nucleotide state. This requires a high degree of synchronization and cooperativity.

However, a calculated Hill coefficient of about 2 led to the conclusion that the only cooperativity is between the GTPase domains of dynamins from adjacent rungs and not between the two monomers of a dynamin dimer (Tuma and Collins, 1994). In addition, to reach the hemi-scission intermediate, the dynamin assembly needs to be long enough in the super-constricted state. A second critical point of this model is the discrepancy between the disassembly kinetics of dynamin and the membrane fluidity. With a calculated viscoelastic time less than 10 ms (Camley and Brown, 2011) the dynamin disassembly, which can last up to a few hundred milliseconds and up to some seconds for complete disassembly (Cocucci et al., 2014), is too slow to apply any stress to the membrane to separate the bud. Rather, a flow of lipids is expected until viscoelastic equilibrium is reached (Antonny et al., 2016).
A solution to these discrepancies might come from the PH-domain. Besides the ability to bind to membranes, this domain harbors a short amphipathic loop that could assist the scission process by its insertion into the membrane (Ramachandran et al., 2009). Cryo-EM data suggest that in the super-constricted state one PH-domain per dynamin dimer is tilted, to push the loop into the membrane leaflet. This could apply mechanical forces to the membrane assisting the scission process (Sundborger et al., 2014).

In the second model (constriction model), GTP hydrolysis is rather used for mechanical work than for disassembly of the dynamin helix. Dynamin is likely to act as a molecular motor powered by several GTP hydrolysis cycles to slide adjacent dynamin rings relative to each other. This leads to the constriction and twisting of the helix causing the separation of CCB from membranes (scission). As structural data indicates, the BSE exists in an open conformation when GTP is present, which also causes trans-dimerization of adjacent G-domains, and in a closed conformation in the GDP+Pi transition state and the nucleotide free state. The movement between these two conformations will adopt the power stroke necessary for constriction (Chappie et al., 2011). In vivo it was shown that efficient scission occurs with at least 13 – 14 dynamin dimers, corresponding to one turn in the non-constricted state and one and a half turn in the super-constricted state (Cocucci et al., 2014). As the interaction of opposite G-domains is important to generate the movement to constrict the dynamin helix, the question arises if only a few interacting G-domains, 1 to 5 are possible with about 14 dynamin dimers, are able to generate a torque of about 1 nN.nm as measured in vitro to constrict the membrane for scission (Morlot et al., 2012, Antonny et al., 2016), which is 25 to 50 times larger than for other known torque generating proteins, like the recombinase A (Lipfert et al., 2010), or the F1-ATPase (Yasuda et al., 1998), 0.02 and 0.04 nN.nm respectively. A point contradictory to

the first model is the fact that the constriction force seems to be directly dependent on the concentration of GTP (Morlot et al., 2012), which is not consistent with the well-defined super-constricted state. Thus, to keep constriction unless the tube breaks spontaneously, GTP must be consumed, whereas the requisite and transient hemi-scission state of the first model is reached right after GTP hydrolysis (Mattila et al., 2015). Also, for this model, it is not clear how dynamin disassembles. Two possibilities are discussed: either disassembly is the consequence of scission, because the membrane template has disappeared, or the constriction stress causes the dynamin helix to fall apart. In both cases GTP hydrolysis is used for mechanical work (Antonny et al., 2016).

To get a more refined picture of the scission process, it is necessary to get a more completely understand how dynamin's GTPase cycle is coupled to scission. Two points are not considered in both models, first the influence of actin and second the functional role of dynamin interacting proteins. Actin together with the Arp2/3 complex and the nucleation factor N-WASP co-localizes with dynamin in a spatially and temporally manner (Merrifield et al., 2004), and in some cells dynamin seems to control actin polymerization at endocytic sites (Taylor et al., 2012). This, together with the fact that a reduced membrane tension causes a delay of scission in vivo (Morlot et al., 2012), and that actin is the main driver of membrane tension, suggests an important role of actin during scission by interacting directly with dynamins PRD-domain or indirectly over PRD-binding proteins. Investigations in yeast revealed actin to be critical for endocytosis (Palmer et al., 2015). Second, the exact role of dynamin binding partners needs to be elucidated. Many of these interactors comprise a BAR-domain in addition to the SH3-domian. While SH3-domains interact with the PRD-domain of dynamin, BAR-domains are able to sense or induce membrane curvature. It is assumed that these interactions recruit dynamin to the neck of CCBs, but it is not clear how or if these proteins are implicated in regulation of dynamins GTPase cycle, the temporal control of scission, or if they directly influence the scission.

1.2 Endocytosis

Endocytosis describes the cellular process in which extracellular material is internalized. Due to the diversity of these materials, organisms developed different pathways (Figure 1-6). Whereas large particles (≥ 0.5 µm) are internalized via processes called phagocytosis and macropinocytosis, several cargo specific pathways for the uptake of small molecules exist. Although their mechanisms are quite different, the main steps are common: (I) cargo recognition, (II) invagination of the plasma membrane, (III) generation of transport carriers, (IV) transport of these carriers to their target and (V) tethering and fusion with the target compartment. In contrast to cargo specific pathways, macropinocytosis mediates the rather unspecific uptake of fluids and therein dissolved molecules as well as of pathogens.

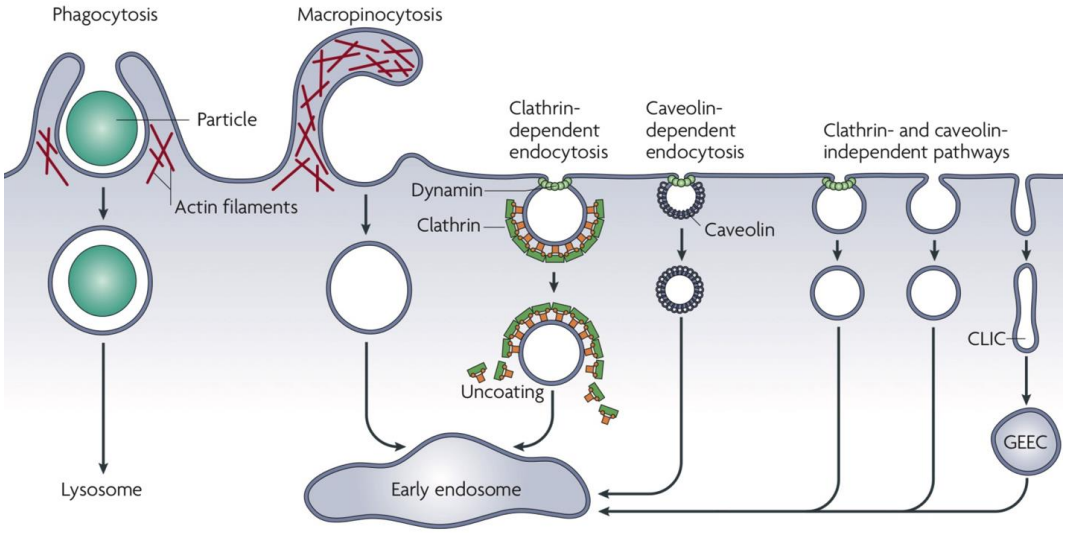

Figure 1-6 Overview of endocytic pathways. The uptake of large particles is mediated by phagocytosis (cell-eating), whereas large amounts of fluid is taken up by a process called micropinocytosis (cell-drinking). Both pathways are highly dependent on large-scale plasma membrane remodeling based on the polymerization of actin. Small molecules can be endocytosed by a subset of pathways. The most studied ones are clathrin- and caveolin-dependent. Other, less known pathways, are independent of the coat proteins clathrin or caveolin. Except for some clathrin- and caveolin-independent pathways, the large GTPase dynamin seems to be the common scission factor. After budding from the membrane, most cargos target via vesicular or tubular carriers directly to the early endosome or indirectly via the ´glycosyl phosphatidylinositol-anchored protein enriched early endosomal compartment´ (GEEC). CLIC: ´clathrin-independent carrier´. Picture taken and modified from (Mayor and Pagano, 2007).

The first described endocytic pathways, up to 135 years ago, were phagocytosis and macropinocytosis, also known as “cell-eating” and “cell-drinking”. Phagocytosis was first described almost 135 years ago, as Elie Metchnikoff studied the “relationship between phagocytes and anthrax” (Metschnikoff, 1884), a process which is nowadays known to be critical for the innate and adaptive immune system. Professional phagocytes take up pathogens via this pathway, thus contributing to the first response upon infections and playing a key role

in the adaptive immune system. Phagocytosis is also used by other cell types, like fibroblasts, epithelial cells or endothelial cells to ingest apoptotic cells. All these processes are mediated via several receptors directly recognizing pathogenic molecules (pattern-recognition receptors), indirectly via opsonic receptors or via specialized receptors recognizing apoptotic cells (Flannagan et al., 2012). A second pathway for the uptake of large particles like pathogens as well as soluble molecules is macropinocytosis, first observed over 80 years ago during the work on rat macrophages (Lewis, 1931). Lewis described this process as an inward folding of cell surface ruffles, which are fusing with the plasma membrane and forming large (0.5 – 5 µm) vacuoles called "macropinosome" (Hewlett et al., 1994). The formation of macropinosomes is stimulated as a response of growth factors like epidermal growth factor (EGF) or macrophage colony-stimulated factor 1 (M-CSF1) (Haigler et al., 1979, Racoosin and Swanson, 1989). In contrast, this process was observed to be constitutive in bone marrow-derived dendritic cells (Norbury et al., 1997). Beside pathogen entry and antigen presentation, macropinocytosis has also relevance in cell motility (Lim and Gleeson, 2011). Both endocytic pathways, phagocytosis and macropinocytosis, are highly dependent on actin polymerization and associated regulators, because actin-induced plasma membrane deformation and remodeling play a central role in these processes. Informative reviews for both endocytic pathways can be found elsewhere (Flannagan et al., 2012, Lim and Gleeson, 2011)

Small scale endocytic pathways, on the other hand, can be divided into clathrin-dependent and clathrin-independent endocytosis. Additionally, the clathrin-independent pathways can further be grouped into dynamin-dependent and -independent ones. The next two sections of this chapter will give an overview of these processes with a detailed view on the by far most studied endocytic pathway including its biogenesis: the clathrin- and dynamin-dependent endocytosis.

1.2.1 Clathrin independent endocytosis

The first endocytic process was the observation of plasma membrane derived vesicles with bristle-like structures at their surface. Later these bristle-like structures were identified as the scaffolding protein clathrin. Ongoing studies to this type of endocytosis revealed the large GTPase dynamin to be critical for the separation of such clathrin-coated vesicles from the plasma membrane. Another type of endocytosis, whose biogenesis is also dependent on dynamin, was already observed 10 years earlier in 1953 and described as little caves invaginate from the plasma membrane (Palade, 1953). However, it lasts 40 years until caveolin, a structural component of these 50 – 100 nm invaginations, was identified (Rothberg et al., 1992). Three types of these integral membrane proteins are known, the non-muscle caveolin-1 and caveolin-2 and the muscle-specific caveolin 3 (Rothberg et al., 1992, Scherer et al., 1996, Way

and Parton, 1995). A second essential coat component are members of the cavin protein family. Four cavin (cavin-1 – cavin-4) isoforms exist in mammalian cells, with cavin-4 as a muscle-specific isoform (Kovtun et al., 2015). Notably, caveolin-1 and cavin-1 seems to be the most important isoforms, as a depletion of them causes a loss of caveolae (Drab et al., 2001, Liu et al., 2008). The actual model of how such carriers are generated is as follows. Initially, cavins trimerizes and assemble into cytosolic oligomers with an average of 50 cavin monomers (Gambin et al., 2013). The trimerization of monomers and the subsequent oligomerization of these trimers is mediated by different domains, termed helical region (HR) 1 and 2 (Kovtun et al., 2014). Then, the cavin oligomers are recruited to the plasma membrane via interactions to the oligomeric caveolins at the plasma membrane and negatively charged lipids, resulting in bud formation (Kovtun et al., 2015). As can be seen on rapid-freeze deep-etch electron micrographs, the cavin oligomers assemble into a characteristic spiral-like coat (Anderson, 1998). Finally, the bud is separated from the plasma membrane through the large GTPase dynamin (Henley et al., 1998) and targeted to the early endosome. Although, caveolae endocytosis is the most investigated pathway among the clathrin-independent ones, its exact mechanism is not fully understood. In addition to the so-far mentioned proteins, Eps15 homology domain (EHD) protein 2 and the F-BAR-domain containing protein kinase C and casein kinase substrate in neurons protein 2 (pacsin2) play a certain role in the biogenesis of caveolae. EHD2 is a dynamin-like ATPase located mainly at the neck of caveolae buds (Ludwig et al., 2013), whose knockdown causes an increased budding of caveolae. This observation implicates EHD2 to be a negative regulator in caveolae biogenesis (Moren et al., 2012). However, the underlying mechanism is not known, but it is linked to the direct or indirect interaction of EHD2 with the actin filament (Stoeber et al., 2012). EHD2 interacts directly with another protein of the caveolae machinery, pacsin2. This protein is implicated in membrane sculpting via its F-BAR domain. In addition, pacsin2 interacts directly with dynamin and caveolin 1 to be regulated by or is regulating these proteins (Senju et al., 2011). Detailed information and further readings to caveolae endocytosis can be found elsewhere (Kovtun et al., 2014, Kovtun et al., 2015).

Besides the caveolae pathway, there are many other less investigated clathrin-independent endocytic pathways internalizing, in some case, a more specific set of cargos. Some of these pathways are also independent of dynamin and/or absent of any coat structure. Two examples for a dynamin-dependent pathway are the RhoA-dependent endocytosis (Lamaze et al., 2001) and the more recently identified fast endophilin mediated endocytosis (FEME) (Boucrot et al.,

2015). The first one does not have a yet identified coat, whereas the latter one generates endophilin coated carriers. Independent on dynamin are endocytic processes associated with Arf6 (Radhakrishna and Donaldson, 1997), flotillin (Glebov et al., 2006) and the uptake of lipid-anchored proteins like glycosylphosphatidylinositol anchored proteins (GPI-APs) via tubular clathrin-independent carriers (CLICs) targeting to a specialized compartment, the GPI-AP enriched early endosomal compartment (GEEC) (Kirkham et al., 2005). Therefore, this pathway is termed CLIC/GEEC-pathway. Informative reviews regarding the clathrin- and caveolin-independent endocytic pathways can be found elsewhere (Kirkham and Parton, 2005, Sandvig et al., 2011, Mayor et al., 2014).

As outlined, many dynamin-independent pathways exist, thus, the question arises of how endocytic carriers are separated from the plasma membrane in the absence of the large mechanochemical GTPase dynamin or a yet not identified component able to replace dynamin as the scission factor. Compared to the scission by dynamin, whose investigation is ongoing since several decades and still not fully understood, the underlying mechanisms of dynamin-independent scission is much less investigated but linked to actin polymerization (Mayor and Pagano, 2007). An example to this hypothesis describes a mechanism of how shiga toxin-induced tubular endocytic membrane invaginations undergo scission without dynamin through a cholesterol-dependent membrane reorganization triggered by actin polymerization. As a consequence of actin polymerization, membrane domains are forming as demonstrated in a liposomal system. In this model, scission is driven by domain boundary forces (Romer et al., 2010). Further investigations to the biogenesis of the different endocytic processes are necessary to figure out whether or not this mechanism can be generalized and if other pathway-specific or common factors are necessary.

1.2.2 Clathrin dependent endocytosis

Clathrin coated vesicles are established carriers within the endosomal system and in endocytosis. Together with the adaptor protein complexes AP-1, AP-2 and AP-3 it is the main component of this class of vesicles. Among the various locations of budding of clathrin coated vesicle, the formation of these carriers at the plasma membrane during endocytosis is best characterized. Here, AP-2 has a crucial role, as (i) it is the central hub within the clathrin endocytic interactome (Schmid and McMahon, 2007), (ii) the uptake of clathrin-dependent cargos (e.g. transferrin, epidermal growth factor or low-density lipoproteins) requires AP-2, and (iii) there is no evidence for clathrin coated structures at the plasma membrane without

AP-2 (Motley et al., 2003, Huang et al., 2004, Boucrot et al., 2010). Although, clathrin and AP-2 are mandatory for the formation of endocytic CCP, there is a set of proteins with specialized functions assisting vesicle biogenesis, a process which is canonically split into five steps (McMahon and Boucrot, 2011). It is initiated with nucleation, forming an 'initiation complex', followed by the selection of cargo and coat assembly to a matured clathrin coated bud. Finally, the bud is separated by dynamin. After the vesicle has formed and before it fuses with the acceptor compartment, the early endosome, the coat is shed off (Figure 1-7).

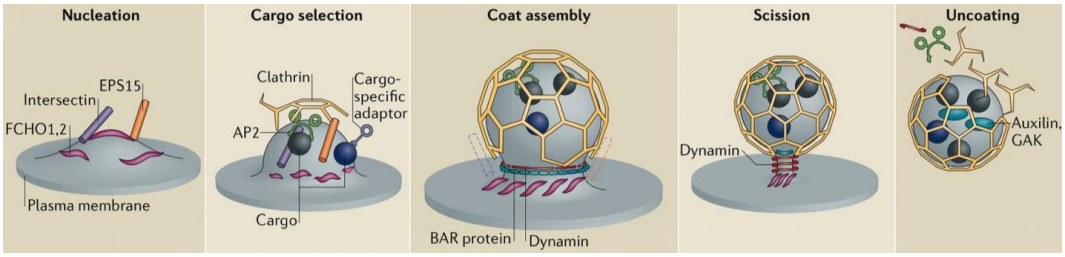

Figure 1-7 Individual steps in the formation of an endocytic clathrin coated vesicle. CCV biogenesis can be split up into five steps: nucleation, cargo selection, coat assembly, scission and uncoating. Nucleation sites define the starting point of CCV-biogenesis. Members of a so-called nucleation module are the BAR-containing FCHo proteins, intersectin and Eps15. Here, FCHo proteins bind specifically to and initially induce a shallow curvature to the plasma membrane, while intersectin and Eps15 cluster FCHo-proteins and also recruit AP-2 to initiation sites. However, a different model suggests that AP-2 and clathrin are the initiation factors and FCHo proteins are important to sustain growth. Upon arrival at the plasma membrane, AP-2 bind to cargos and also recruit further monomeric clathrin associated sorting proteins to the membrane. Both recruit clathrin to the membrane. During maturation, BAR-containing proteins are recruited to the growing edge of CCPs, most likely for regulatory purposes and for neck narrowing. Finally, these proteins recruit dynamin to separate the CCBs from the membrane. Prior fusion, the coat proteins are shed off with the help of Hsc70, auxilin/GAK and synaptojanin. The picture was taken and modified from (McMahon and Boucrot, 2011)

Recent studies suggest a putative 'nucleation module' to be the initial step in CCV formation. Thus, sites of CCV formation are not marked by AP-2 recruitment. This nucleation module is defined by the proteins FCHo 1/2, Eps15 and intersectin. The FCHo proteins bind specifically to the plasma membrane via its shallow curved F-BAR domains and sense and/or induce low curvature to the plasma membrane, which is important for CCP progression, as AP-2 and clathrin remain cytosolic when FCHo proteins are downregulated using RNAi (Henne et al., 2010, Stimpson et al., 2009). Two other proteins, Eps15 and intersectin, bind to and cluster FCHo proteins to define the site of nucleation and also interact directly with AP-2. Thus, they are bridging the nucleation step with the cargo selection step (Henne et al., 2010). Almost at the same time, a contradictory model was put forward, in which AP-2 and clathrin seem to be the initiation factors, whereas FCHo proteins are required to sustain growth (Cocucci et al., 2012). Thus, the exact mechanism of CCP initiation is not clear.

AP-2 together with other monomeric clathrin associated sorting proteins (CLASPs) bind to and recruit cargos to nucleation sides of CCV. CLASPs typically bind to lipids, to AP-2, and can also function as clathrin adaptors (Traub, 2009). Likewise, in yeast the FCHo-homologue Syp1 is implicated in cargo sorting (Reider et al., 2009). The mechanism of how AP-2 interacts with the membrane was investigated in detail (Jackson et al., 2010). As mentioned in a previous chapter, AP-2 binds specifically to $PI(4,5)P_2$ at the plasma membrane. AP-2 harbors a total of four binding sites for this lipid, one in each of the two large subunits α and β, and two within the μ-subunit. Both large subunits seem to have a key role in initial membrane binding, whereas the binding sites within the μ-subunit drive the rearrangement from a closed to an open conformation of the adaptor complex. In the open conformation all binding sites become coplanar, allowing the simultaneous binding to lipids and cargo (Jackson et al., 2010, Kelly et al., 2014). A further regulatory mechanism in cargo binding is phosphorylation. The μ-subunit of AP-2 can be phosphorylated at a threonine residue at position 156 by adaptor-associated kinase 1 (AAK1) (Conner and Schmid, 2002). This phosphorylation does lead not only to a stabilized open conformation but also to an increased affinity to YxxΦ-, but not dileucine-motifs (Olusanya et al., 2001, Ricotta et al., 2002, Honing et al., 2005). In addition, Crystallographic and biochemical studies identified a conformation-dependent mechanism for the interaction of AP-2 with clathrin (Kelly et al., 2014). In the closed cytosolic conformation of AP-2, clathrin binding sites are occupied by folding of the β-appendage domain back to the trunk domain via interactions with the C-terminus of AP-2μ. Only the membrane bound open conformation, when the β-appendage domain is released from the trunk, allows AP-2 to bind to clathrin. So far, no similar mechanisms were identified for other clathrin binding CLASPs. Although these CLASPs are able to recruit clathrin to plasma membranes, CCP were remarkably reduced in AP2-depleted cells (Motley et al., 2003). Thus, AP-2 seems to be a major hub in the protein interaction network during CCV maturation.

While sorting cargo to sites of CCV formation, also clathrin is recruited to assemble a lattice around the forming bud. Whether or not clathrin polymerization generates enough force to bend the plasma membrane and form a matured bud is not known. In vitro, AP-2 and clathrin are reported to be sufficient for bud formation when recruited to liposomes (Kelly et al., 2014). Alternatively, accessory proteins able to induce membrane curvature could bend the membrane at the rim of a growing bud, while the recruitment of clathrin would stabilize the curvature. Two proteins, shown to be displaced to the rim are Eps15 and epsin (Tebar et al., 1996, Saffarian et al., 2009). Epsins are a type of CLASPs interacting with AP-2, clathrin, Eps15 and sort ubiquitinated proteins into CCV (Chen et al., 1998, Rosenthal et al., 1999). Actually, there

are three identified epsin isoforms. Epsin-1 and 2 are expressed ubiquitously, however, they are enriched in the brain. Epsin-3 is closely related to the former ones, but seems to have a quite restricted expression pattern to wounded epithelia cells and the stomach (Spradling et al., 2001, Ko et al., 2010). The domain architecture of the epsin family members can be split into a N-terminal PI(4,5)P_2 binding domain, termed epsin N-terminal homology (ENTH) domain and a mostly unstructured C-terminal part which can be referred to as the protein-protein interaction platform (Sen et al., 2012). A related protein was identified as an AP-1 interacting protein at the TGN, epsinR. Although, epsinR possess a similar domain architecture including an ENTH-domain interacting with PI4P, it relocalizes into the cytosol upon brefeldin A treatment, indicating an Arf-dependent recruitment (Hirst et al., 2003). The important feature of epsin-1 to 3, necessary for the progression of CCP to a matured CCB, is the membrane bending activity of the ENTH-domain. This membrane bending activity is caused by an additional α-helix, which becomes structured and inserted into the inner leaflet like a wedge upon membrane binding (Ford et al., 2002). At the rim of a CCP, epsin could induce the curvature necessary for bud formation, while Eps15 recruits further AP-2 complexes. When recruited, clathrin stabilizes the curvature and pushes Eps15 and epsin further towards the rim. Additional proteins able to sense and/or induce curvature, like BAR-containing proteins, assist CCP progression to form a spherical CCB (McMahon and Boucrot, 2011, Daumke et al., 2014). BAR-containing proteins implicated in curvature progression are amphiphysin, endophilin and sorting nexin 9 (SNX9), all of which are known to interact with the scission factor dynamin (Dawson et al., 2006). Furthermore, synergy between dynamin and BAR-containing proteins seems to facilitate scission (Meinecke et al., 2013), the last step in CCV formation. The exact mechanism of how dynamin separates CCV form the membrane is still unclear. Putative models are outlined in chapter 1.1.3.3. In contrast to the common view in the endocytosis field, epsin was also suggested to mediate CCV release even when dynamin was absent (Boucrot et al., 2012). The predicted mechanism, in which insertion of the N-terminal α-helix generates mechanical forces at the neck of a CCB that finally lead to fusion of the membranes adjacent in the neck and thus to the release of a vesicle, is similar to those described for Arf1 and Sar1 in the early secretory pathway.

Finally, the vesicle coat is shed off by the chaperone heat shock cognate 70 (Hsc70) that, in conjugation with its cofactor auxilin, destabilizes the clathrin coat (Schlossman et al., 1984, Ahle and Ungewickell, 1990, Prasad et al., 1993). In addition, the endophilin-recruited phosphatase synaptojanin degrades PI(4,5)P_2, which leads to the release of phosphoinositide-based membrane associated proteins like AP-2 or epsin (Milosevic et al., 2011, Sousa and

Lafer, 2015). After disassembly, released coat components can be used for a next round of CCV biogenesis.

1.3 Objective

As has been mentioned earlier, Dynamin has a pivotal role in the scission of a CCB. Dynamin itself is a large GTPase. Actually, three isoforms are known which are expressed more or less tissue specific. It is thought that Dynamin has to catalyze GTP hydrolysis, which leads to a conformational change and finally separates the CCV from the plasma membrane (see section 1.1.3.3). However, recent studies pointed out that Dynamin may not be the direct or exclusive scission factor for CCV. Rather, insertion of the N-terminal amphipathic helix of epsin, the ENTH-domain, into membranes was shown to induce scission in the absence of Dynamin (Boucrot et al. 2012).

The classical adaptors in CCV biogenesis are the adaptor protein complexes (AP-complexes). So far, five of these tetrameric complexes are described. Three of them (AP-1, AP-2 and AP-4) are recruited in an Arf-dependent manner to their donor membrane, whereas the endocytic adaptor complex AP-2 is recruited to the plasma membrane independent of Arf. Rather, AP-2 harbors binding sites for phosphatidylinositol-(4,5)-bisphosphate to be recruited to the plasma membrane. In AP1-, AP3- and AP4-dependent formation of CCVs, Arf is likely to play a distinct role in the mechanism of vesicle scission via its myristoylated amphipathic helix, as has been shown for Arf´s role in COPI vesicle scission. In case of AP-2 no Arf is present (or it is actually not known), but it has been shown that epsin that like Arfs contains an amphipathic helix is an important accessory protein involved in the biogenesis of endocytic clathrin coated vesicles (Kalthoff et al. 2002). Thus, the exact mechanism of CCV scission is still under debate.

In vitro reconstitution experiments are powerful tools to dissect biological processes in detail. To date, only CCV reconstitution studies were carried out using, besides some purified components, the whole cytosol or component-depleted cytosol for generating CCV in vitro. Moreover, formation of endocytic CCVs was also described to occur in the presence of the non-hydrolysable nucleotide GTPγS (Miwako et al. 2003).

Therefore, to investigate which factors are required to generate and separate a CCV after a CCB has formed and to answer the question of a general scission mechanism among vesicle types (COPI-, COPII- and clathrin-coated), I will establish an in vitro reconstitution system with chemically defined components to mechanistically dissect steps in CCV biogenesis.

2 Results

In this thesis, I want to investigate in detail how an endocytic clathrin coated vesicle is separated from the plasma membrane after a clathrin coated bud has formed. To get detailed insight into the mechanisms underlying this process, recombinant proteins were used in a defined system to reconstitute receptor mediated endocytosis. First, the recombinant expression and purification of the protein components needed for this study were established in our laboratory. Besides *E. coli* expression systems, a baculoviral expression system (Berger et al., 2004, Stowell et al., 1999) was employed. All Proteins were tested for functionality and finally used for reconstitution experiments. The following sections will describe all steps in detail.

2.1 Cloning Strategies

For the recombinant expression of the components, the cDNAs for AP-2, clathrin, dynamin-1 and 2 as well as mutants of these proteins were cloned into a baculovirus expression system (Berger et al., 2004). Epsin-1 and its truncated version ΔENTH-epsin-1 were expressed in a *E. coli* expression system. Except the human cDNA for dynamin-1 all proteins were from rat.

2.1.1 AP-2

During receptor mediated endocytosis, the clathrin coat is recruited to the membrane via several adaptors. The main adaptor in this process is the tetrameric adaptor protein 2 complex. Its four subunits (α, β, μ and σ) were cloned into the pFBDM vector, suitable for insect cell expression of multi subunit complexes. For purification purposes, the AP-2α subunit was tagged with a N-terminal OST-tag. The pFBDM vector harbors two independent expression sites, one site is under the control of the polyhedrin-promotor and the second site under the control of the p10-promotor. Two or more of these vectors can be combined by cutting out the expression cassette (PmeI and AvrII) and ligating this cassette into the multiplication-module (open with SpeI and NruI) of another pFBDM vector. The product of these steps is a pFBDM vector with four expression sites. Another round of combination will yield six expression sites and so on. Using this system, all subunits can be expressed in insect cells within one virus.

First, the α-subunit together with the σ-subunit and the β-subunit together with the μ-subunit were cloned into two individual pFBDM plasmids and both vectors were combined afterwards as described above (Figure 2-1 A). Finally, the genes were inserted into the bacmid via Tn7 transposition. Two mutants of the μ-subunit were generated (T156D and T156E) mimicking a

phosphorylated amino acid residue. The mutated µ-subunit was combined with the other three subunits as described.

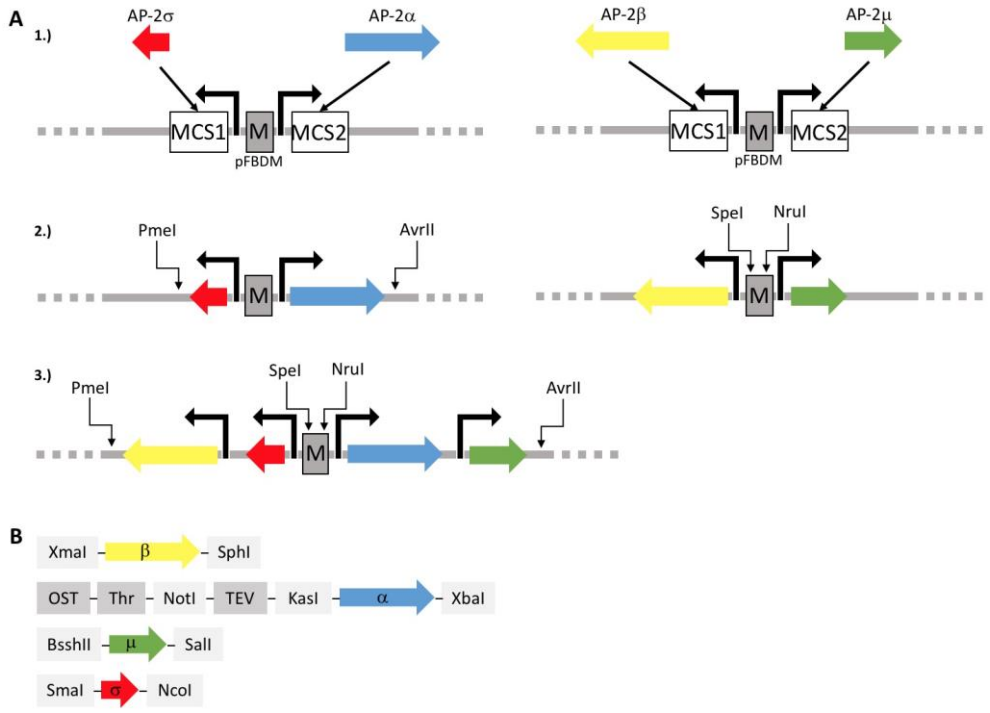

Figure 2-1 Cloning strategy for the expression of AP-2 in Sf9 cells. (A) The subunits σ and α or the subunits β and µ were cloned into two individual pFBDM plasmids as indicated in (B) before both were combined, resulting in a single plasmid harboring all four subunits of the AP-2 complex. The pFBDM plasmid was incorporated into the baculoviral genome via Tn7 transposition in *E. coli* DH10MultiBac^{Cre}. Recognition sites for restriction endonucleases are indicated in light grey. OST, One-Strep-Tag (WSHPQFEKGGGSGGGSGGGSWSHPQFEK); Thr, Thrombin cleavage site; TEV, Tobacco Etch Virus cleavage site; M, multiplication-module; MCS, multiple cloning site.

2.1.2 Epsin-1

Epsin-1, a monomeric clathrin adaptor that sorts ubiquitinated cargo into endocytic vesicles, was cloned as a C-terminal GST-fusion protein and its truncated version ΔENTH-epsin-1 (amino acid 144-575) as a N-terminal His-fusion protein, both in pET29a (Figure 2-2).

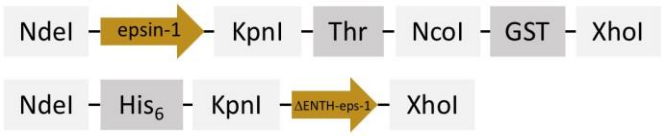

Figure 2-2 Cloning strategy for the expression of epsin-1 in *E. coli*. Both constructs were expressed with the help of the bacterial expression vector pET29a. In case of full length epsin-1, a GST-tag was cloned into the plasmid before epsin-1 was inserted. Recognition sites for restriction endonucleases are indicated in light grey. GST, Glutathione S-transferase-tag; His_6, Hexahistidine-tag.

2.1.3 Clathrin

The two subunits of the scaffolding protein clathrin, the heavy chain (HC) and the light chain (CLC), build up a trimer of dimers called triskelion. Initially, both subunits were cloned into one pFBDM plasmid. However, this construct yields a stoichiometry of about 19 CLC for 1 CHC, rather than a stoichiometry of 1:1. To improve the expression level of the CHC, two copies of the CHC cDNA were cloned into the pUCDM plasmid (Figure 2-3). The overall structure of this plasmid is similar to that of the pFBDM plasmid, however the incorporation into the bacmid for virus production is mediated via *cre-lox* site-specific recombination. Several restriction sites within the cDNA of CHC made it impossible, without mutagenesis, to combine two pFBDM plasmids, as it was done for the AP-2 complex. Genes within both vectors can be incorporated into one bacmid, the pFBDM vector via transposon elements, and the pUCDM vector via recombination. This will increase the mRNA level and therefore could improve the expression of the clathrin heavy chain.

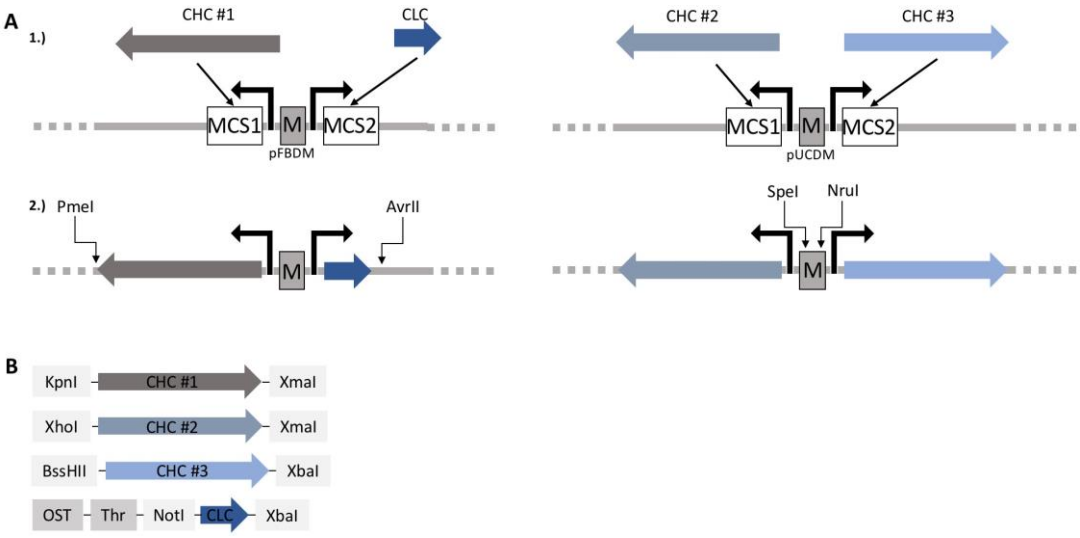

Figure 2-3 Cloning strategy for the expression of clathrin in Sf9 cells. (A) Three cDNA copies of the CHC and one of the CLC were cloned as indicated (B) into the pFBDM (CHC/CLC) and the pUCDM plasmid (2x CHC). First, the two CHC copies from the pUCDM vector were inserted into the baculoviral genome via recombination in *E. coli* DH10MultiBac^{Cre}. Bacteria were screened for the correct incorporation via chloramphenicol resistance and colony PCR and used in a second step to incorporate the cDNAs on the pFBDM plasmid into the bacmid via transposition. Recognition sites for restriction endonucleases are indicated in light grey.

2.1.4 Dynamin

The last step of endocytosis, the scission of a newly formed bud, is described to be mediated by the scissase dynamin. For this study, dynamin isoforms 1 and 2 were cloned as N-terminal OST-fusion proteins into a modified version of the pFBDM plasmid. This plasmid was modified such, that one multiple cloning site (MCS) was eliminated and only the site controlled by the polyhedrin promotor was left (Figure 2-4). For mechanistic studies to the role of dynamin in the scission process a mutant of dynamin-2 (K44A) was generated that cannot bind GTP (Marks et al., 2001).

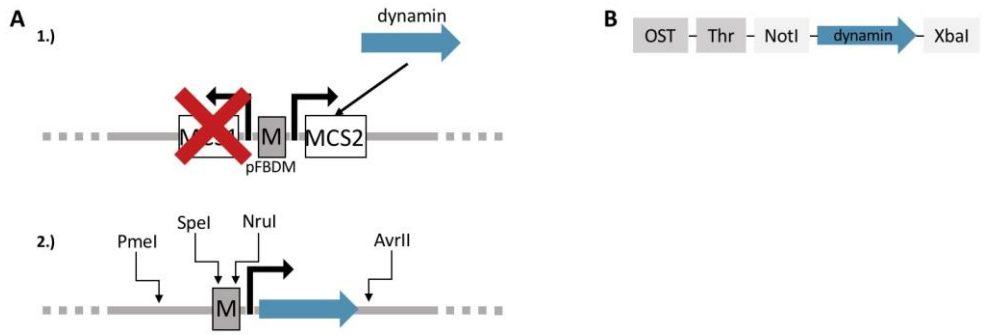

Figure 2-4 Cloning strategy for the expression of dynamin in Sf9 cells. The MCS1 including the termination region was first eliminated and only the MCS controlled by the polyhedrin promotor was left (A). Then, the cDNAs of dynamin-1, dynamin-2 and the dynamin-2 mutant were inserted into the plasmid as indicated in B. Recognition sites for restriction endonucleases are indicated in light grey.

2.1.5 AAK1

Biogenesis of endocytic vesicles is, like all other vesicle types, tightly regulated. One of these regulation mechanisms is phosphorylation. Phosphorylation of the µ-subunit of AP-2 plays a crucial role in the uptake of cargo into the cell (Olusanya et al., 2001). Later on, the corresponding kinase, that was co-purified with AP-2, was identified and named adaptor associated kinase 1 (AAK1) (Conner and Schmid, 2002). The kinase was cloned as a C-terminal OST-fusion protein in the same plasmid that was used for dynamin and its mutants (Figure 2-5).

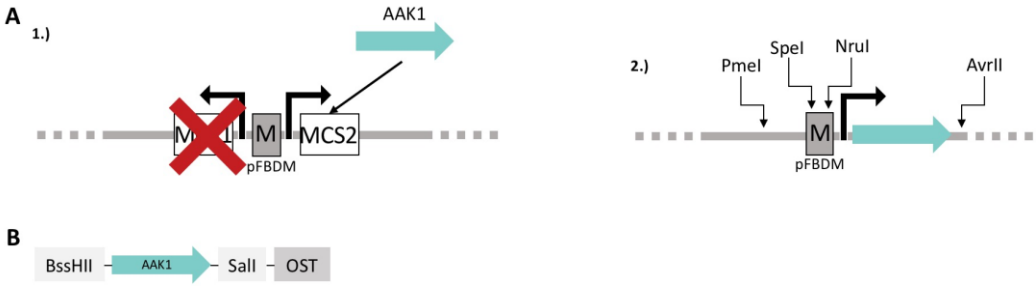

Figure 2-5 Cloning strategy for the expression of AAK1 in Sf9 cells. (A) AAK1 was cloned into the same plasmid as it was used for the dynamin cloning strategy. The kinase was inserted into the plasmid as indicated in (B). Recognition sites for restriction endonucleases are indicated in light grey.

2.2 Expression and Purification

For insect cell expression, the pFBDM constructs were transformed into *E. coli* DH10MultiBac^{Cre} via electroporation and subjected to blue-white screening, in which white colonies indicate a successful incorporation of the constructs into the baculoviral genome. In case of clathrin, two copies of the CHC gene harbored in the pUCDM vector were first transformed into *E. coli* DH10MultiBac^{Cre} and screened for a successful incorporation (recombination) via chloramphenicol resistance and colony-PCR, using primers annealing on the CHC gene and the baculoviral genome. An amplified product can only be observed when the CHC genes were incorporated into the baculoviral genome via recombination. The third copy of the CHC gene and the single copy of the CLC gene, both harbored on the pFBDM vector, were incorporated into chloramphenicol resistant *E. coli* DH10MultiBac^{Cre}-2xCHC and screened for correct incorporation into the baculoviral genome by blue-white screening. Sf9 cells were transfected with the isolated bacmid DNA to amplify baculoviruses used for expression of the components needed to reconstitute receptor mediated endocytosis (Berger et al., 2004).

Epsin-1 and its ΔENTH-truncated version were expressed in *E. coli* BL21pLysS at 37 °C either overnight using an auto-induction medium or for 4 hours after induction with 1 mM IPTG in LB-medium (induction at OD_{600}: 0.6) (Figure 2-6).

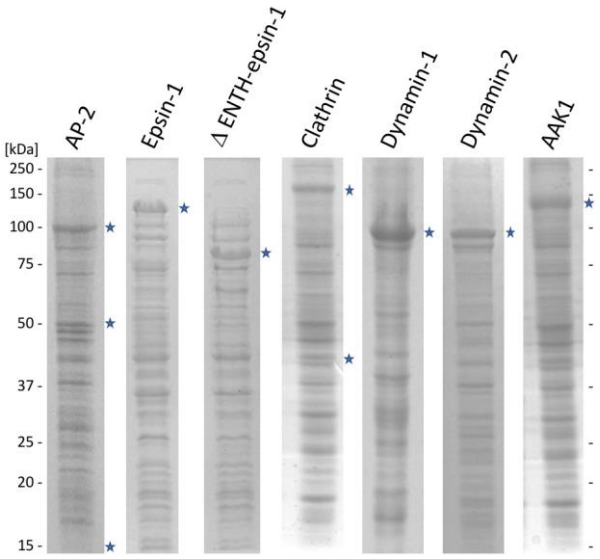

Figure 2-6 SDS-gel of whole cell lysates form the expressions of endocytic proteins. Except the bacterial expression of epsin-1, all proteins were expressed in Sf9 cells. Expressed proteins within the coomassie stained gel are marked (★).

The endocytic proteins dynamin-1 and 2, AP-2, clathrin and AAK1, as well as their mutants were purified with Strep-Tactin sepharose and in case of AP-2 further subjected to gel filtration to get rid of any co-purified endogenous clathrin. Here, soluble aggregates appear in the void at a retention volume of about 48.2 ml, the second peak at a retention volume of about 61.1 ml corresponds to the AP-2 complex. Comparing with standard proteins, the calculated mass of the complex is 291 kDa, which is close to the molecular mass of 281 kDa calculated from the primary structure (Figure 2-7).

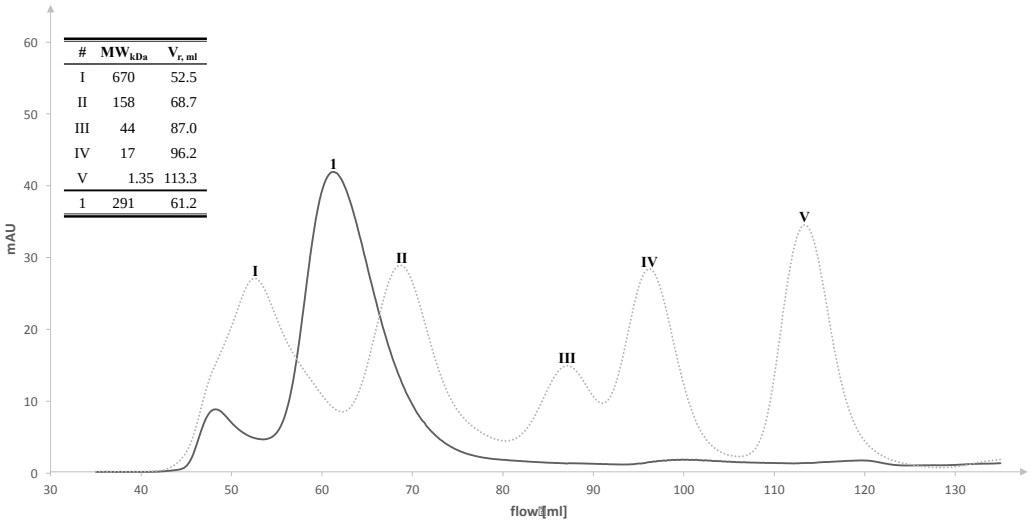

#	MW_{kDa}	$V_{r, ml}$
I	670	52.5
II	158	68.7
III	44	87.0
IV	17	96.2
V	1.35	113.3
1	291	61.2

Figure 2-7 Gel filtration of AP-2 on a Superdex 200 pg column. Affinity purified AP-2 contains endogenous clathrin as a co-purifying contamination. Therefore, the proteins were separated using a HiLoad 16/600 column filled with Superdex 200 prep grade. Roman numerals indicate standard proteins (·····) (Bio-Rad Laboratories GmbH, Munich). The table inside the graph lists the retention volumes ($V_{r, ml}$) with the corresponding molecular masses (MW_{kDa}) for the marked peaks.

Epsin-1 was initially purified via glutathione sepharose. After elution, the 25 kDa GST-tag was cleaved by incubating with thrombin at an activity of 10 U/mg-epsin overnight at 4 °C, and subsequently separated by gel filtration. Soluable aggregates appear in the void at about 48 ml. The cleaved GST-tag elutes from the column after 86.7 ml (≈ 44 kDa) as a dimer (50 kDa). Epsin-1 without the tag elutes at a retention volume of 64.7 ml (Figure 2-8). Although epsin-1 is a 60 kDa protein and its predominant cytocolic form is monomeric, it behaves like a 245 kDa protein, which is caused by its flexible carboxyterminal part with litte or no conventional secondary structures (Kalthoff et al., 2002).

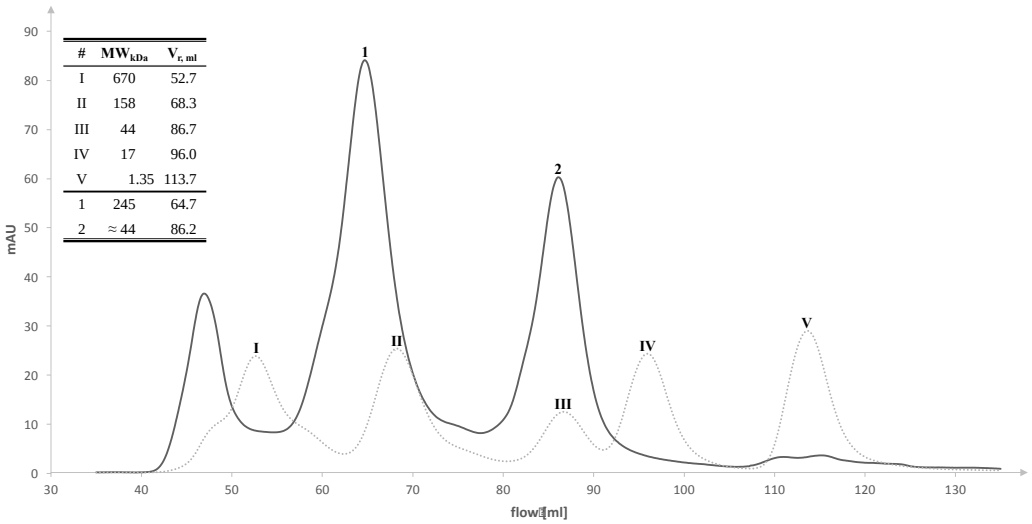

Figure 2-8 Gel filtration of epsin-1 pre-incubated with Thrombin on a Superdex 200 pg column. Affinity purified epsin-1 was incubated with thrombin (10 U/mg-epsin) over night at 4 °C to cleave the GST-tag and the products were subsequently subjected to gel filtration- Roman numerals indicate standard proteins (·····) (Bio-Rad Laboratories GmbH, Munich). The table inside the graph lists the retention volumes ($V_{r, ml}$) with the corresponding molecular masses (MW_{kDa}) for the marked peaks.

Frozen bacterial pellets of the expression of ENTH-domain truncated epsin-1 were resuspended and homogenized in the presence of 25 mM imidazole. The clarified homogenate was incubated for two hours with 3 ml (1 column volume, (CV)) nickel sepharose, washed with 3 CV of 25 mM imidazole and eluted stepwise with 3 CV of increasing concentrations of imidazole (Figure 2-9). For the reconstitution experiments the 100 mM imidazole fraction was subjected to a desalting column (PD-10 Desalting Column) for the exchange of the purification buffer with storage buffer.

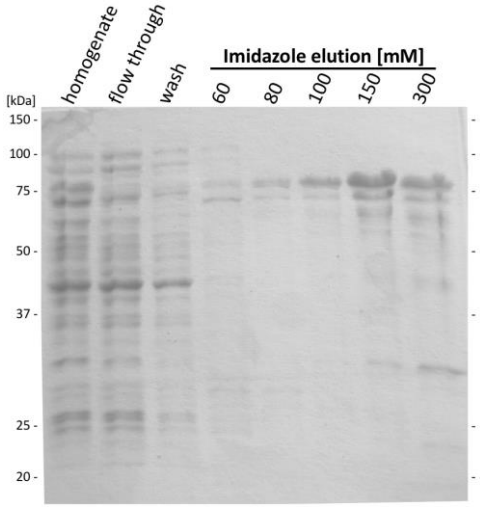

Figure 2-9 Imidazole elution pattern of ΔENTH-epsin-1 analyzed by SDS-gel electrophoresis. Frozen bacterial pellets, expressed the ENTH-truncated version of epsin-1, were homogenized in the presence of 25 mM imidazole. The clarified homogenate was then incubated with nickel sepharose, washed with 3 CV of 25 mM imidazole and eluted stepwise with increasing concentrations of imidazole. The 100 mM imidazole fraction was subjected to a desalting column for the removal of imidazole. Aliquots were flash frozen in liquid nitrogen and stored at -80 °C. The gel was stained with Coomassie

The coomassie stained gel in Figure 2-10 shows representative samples of all purified proteins. Staining intensity of the two complexes, AP-2 and clathrin is in line with the expected 1:1 stoichiometry of their subunits. Similar to gel filtration, epsin-1 and its ENTH-domain truncated version migrate in a SDS-gel like much bigger proteins.

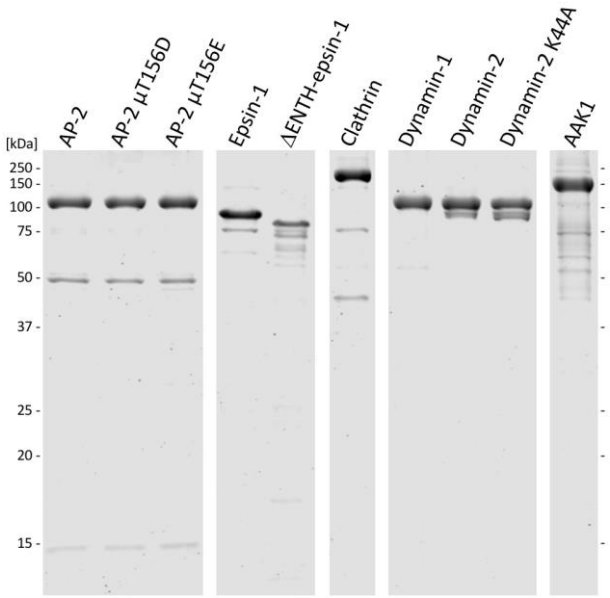

Figure 2-10 SDS-gel of purified endocytic proteins. 0.5 µg of all purified proteins was loaded on a 10 % SDS-gel and stained with colloidal coomassie after separation.

2.3 Functional characterization

Before reconstitution experiments could be performed, it was of course necessary to test all proteins with regard to their membrane binding, protein-protein interaction and enzymatic activity as it is described in the literature. Membrane binding and protein-protein interactions were tested using liposomes as donor membranes. Proteins bound to membranes were separated by sucrose gradient centrifugation and subsequently analyzed via immunoblotting. The enzymatic activity of AAK1 to phosphorylate the µ-subunit of AP-2 was tested via immunoblotting using antibodies raised against phosphorylated amino acid residues. To determine the nucleotide state of the large GTPase dynamin and its ability to hydrolyze GTP to GDP a HPLC-based approach was applied.

2.3.1 Clathrin adaptors need structural motifs to bind to membranes

AP-2 is initially recruited to membranes via phosphatidylinositol 4,5-bisphosphate ($PI(4,5)P_2$) and are subsequently stabilized via binding to a cargo signal motif and further $PI(4,5)P_2$ binding sites. The last step goes along with a conformational change and is favored, besides the binding to a cargo, by phosphorylation of the AP-2µ subunit at threonine 156, mediated by the AAK1

kinase (Collins et al., 2002, Conner and Schmid, 2002, Honing et al., 2005, Kelly et al., 2014, Ricotta et al., 2002). Also, epsin-1 binds PI(4,5)P_2-dependent to the inner leaflet of plasma membrane via its N-terminal ENTH-domain. The interaction with the plasma membrane enriched lipid PI(4,5)P_2 induces the formation of an additional helix, referred to as "helix zero" (H0), which inserts into the inner leaflet, thus causing an asymmetry that results in membrane curvature (Ford et al., 2002). Liposomes used for the characterization as well as for the first reconstitution experiments were made from a Brain Polar Lipid Extract (BPLE, Avanti Polar Lipids Inc., Alabaster, US), used by Dannhauser and Ungewickell (2012) for their reconstitution experiments. This extract was supplemented with PI(4,5)P_2 and a lipopeptide containing a sequence YxxΦ of the cargo signal from the *trans*-Golgi network integral membrane protein TGN38, the AP-2µ subunit binds to. For this purpose, a peptide of 15 amino acids including the cargo-signal at its C-terminal end (Figure 2-11), was linked to a maleimide-functionalized lipid.

```
        10         20         30         40         50         60
MQFLVALLLL SVAVARALPS ASKPNNTSSE NNPPIQPSTP LPPGVDISQQ VKTNRPTDQR

        70         80         90        100        110        120
LESDKEGQDK TVARTSASVS SGVESATNLN LDDSKKHPET ADAKLKETLQ QLLPVDPKQE

       130        140        150        160        170        180
KSGQKFTKDS GSPTGGDSDN TTGGDSNKTT GVDSDKTSGG DSNKPTGSDN DKPTGGDSNK

       190        200        210        220        230        240
PTSKVPSNTE TPKIDKVQLT EKGQKPTLIS KTESGEKLAG DSDFSLKPEK GDKSSEPTED

       250        260        270        280        290        300
VETKEIEEGD TEPEEGSPLE EENEKVLGPS SSENQEGTLT DSMKDEKDDH YKDNSGNTSA

       310        320        330        340        350
ESSHFFAYLV TAAVLVAVLY IAYHNKRKII AFALEGKRSK VTRRPKASDY QRLNLKL
```

Figure 2-11 Amino acid sequence of TGN38 from rat. Underlined in blue is the cytoplasmic part of TGN38 and in red the peptide that was linked to a maleimide group containing lipid (MPB-PE (16:0), Avanti Polar Lipids Inc., Alabaster, US). The peptide was synthesized with a N-terminal cysteine. At its C-terminus the peptide harbors the sorting signal (YQRL) which is recognized by the cargo binding motif YxxΦ of AP-2.

To test the dependencies on PI(4,5)P_2 and/or a cargo-motif of adaptors for the binding to membranes, 0.5 µM of AP-2, epsin-1 or ΔENTH-epsin-1 were incubated (15 min at 37 °C) with 25 µg liposomes derived from a brain polar lipid extract. For the binding studies with epsin-1 and AP-2, the liposomes were supplemented with 5 % (w/w) PI(4,5)P_2 and/or 5 % (w/w) TGN38-lipopeptide and in case of ΔENTH-epsin-1 with or without 5 % (w/w) of a nickel chelating lipid. Bound material was subsequently separated via sucrose gradient centrifugation and analyzed by immunoblotting.

In the absence of any endocytic signal, AP-2 and epsin-1 did not bind to membranes (Figure 2-12 lane 9 & 13). Efficient epsin-1 recruitment could only be observed when PI(4,5)P_2 was present (Figure 2-12lane 14) and in case of AP-2 the presence of both signals, PI(4,5)P_2 and TGN38-lipopeptide are needed, for efficient recruitment to membranes (Figure 2-12, compare lanes 10, 11 & 12). ΔENTH-epsin-1 bound specifically to liposomes through interaction of its C-terminal polyhistidine tag to the nickel chelating lipid (Figure 2-12, compare lanes 15 & 16).

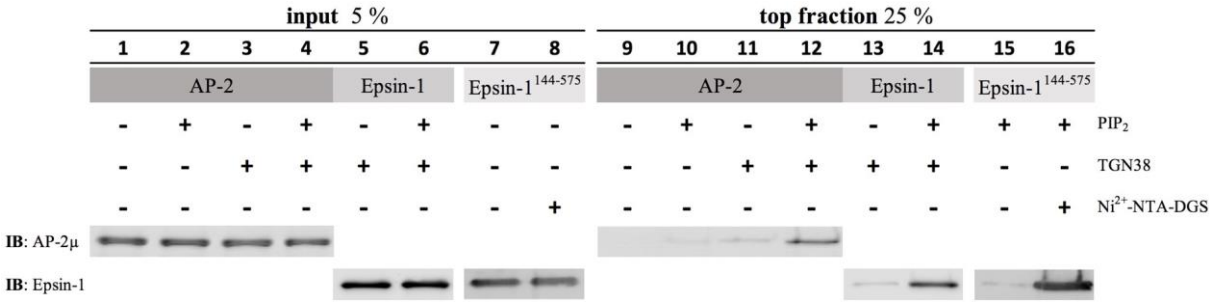

Figure 2-12 Signal dependent membrane binding of AP-2 and epsin-1. 0.5 µM clathrin adaptor (AP-2, epsin-1 or ΔENTH-epsin-1) was incubated with 25 µg liposomes derived from a brain polar lipid extract (BPLE). For AP-2 and epsin-1 the extract was supplemented with 5 % (w/w) PIP_2 and/or TGN38-lipopeptide and in case of ΔENTH-epsin-1 with 5 % (w/w) of a nickel chelating lipid. After incubation at 37 °C for 15 minutes the bound material was subsequently separated via sucrose gradient centrifugation. The top fraction was analyzed by immunoblotting for the presence of clathrin adaptors. Epsin-$1^{144-575}$ = ENTH-domain replaced by a His_6-tag.

Further titration experiments were carried out to determine the saturation concentrations for the liposome-bound adaptors. To this end, liposomes (0.5 mg/ml) were incubated with different amounts of adaptor and pelleted at 16000 g for 10 min, the pellet was washed twice with buffer. Liposome bound adaptor were quantified via western blot analysis. For AP-2 and epsin-1 the binding saturation is reached at assay concentrations of about 0.7 µM and 1 µM, respectively. The saturation for bound ΔENTH-epsin-1 is above 1.8 µM (Figure 2-13).

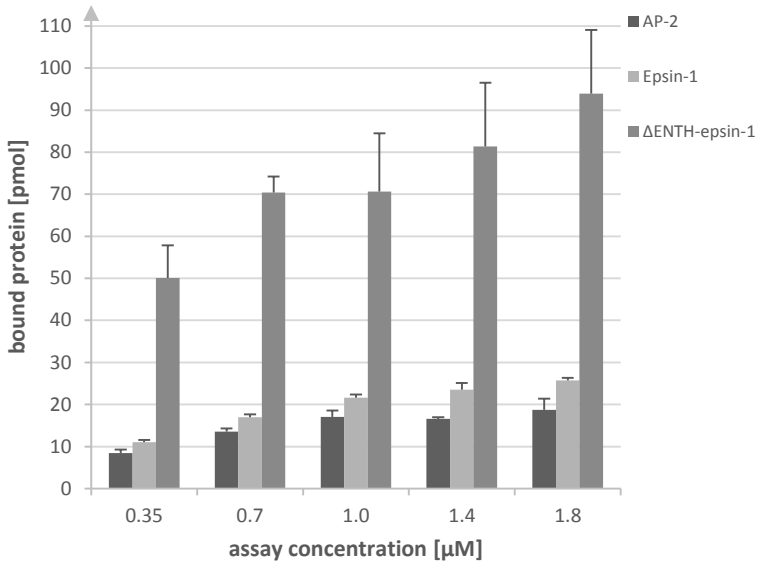

Figure 2-13 Titration of AP-2 and epsin-1 to liposomes. AP-2, epsin-1 or ΔENTH-epsin-1 were incubated at different amounts with liposomes for 15 min at 37 °C. Liposomes were supplemented with 5 % (w/w) PI(4,5)P_2/TGN38-lipopeptide for the recruitment of AP-2 and full length epsin-1 and in case of ΔENTH-epsin-1 with 5 % (w/w) of a nickel chelating lipid. After incubation, the liposomes were pelleted at 16 000 g for 10 min, washed twice with buffer and analyzed for AP-2, epsin-1 or ΔENTH-epsin-1 by western blot. The amount of bound proteins was quantified using the Li-COR Image Studio™ software.

2.3.2 AP-2 is not sufficient for budding

As shown the previous section, all clathrin adaptors used in this study are able to bind to membranes in a signal dependent manner, as prerequisite for the recruitment of clathrin to membranes, leading to the formation of clathrin coated buds at sites of endocytosis. In order to reconstitute the process, 1 µM of the clathrin adaptors were incubated either individually or simultaneously in the presence of BPLE-derived liposomes (0.5 mg/ml) and clathrin (0.4 µM) for 15 minutes at 37 °C. Bound material was separated by sucrose gradient centrifugation and analyzed via immunoblotting. Again, AP-2 and epsin-1 bound cargo signal- and/or PI(4,5)P_2-dependent to liposomes to a similar extend, with comparable amounts of bound clathrin (Figure 2-14, lane 3 & 4, respectively). However, when both clathrin adaptors were incubated simultaneously, the amount of each bound protein increased two- to threefold (Figure 2-14, lane 5). Without any of the required recruitment signals (Figure 2-14, lane 1 & 2) or when incubating clathrin alone with the liposomes (Figure 2-14, lane 6), almost no bound protein was detectable.

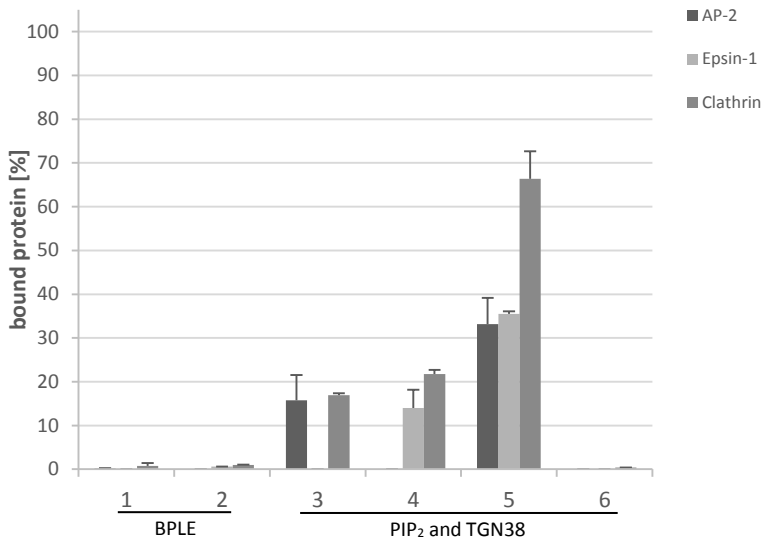

Figure 2-14 Clathrin recruitment to liposomes by AP-2 and epsin-1. Both adaptors (1 µM) were incubated either individually (AP-2: **1** & **3**, epsin-1: **2** & **4**) or simultaneously (**5**) in the presence of liposomes and clathrin for 15 min at 37 °C. In condition (**6**), clathrin alone was incubated with liposomes. The bound material was subsequently separated from the reaction by sucrose gradient centrifugation and analyzed via immunoblotting for bound proteins. BPLE-liposomes were supplemented with 5 % (w/w) PIP_2 and TGN38-lipopeptide (conditions 3 – 6) or not (condition 1 and 2). The amount of proteins recruited to liposomes was quantified using the Li-COR Image Studio™ software.

Aliquots of samples from the conditions above were pelleted for Epon-embedding to analyze ultra-thin sections by electron microscopy for the presence of clathrin coated buds. Using AP-2 alone did not result in budding (Figure 2-15 A), rather it seems that clathrin structures, probably clathrin cages, are recruited to the membranes due to interaction with AP-2. Invaginated structures, coated with clathrin, could only be observed when AP-2 was replaced by epsin-1 (Figure 2-15 B) or in addition of epsin-1 (Figure 2-15 C).

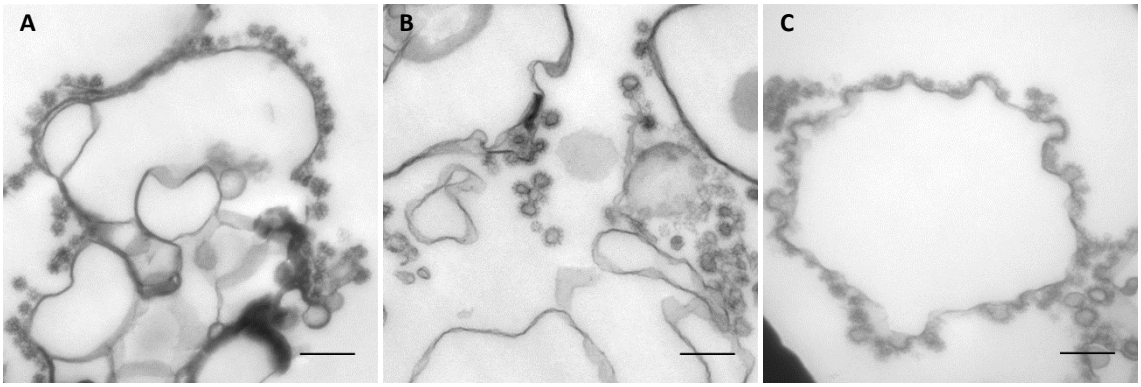

Figure 2-15 Formation of clathrin coated buds using AP-2 or epsin-1. Both adaptors were incubated either individually (**A**: AP-2 and **B**: epsin-1) or simultaneously (**C**) in the presence of liposomes and clathrin for 15 min at 37 °C. The donor membranes were pelleted for Epon-embedding to analyze ultra-thin sections by electron microscopy. Scale bar, 250 nm.

2.3.3 Assembly-dependent GTP hydrolysis

For vesicle formation experiments carried out with dynamin, it is important to check the nucleotide state of the protein in order to allow interpretation of the results, specifically when incubating with a non-hydrolysable GTP analog (GTPγS, GMPPNP) or GDP. For this experiments dynamin must be free of GTP in the first place.

The amount of bound nucleotide was checked using reversed phase chromatography on a HPLC system. Before loading onto the column, 150 µl (15 - 20 µM) of each dynamin isoform and GDP loaded Arf1, as a control, were heated up to 95 °C for 1 min, then precipitated material was pellet by centrifugation. Standard GDP and GTP (10 nmol each) eluted after 4.7 minutes and 6 minutes. Arf1, as a control, showed the expected signal for GDP, whereas the chromatogram for dynamin-1 and dynamin-2 did not show any signal for GDP or GTP. These data were confirmed by mass spectrometry.

To analyze if recombinant dynamin is able to hydrolyze GTP to GDP, the same assay was applied. From the literature it is known that dynamin assembles around the neck of a formed clathrin coated bud in a spiral-like fashion, and that the dimerization of its G-domain with another dynamin molecule from an adjacent ring of the spiral is required for its assembly-stimulated GTPase activity (Chappie et al., 2010, Stowell et al., 1999). Therefore, 1 µM dynamin was incubated in the presence of 2 mM GTP with or without 0.1 mM liposomes at 37 °C for 30 minutes. At various time points samples were taken, diluted 1:15 with assay buffer including 5 mM EDTA and flash frozen in liquid nitrogen to stop the reaction. Then, the thawed samples were prepared for reversed phase chromatography as described for the determination of the nucleotide state of dynamin.

No detectable GTP hydrolysis activity was observed when liposomes were absent or when the dynamin-2 K44A mutant was used. However, the presence of liposomes in the reaction led to calculated GTP hydrolysis rates for dynamin-1 and dynamin-2 of 3,75 U/mg and 2,75 U/mg, respectively.

2.3.4 AP-2 phosphorylation does not increase its affinity to membranes

As in a previous section already mentioned, AP-2 recruitment to the plasma membrane starts with the binding to $PI(4,5)P_2$ at the plasma membrane, which leads to a conformational change, the so called "open conformation". This conformation is further stabilized via binding to a cargo signal and by a mono-phosphorylation of the AP-2µ subunit at threonine 156. This phosphorylation, mediated by the AAK1 kinase, enhances the affinity to YxxΦ-motifs but not to dileucine-motifs (Collins et al., 2002, Conner and Schmid, 2002, Honing et al., 2005, Ricotta et al., 2002). Point mutants were generated (T156D, T156E), mimicking the phosphorylated state of the µ-subunit. However, both mutants showed a decreased affinity to liposomes harboring $PI(4,5)P_2$ and the YXXΦ-motif of TGN38. In order to analyze this surprising behavior in more detail, the respective kinase for AP-2µ phosphorylation, AAK1, was expressed and purified. The kinetics of phosphorylation by AAK1 was analyzed by time-course measurements read out by half-quantitative immunoblotting against phosphorylated threonine. AP-2 and AAK1 (both 0.5 µM) were incubated at 37 °C. Samples were taken at various time points (Figure 2-16).

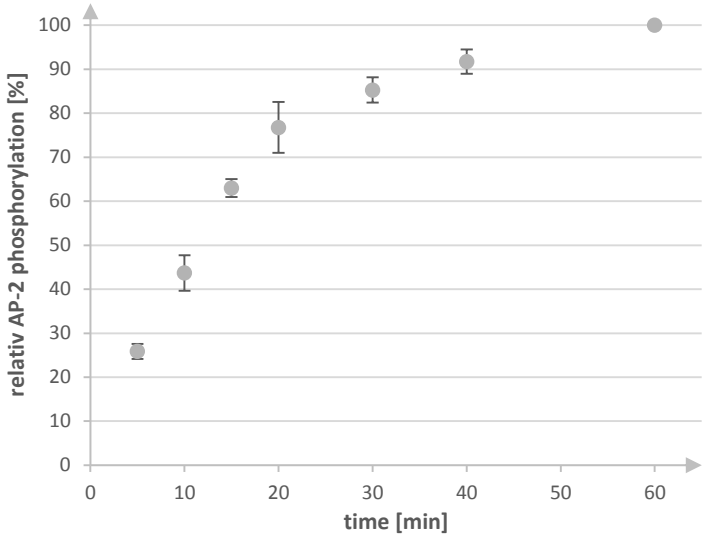

Figure 2-16 Phosphorylation kinetic of AP-2µ by AAK1. 0.5 µM AP-2 and AAK1 was incubated with 2 mM ATP at 37 °C for 60 minutes. At various time points samples were taken and analyzed by Western Blot using an antibody against phosphorylated threonine. Quantification was carried out with Image Studio lite (LI-CORE Biotechnology, US). The highest phosphorylation signal (60 min) was set to 100 % relative AP-2µ phosphorylation. All reactions were supplemented with 1mM Na-orthovanadate and Na-fluoride.

To further analyze if AAK1 specifically phosphorylates the µ-subunit of AP-2, the adaptor complex was incubated with the kinase and immunoblotted using antibodies detecting

phosphorylated threonine, serine and tyrosine residues. According to the time-course measurements the following experiments were carried out at 37° C for 30 minutes.

Phosphorylated threonine residues could not be detected for the purified AP2-complex (Figure 2-17, lane 1), whereas the µ-subunit and either the α-subunit, the β-subunit or both are already phosphorylated at serine residues (Figure 2-17, lane 6). Further serine- or threonine-phosphorylations in the presence of ATP was not detectable (Figure 2-17, lane 2 & 7), showing that the purified AP2-complex is not contaminated with kinases phosphorylating the adaptor complex. However, AAK1 specifically phosphorylates threonine residues within the µ-subunit of AP-2 when incubated with ATP (Figure 2-17, compare lane 4 & lane 9).

AAK1 was also shown to phosphorylate the α-, β-subunit, dependent on the presence of magnesium, but not manganese ions (Ricotta 2002). However, the use of manganese instead of magnesium ions decreased the level of AP-2µ phosphorylation (compare Figure 2-17, compare lane 4 & 5), and in spite of the presence of magnesium ions, AAK1 is not capable of auto phosphorylation (Figure 2-17, lane 5). Threonine residues from the two large subunits were not phosphorylated at a detectable level, neither in the presence of magnesium ions nor with manganese ions (Figure 2-17, lane 4 & 5). Any phosphorylated tyrosine residue could not be detected (Figure 2-17, IB: pTyr).

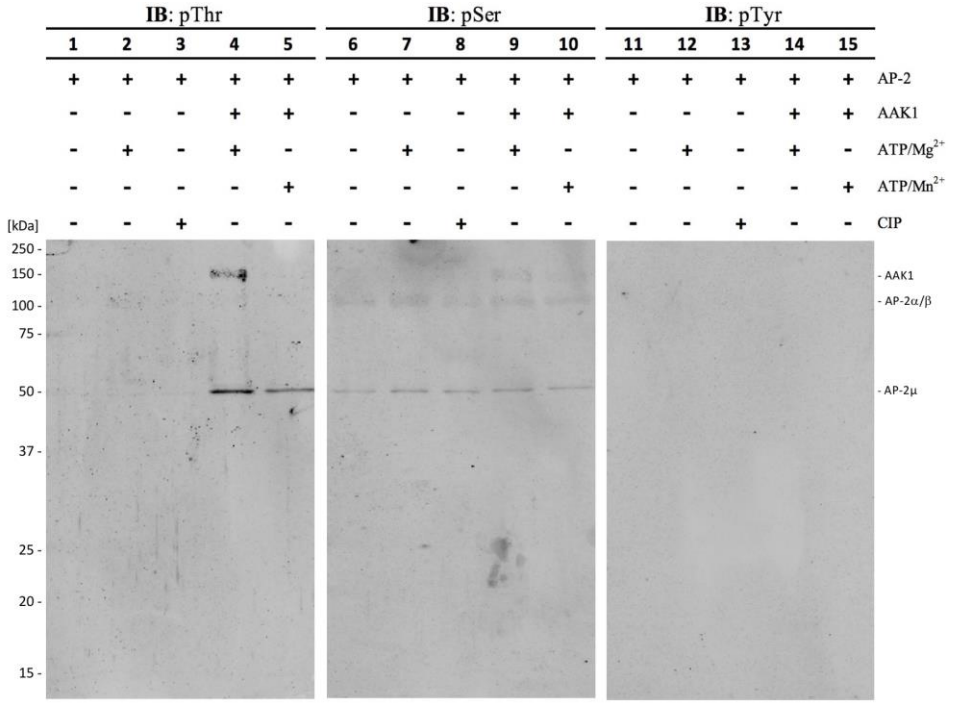

Figure 2-17 AP-2 phosphorylation by AAK1. Equimolar amounts (0.5 µM) of AP-2 and AAK1 were incubated at 37° C for 30 minutes with 2 mM ATP. The Western blot was analyzed using antibodies detecting the phosphorylated amino acids threonine (pThr), serine (pSer) and tyrosine (pTyr). Except the reaction with CIP (calf intestinal phosphatase) all reactions were supplemented with 1mM Na-orthovanadate and Na-fluoride.

To further characterize the specificity of the AP-2µ phosphorylation, phosphomimetic mutants of AP-2, which cannot be phosphorylated at position 156 of the µ-subunit anymore, were incubated with AAK1 and ATP as before, and compared with wild type AP-2. Indeed, no detectable AP-2µ phosphorylation for the phosphomimetic mutants could be observed by immunoblotting, indicating the specific phosphorylation of only the threonine residue at position 156 of AP-2µ (Figure 2-18, IB: pThr).

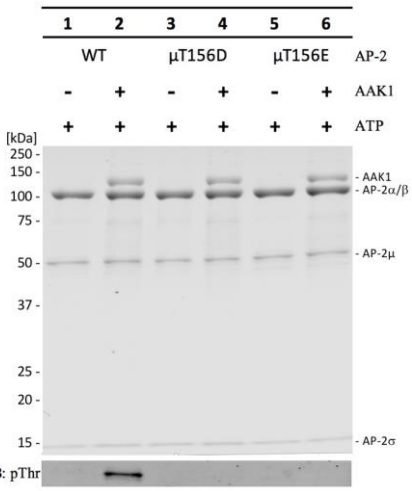

Figure 2-18 AAK1 specifically phosphorylates AP-2µ at position 156. AAK1 was incubated with AP-2 wild type or a phosphomimetic mutants of the AP-2µ-subunit (0.5 µM each) for 30 min at 37 °C. The picture does show a coomassie stained SDS-gel of the incubated reaction mixtures. An aliquot from each reaction was subjected to immunoblotting. An antibody detecting phosphorylated threonine residues (pThr) was used to analyze if AP-2µ is specifically phosphorylated at position 156 (**IB**: pThr). All reactions were supplemented with 1mM Na-orthovanadate and Na-fluoride.

To compare the affinity of phosphorylated and non-phosphorylated AP-2 to liposomes, the adaptor complex was incubated (30 min at 37 °C) with AAK1, ATP and BPLE-derived liposomes (25 µg). The bound material was separated from the unbound material using sucrose gradient centrifugation and analyzed by immunoblotting. An increased binding of the phosphorylated (Figure 2-19 lane 10) AP2-complex as compared to the non-phosphorylated complex (Figure 2-19 lane 9) could not be detected. AAK1 does not have a known membrane interacting domain, but can be recruited to membranes via the interaction with the appendage domain of AP-2α (Figure 2-19 lane 9 & 10), AAK1 recruitment in the absence of AP-2 may indicate for electrostatic interactions of the kinase with charged lipids within the liposomal membrane (Figure 2-19 lane 6).

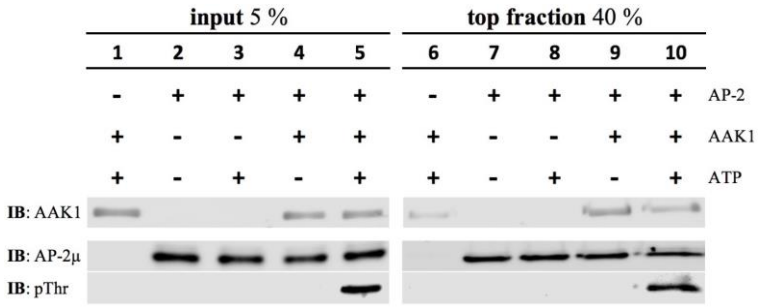

Figure 2-19 Binding of phosphorylated and non-phosphorylated AP-2 to liposomes. The AP-2 complex, AAK1 (both 0.5 µM), ATP (2 mM) and BPLE-derived liposomes (25 µg) including 5 % (w/w) PI(4,5)P_2 and TGN38-lipopeptide were incubated for 30 minutes at 37 °C. The bound material was separated from the unbound material using sucrose gradient centrifugation and analyzed by immunoblotting. Phosphorylated threonine residues (pThr) within AP-2µ were detected with an antibody (IB: pThr). All reactions were supplemented with 1 mM Na-orthovanadate and Na-fluoride.

In 2005, Höning and colleagues investigated the binding of phosphorylated AP2-core (that is AP-2 without the appendage domains of the α- and β-subunit that are necessary for interactions with endocytic accessory proteins and clathrin) to TGN38-lipopeptide in a surface plasmon resonance (SPR)-based approach. They calculated a 12-fold lower K_D for the phosphorylated AP2-core (36 nM) as compared to the non-phosphorylated (450 nM) core. With the same approach, they also calculated dissociation constants for the binding of phosphorylated and non-phosphorylated AP2-core to PI(4,5)P_2 (10 % (w/w)) and PI(4,5)P_2/TGN38-lipopeptide (both 10 % (w/w)) containing liposomes (60-80 % (w/w) PC and 20 % (w/w) PE). The K_D-value for the binding of the non-phosphorylated AP2-core to PI(4,5)P_2-containing liposomes was 24-fold higher, and 40-fold higher to liposomes containing the TGN38-lipopeptide in addition, as compared to the phosphorylated AP2-core. According to this finding one should expect an increased binding of AP-2 to liposomes in its phosphorylated state. Flotation experiments, however, using the same lipid mixture, do not reflect these findings. Without any of the required recruiting signals AP-2 did not bind to liposomes derived from the lipid mixture above, neither with or without AAK1 (Figure 2-20, lane 1 & 2, top fraction). The non-phosphorylated AP2-complex showed the expected increase of membrane recruitment in the presence of both, the cargo-signal (TGN38) and the lipid PI(4,5)P_2 (Figure 2-20, compare lane 3 & 5, top fraction). However, the amount of membrane bound AP-2 did not further increase when the µ-subunit was phosphorylated at position 156 (threonine) by AAK1 as compared to the non-phosphorylated AP2-complex (Figure 2-20, compare lane 5 & 6, top fraction), although the phosphorylation level was about 70 % - 80 %, as determined via the amount of generated ADP. The obtained signals from the western blot analysis were normalized by measuring the fluorescence of the floated liposomes via incorporated PE-rhodamine.

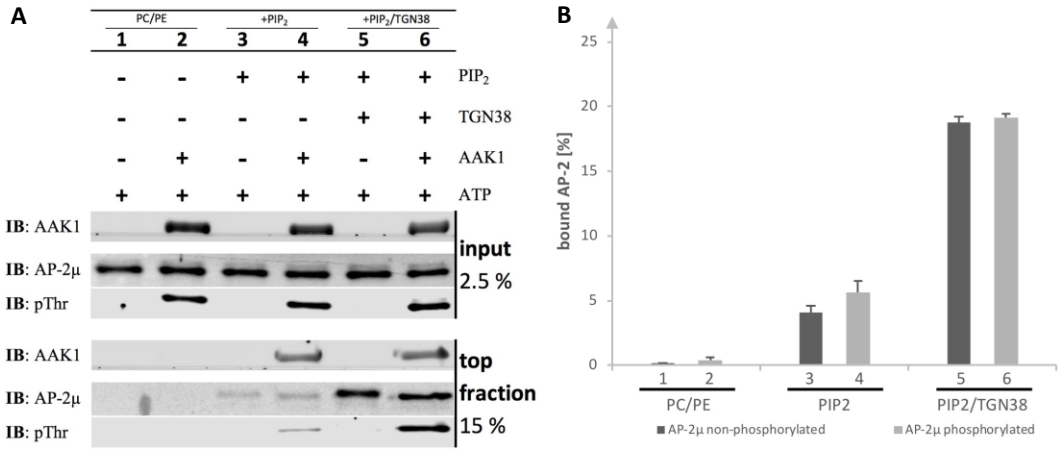

Figure 2-20 Binding of phosphorylated and non-phosphorylated AP-2 to liposomes with a high content of PIP_2. The adaptor complex 2, AAK1 (both 0.5 µM), ATP and liposomes (25 µg, 60 – 80 % (w/w) PC and 20 % (w/w) PE) harboring 10 % (w/w) TGN38-lipopeptide and/or 10 % (w/w) $PI(4,5)P_2$ were incubated for 25 minutes at 37 °C. (**A**) The bound material was separated from unbound material using sucrose gradient centrifugation and analyzed by immunoblotting. All reactions were supplemented with 1mM orthovanadate. (**B**) The amount of membrane bound AP-2 (top fraction) was quantified using the Li-COR Image Studio™ software. For quantification, the amount of floated membranes in the top fractions using fluorescence was taken in account. Phosphorylated threonine residues within AP-2µ were detected with an antibody (pThr). All reactions were supplemented with 1 mM Na-orthovanadate and Na-fluoride.

2.4 Reconstitution of endocytic clathrin coated vesicles

To date, only reconstitution studies were carried out using (besides some purified components) the whole cytosol or component-depleted cytosol for generating CCV in vitro. Moreover, AP2-vesicle formation was also described to occur in the presence of the non-hydrolysable nucleotide GTPγS (Gilbert et al., 1997, Lin et al., 1991, Miwako et al., 2003). In 2012, Dannhauser and Ungewickel published the reconstitution of CCV using the artificial clathrin adaptor ΔENTH-epsin-1, clathrin, dynamin-1 and GTP. The ENTH-domain of ΔENTH-epsin-1 was replaced by a polyhistidine-tag and recruited to liposomes using a nickel chelating lipid. However, the authors did not investigate the influence of full length epsin-1 and excluded the main endocytic clathrin adaptor AP-2 in their reconstitution experiments.

2.4.1 Dynamin-driven vesicle formation with a truncated clathrin adaptor

In order to validate the reconstitution system used in my studies, a first aim was to reproduce the results of Dannhauser and Ungewickel with the purified proteins. For this, ΔENTH-epsin-1 (1.8 µM) was first incubated with BPLE-derived liposomes (0.5 mg/ml) harboring 5 % (w/w) of a nickel chelating lipid. To remove unbound proteins, the liposomes were pelleted and then resuspended in buffer containing clathrin (0.4 µM) and dynamin-1 (0.3 µM). After pre-incubation with the proteins, GTP (2 mM) was added. Then, the larger

liposomes were pelleted (10 min at 10000 g (LSP)) and the supernatant was centrifuged at 100000 g for 30 min (HSP). The pellets were analyzed by Coomassie stained SDS-gel, western blot and electron microscopy. The experiments showed a result (Figure 2-21 B) very similar when compared to the published data of Dannhauser and Ungewickel (Figure 2-21 A). However, the efficiency of the vesiculation process is very low in both cases. Besides some reconstituted CCV mostly clathrin aggregates are visible.

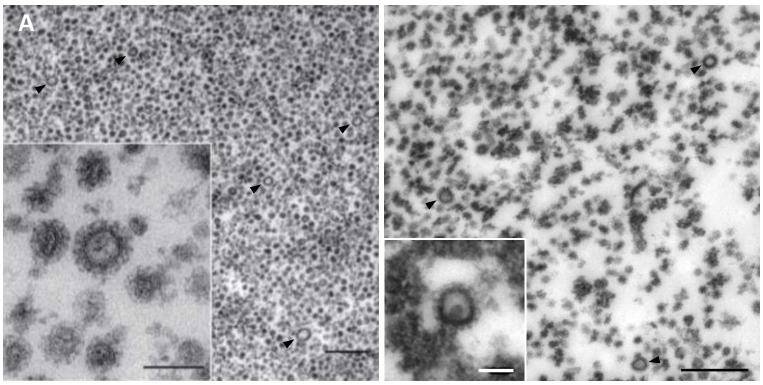

Figure 2-21 Epon-embedded EM pictures of vesicle formation experiments with ΔENTH-epsin-1. The adaptor was incubated with BPLE-derived liposomes (5 % (w/w) Ni^{2+}-NTA-DGS), clathrin, dynamin-1 and GTP. Donor membranes were pelleted at 10000 g and the supernatant at 100000 g (HSP). The HSP were embedded in Epon and ultrathin sections were analyzed by EM. (**A**) Reconstitution by Dannhauser & Ungewickel published in 2012. (**B**) Representative image of an experiment described here. The inset shows a magnified view of a reconstituted CCV. Scale bars: 500 nm, 100 nm (inset in A and B). Vesicles are marked by black arrowheads.

2.4.2 CCV generation with full length proteins in a liposomal system

The experiments from Dannhauser and Ungewickel (2012) have demonstrated, that a minimal machinery, in this case the artificial clathrin adaptor ΔENTH-epsin-1, clathrin and dynamin, can generate clathrin coated vesicles in a GTP dependent manner. However, they did not use full length epsin-1 nor the main clathrin adaptor AP-2, which is the major hub for accessory proteins as well as for the sorting of receptor bound ligands into a forming clathrin coated vesicle.

To fill this gap, AP-2 and epsin-1 were tested either individually or simultaneously for their ability to generate clathrin coated vesicles in the assay by Dannhauser and Ungewickel. Unfortunately, however, a direct comparison was hampered by the very different behavior of adaptor loaded liposomes in the first step of the assay. Such liposomes behaved differently in their sedimentation characteristics, an in the quality of the resulting pellet that could not be efficiently resuspended. Therefor I aimed at analyzing potentially formed vesicles in a way avoiding the first pelleting step. To this end, the components were incubated as before, but without removal of the excess of adaptor. After the incubation steps, the donor membrane was pelleted and the supernatant centrifuged as before, but the pellet was resuspended in assay

buffer for negative-stain electron microscopy rather than embedded in Epon. In the final contrasting step with uranyl acetate, vesicular structures were preserved by using a mixture with methyl cellulose as an embedding reagent. For the conditions outlined in Table 2-1, the concentration of AP-2 and epsin-1 was 1 µM. The concentrations of clathrin and dynamin-2 were kept at 0.4 µM and 0.3 µM, respectively.

Table 2-1 Protein compositions tested for the formation of CCVs in vitro.

01.		+ AP-2	+ Epsin-1	+ Clathrin	+ Dynamin-2	+ GTP
02.	Liposomes	+ AP-2	+ Epsin-1	+ Clathrin		- GTP
03.	Liposomes	+ AP-2		+ Clathrin	+ Dynamin-2	- GTP
04.	Liposomes	+ AP-2		+ Clathrin	+ Dynamin-2	+ GTP
05.	Liposomes		+ Epsin-1	+ Clathrin	+ Dynamin-2	- GTP
06.	Liposomes		+ Epsin-1	+ Clathrin	+ Dynamin-2	+ GTP
07.	Liposomes	+ AP-2	+ Epsin-1	+ Clathrin	+ Dynamin-2	- GTP
08.	Liposomes	+ AP-2	+ Epsin-1	+ Clathrin	+ Dynamin-2	+ GTP

Using AP-2 alone as adaptor, negative staining EM revealed only clathrin aggregates (Figure 2-22 B), similar to a sample of a reaction without liposomes but with the whole set of proteins (Figure 2-22 A). On the other hand, epsin-1 as adaptor generated clathrin coated vesicle structures even in the absence of GTP (Figure 2-22 C). When comparing epsin-1 alone as adaptor (Figure 2-22 C) with the combined adaptors AP-2 and epsin-1 (Figure 2-22 D & E), the latter sample result in many more vesicle-like structures. Note that in all cases there is no striking difference between the presence or absence of GTP. Finally, similar numbers of vesicle-like structures could be observed when incubating AP-2, epsin-1 and liposomes together with clathrin but without the ‘scissase’ dynamin and GTP (Figure 2-22 F).

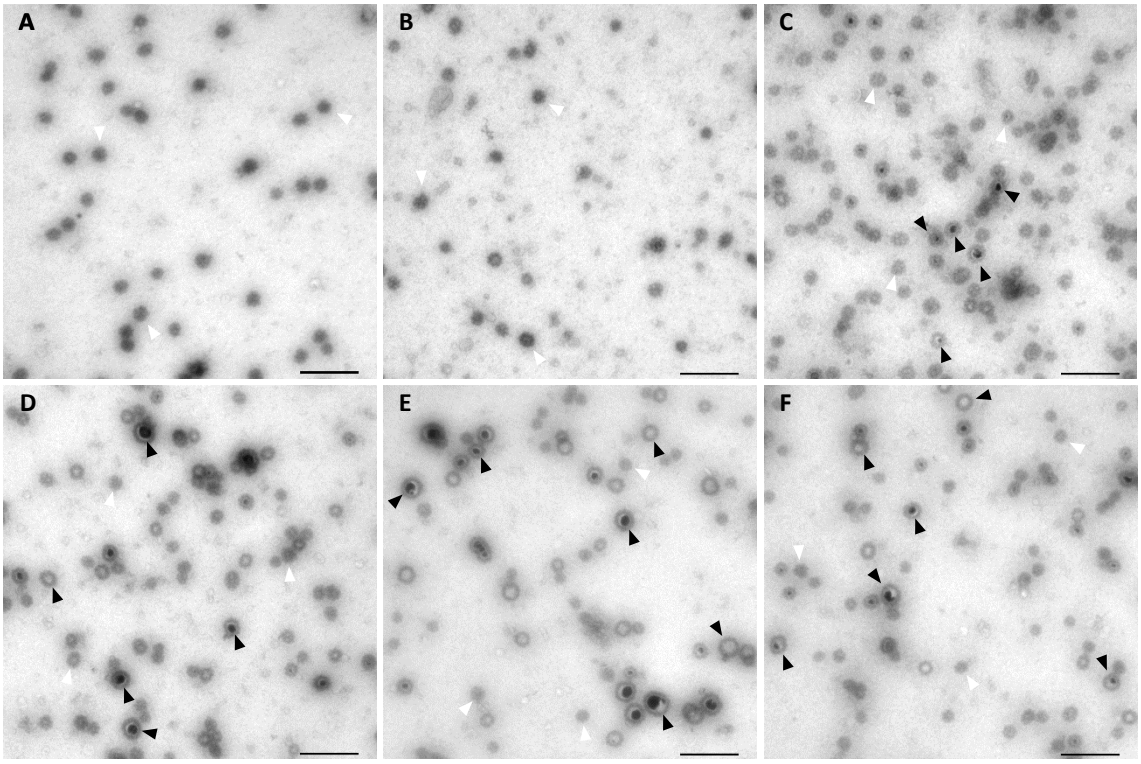

Figure 2-22 Vesicle fractions of various assay conditions captured with negative stain electron microscopy. Liposomes were incubated with proteins as outlined in Table 2-1, then donor membranes were first pelleted at 10 000 g and the resultant supernatant at 100 000 g (high speed pellet (HSP)). Finally, the HSPs were resuspended in assay buffer and subjected to freshly glow discharged carbon-coated copper grids for negative stain EM-analysis. Only clathrin aggregates could be observed when incubating the protein without liposomes (**A)**. Clathrin adaptors were incubated either individually (**B**: AP-2 (+GTP) & **C**: epsin-1 (-GTP)) or simultaneously (**D** (-GTP) & **E** (+GTP)) with liposomes, clathrin, dynamin-2 and nucleotide. Assay conditions by which AP-2 and epsin-1 together with liposomes and clathrin, but without dynamin and GTP (**F**) were incubated, resulted in similar amounts of vesicle like structures as for condition with dynamin 2. Vesicle structures and clathrin aggregates/cages are exemplified by black and white arrowheads, respectively. Scale bars: 250 nm.

In the reconstitution experiments described so far, the presence of dynamin-2 and GTP did not significantly increase the number of vesicle-like structures. In contrast to the literature vesicle formation did not seem to be dynamin- and GTP-dependent. Unfortunately, these findings were not robust. In a second round of reconstitutions, vesicle formation showed dynamin as well as GTP dependency. Without the scissase dynamin-2 (Figure 2-23 A), or when incubating with all proteins, but without GTP (Figure 2-23 B), only clathrin aggregates were observed. Only in the presence of both, dynamin-2 and GTP (Figure 2-23 C), vesicle like structures could be observed. In contrast to the first set of experiments the overall number of these vesicular structures decreased massively (compare Figure 2-23 C & Figure 2-22 E).

These opposing findings led us to the assumption that the liposome preparations used contain small liposomes with a diameter similar to that of CCV that can become coated, rather than being formed de novo. Under such conditions it is not possible to distinguish between small coated liposomes and newly generated CCV. Therefore, to get a more robust assay and a faster

readout, the donor membrane system was switched to giant unilamellar vesicles (GUVs). With differential centrifugation steps, it is possible to remove from GUVs small liposomes almost completely.

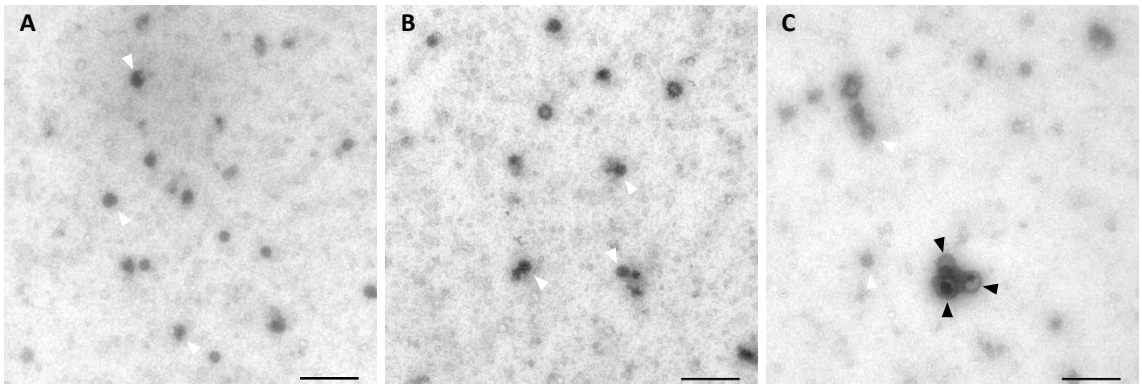

Figure 2-23 The formation of endocytic clathrin coated vesicles depends on the hydrolysis of GTP by dynamin. Liposomes were incubated with proteins as outlined in Table 2-1, then donor membranes were first pelleted at 10 000 g and the resultant supernatant at 100 000 g (high speed pellet (HSP)). Finally, the HSPs were resuspended in assay buffer and subjected to freshly glow discharged carbon-coated copper grids for negative stain EM-analysis. The repetition of the vesicle reconstitution experiments did show an opposing result. Whereas vesicle formation in the first round seems not to be dynamin-2 and GTP dependent, the repetition showed vesicle-like structures exclusively in the presence of dynamin-2 and GTP (**C**). Only clathrin aggregates could be observed when incubating without dynamin-2 (**A**) or without GTP (**B**). The pictures are showing conditions, in which AP-2 and epsin-1 were used as clathrin adaptor. Vesicle structures and clathrin aggregates/cages are exemplified by black and white arrowheads, respectively. Scale bars: 250 nm.

2.4.3 Vesicle formation from Giant Unilamellar Vesicles

Liposomes used so far were generated by ten freeze-thaw cycles to make them unilamellar. However, this harbors the risk of producing small liposomes with a diameter of <100 nm, which, when coated, could be confused with vesicles generated by budding and scission. To minimize the number of small liposomes, the donor membrane system was switched to the use of giant unilamellar vesicles (GUVs). By differential centrifugation, first at 100 g followed by 5000 g, it is possible to separate the GUVs from aggregates, multilamellar GUVs and small liposomes with sizes corresponding to diameters typical for endocytic clathrin coated vesicles. For reconstitution experiments with GUVs as donor membranes, a two-step assay was employed. First, the GUVs (10 nmol) were incubated in 50 µl assay buffer with adaptors (10 pmol) and clathrin (5 pmol) and pelleted together with their bound proteins through 5 % sucrose. Then, the coated GUVs were resuspended in 50 µl assay buffer and incubated with dynamin and GTP (5 pmol and 2 mM, respectively). Finally, the donor membranes were pelleted in a low-speed centrifugation step (5000 g for 10 min) and the supernatant were centrifuged at 120k g for 1 hour. The high-speed pellet was then analyzed by immunoblotting using antibodies raised against the coat proteins. However, due to interaction of epsin-1 with

AP-2, the GUVs tend to aggregate in the first incubation step. The aggregation of the GUVs was analyzed via rhodamine fluorescence. Here, titration experiments revealed a high affinity between both clathrin adaptors. In these experiments, the ratio between proteins and lipids was titrated from 1:1000 to 1:5000. No aggregation was observed when incubating both clathrin adaptors individually with the GUVs at a ratio of 1:1000 (5 nmol GUV and 5 pmol protein). However, GUVs start to aggregate massively when AP-2 and epsin-1 were incubated simultaneously at a protein to lipid ratio of 1:1000. Decreasing the protein concentration fivefold (1:5000) led to minimal aggregation. The appearance of GUV aggregates stayed similar when keeping the AP-2 concentration as before and titrating epsin-1 down to amounts of 500 fmol (Figure 2-24).

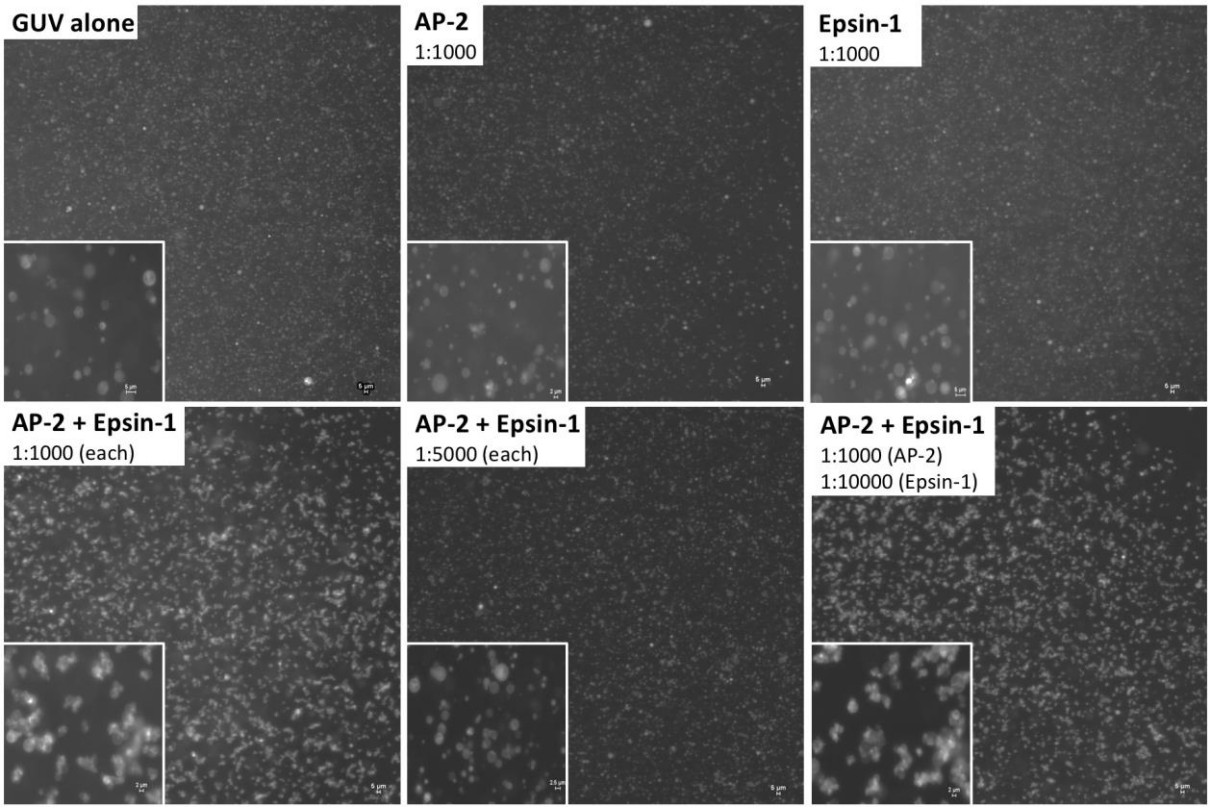

Figure 2-24 Fluorescence microscopy analysis of the interaction of AP-2 and epsin-1 that causes GUV aggregation. GUVs were incubated with clathrin adaptors for 15 min at 37° C as indicated. The numbers in the top left corners indicate the ratio between proteins and GUVs (GUVs were kept at 5 nmol). GUVs were visualized by rhodamine fluorescence (Ex: 510-560, Em: 590 cut-on).

Therefore, when using both adaptors combined, in the following reconstitution experiments a protein to lipid ratio of 1:1000 was used. In the first step 20 nmol GUVs were incubated with 20 pmol AP-2 or epsin-1 and 10 pmol clathrin in a total assay volume of 100 µl. When incubating the GUVs with both adaptors, 10 pmol of each adaptor was used to keep the total

amount of adaptors constant. 10 pmol dynamin-2 and 2 mM GTP where added after GUV recovery. Finally, after pelleting the donor membranes, the supernatants were centrifuged and the resulting pellets analyzed by immunoblotting for released vesicles. After GUV recovery, controls without GUVs do not show any or very low amounts of coat proteins (Figure 2-25, lane 3), indicating efficient separation of the coated GUVs from non-bound material, prerequisite when immunoblot for coat proteins is used to analyze vesicle release. When comparing the vesicle fractions (pellet fractions), the signal for clathrin is about 5-fold higher when GTP and dynamin-2 is present (Figure 2-25, lane 10), as compared to a reaction without GTP but with dynamin-2 (Figure 2-25, lane 9). This observation argues for an GTP dependent release of vesicles. However, there is an unexpected release when dynamin-2 is not present (Figure 2-25, lane 8). The signals for the adaptors are similar.

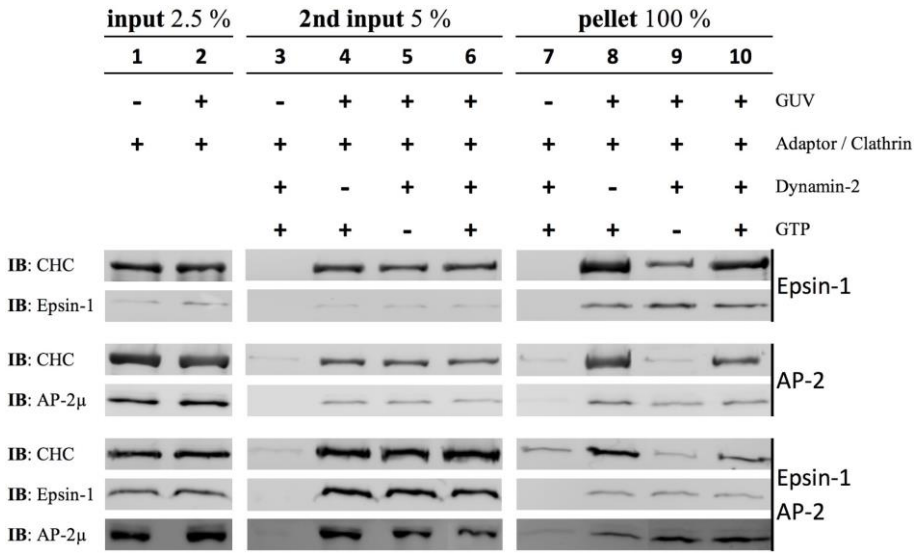

Figure 2-25 Vesicle reconstitution experiments using GUVs. First the GUVs were incubated with various adaptors or their combination and clathrin (input). After the incubation for 15 min at 25° C, the coated GUVs were recovered by centrifugation through 5 % sucrose (w/w) and incubated with dynamin-2 and GTP (2nd input) for 30 min at 37 °C. The reaction was cleared from the donor membrane via centrifugation and the vesicles were pelleted for 1 h @ 120 000 g. Inputs and the pellets were analyzed by immunoblotting.

A more direct approach will be to incubate all components at once, pellet the donor membranes and visualize the generated vesicles by capturing negative stain EM-pictures from the supernatant. Therefore, GUVs were incubated first with adaptors and clathrin at 25 °C for 30 minutes before dynamin-2 and GTP was added for a further 30 minutes incubation step at 37 °C. After pelleting the donor membranes at 10 000 g for 10 minutes, the cleared supernatant was subjected to a freshly glow discharged carbon-coated copper grid and analyzed by negative stain electron microscopy.

This approach clearly reveals a dynamin- and GTP-dependent formation of endocytic clathrin coated vesicles. Comparing the different clathrin adaptors, a dynamin 2- and GTP-dependent vesicle formation could be observed for epsin-1 alone (Figure 2-26, compare B & E) or in addition of AP-2 (Figure 2-26, compare, C & F) as adaptors for clathrin. AP-2 alone is not sufficient to generate clathrin coated vesicles (Figure 2-26 A & D). Reactions in which dynamin-2 was omitted, did not result in any vesiculation, neither for epsin-1 (Figure 2-26 G) alone or in addition of AP-2 (Figure 2-26 H), as compared with previous experiments using liposomes, generated by freeze-thaw cycles, as donor membranes. To further illustrate the necessity of the GTP-hydrolysis by dynamin for vesicle biogenesis, reaction conditions were chosen to abolish its GTPase activity either due to the addition of the non-hydrolysable GTP analog GTPγS (Figure 2-26 I) or by introducing a lysine to alanine mutation at position 44 of dynamin-2 (dynamin-2 K44A, Figure 2-26 J). This mutant lacks the ability to bind GTP. Indeed, both conditions did not generate any clathrin coated vesicle. To further demonstrate, that dynamin does not vesiculate the GUVs by itself, membranes were first incubated with dynamin-2 and GTP for 30 min at 37 °C, GTP hydrolysis blocked by the addition of 5 mM EDTA and further incubated for 30 min at 37 °C with epsin-1 and clathrin (Figure 2-26 L). Vesicle-like structures should only be observable in case dynamin exhibits any vesiculation activity under the assay conditions. However, only clathrin aggregates and cages were observed like incubating the whole set of components without GUVs (Figure 2-26 K).

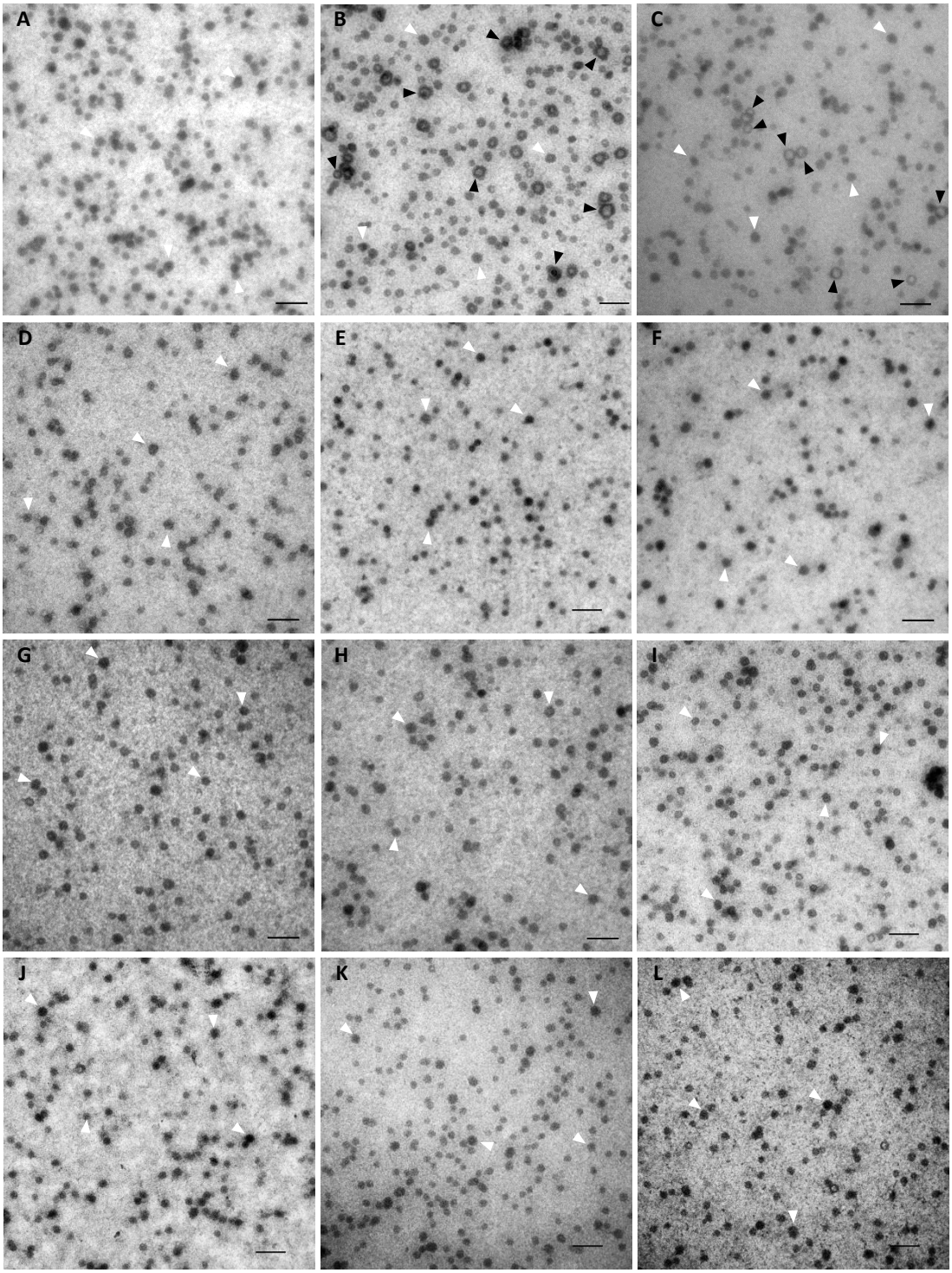

Figure 2-26 Dynamin- and GTP-dependent formation of endocytic clathrin coated vesicles from GUVs. AP-2 (**A** (+GTP) & **D** (-GTP)) and epsin-1 (**B** (+GTP) & **E** (-GTP)) were incubated either individually or simultaneously (**C** (+GTP) & **F** (-GTP)) with GUVs, clathrin, dynamin and GTP. dynamin-2 was omitted to analyze a potential scission activity of epsin-1 alone (**G**) or in addition of AP-2 (**H**). The necessity of dynamin´s GTPase activity for clathrin coated vesicle biogenesis was shown for conditions in which the non-hydrolysable GTP analog GTPγS was introduced (**I**) and by using the dynamin-2 mutant K44A, lacking the ability to bind GTP (**J**). Epsin-1 alone was used as clathrin adaptor in (I) and (J). Incubating the whole set of proteins but without GUVs, only clathrin aggregates and cages were observed (**K**). A possible vesicle forming activity by dynamin-2 was assessed by first incubating dynamin-2 with GUVs and GTP for 30 min at 37 °C, whereby GTP hydrolysis was blocked by the addition of 5 mM EDTA, and further incubating for 25 min at 25 °C with epsin-1 and clathrin (**L**). The donor membrane-cleared supernatant was subjected to freshly glow discharged carbon-coated copper grids for negative stain EM-analysis. Vesicle structures and clathrin aggregates/cages are exemplified by black and white arrowheads, respectively. Scale bars: 250 nm.

Vesicles generated either with epsin-1 alone or with AP-2 in addition were analyzed for their inner diameter (Figure 2-27). The average diameter of vesicles generated with epsin-1 is about 50 nm and thus 10 nm smaller as compared to those generated with epsin-1 and AP-2 together (about 60 nm).

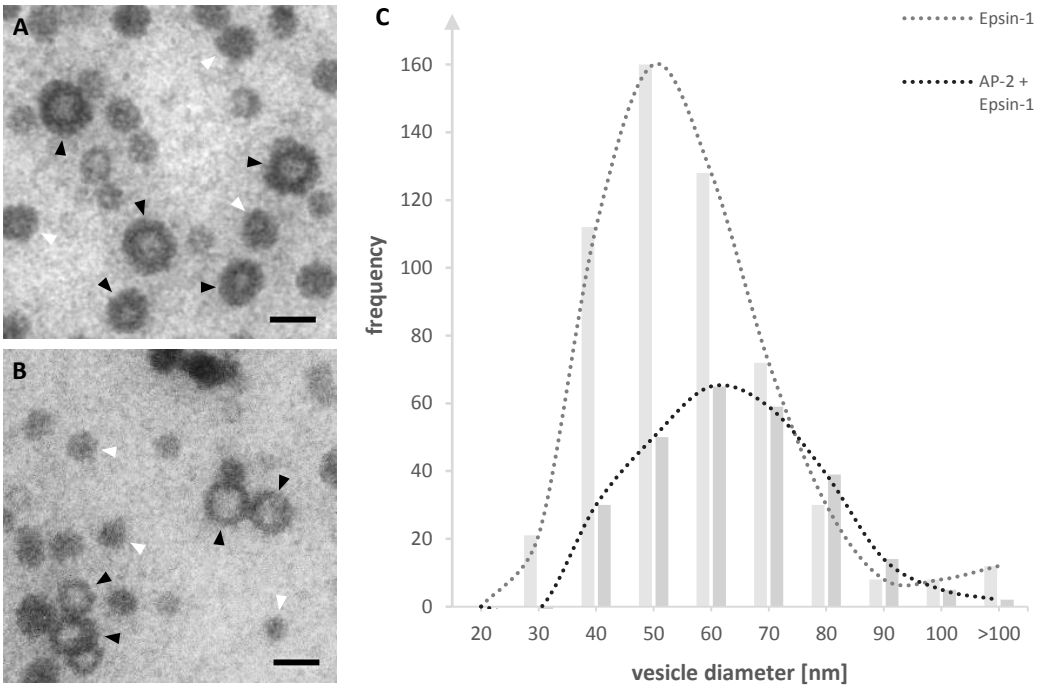

Figure 2-27 Vesicle size distribution using epsin-1 alone or AP-2 in addition as clathrin adaptors. Epsin-1 were incubated either alone (**A**) or in addition of AP-2 (**B**) with GUVs, clathrin, dynamin and GTP. After pelleting the donor membranes by centrifugation, the supernatants were subjected to freshly glow discharged carbon-coated copper grids for negative stain EM-analysis. (**C**) The histogram shows the size distribution of the inner vesicle diameter measured with ImageJ (Schneider et al., 2012). Vesicle structures and clathrin aggregates/cages are exemplified by black and white arrowheads, respectively. Vesicles from at least three individual experiments were analyzed. $n_{epsin\text{-}1} = 551$, $n_{epsin\text{-}1 + AP\text{-}2} = 265$. Scale bars: 100 nm.

The donor membrane cleared and vesicle containing supernatant was further subjected to sucrose gradient centrifugation and analyzed via immunoblotting. To this end, the vesicle containing supernatant was set to 50 % sucrose (w/w), overlaid with 45 % (w/w) sucrose and assay buffer. The gradient was centrifuged for one hour at 40 000 rpm in a SW60 rotor. The interface between assay buffer and 45 % sucrose was collected for analysis. Before loading on the SDS-gel, all floated samples were subjected to chloroform-methanol-precipitation. In both cases, when epsin-1 (Figure 2-28 A) alone was used or together with AP-2 (Figure 2-28 B), very low but significant amounts of the coat proteins were released.

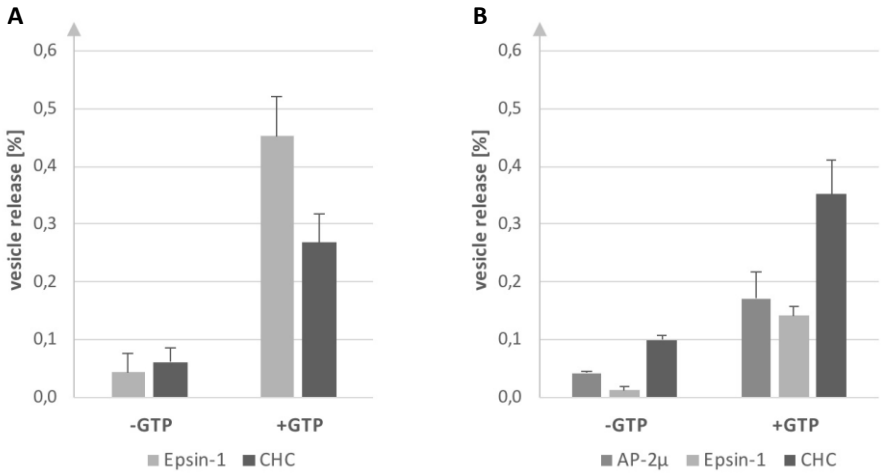

Figure 2-28 Flotation of GUV-derived clathrin coated vesicles. Epsin-1 alone (**A**) or together with AP-2 (**B**) were incubated with GUVs, clathrin, dynamin and GTP. The donor membrane cleared supernatant (10 min at 10 000 g) was subjected to sucrose gradient centrifugation. The floated material was analyzed by immunoblotting after precipitation and quantified using the Li-COR Image Studio™ software.

3 Discussion

In this thesis I investigated steps in the formation of CCVs, including how an endocytic clathrin coated vesicle is separated from the plasma membrane once a clathrin coated bud has formed. In the last years it has been pointed out that dynamin has a pivotal role in the scission of a CCB. It is thought that dynamin catalyzes GTP hydrolysis, leading to a conformational change and final separation of the CCV from the plasma membrane. However, recent studies indicated that dynamin may not be the direct scission factor for CCV. Rather, insertion of the N-terminal amphipathic helix of epsin's ENTH-domain into the membrane was suggested to induce scission (Boucrot et al., 2012). Moreover, endocytic CCV formation was also described to occur in the presence of the non-hydrolysable nucleotide GTPγS (Miwako et al., 2003). The last two points would argue for a more general scission mechanism shared by COPI-, COPII- and clathrin-vesicles. The scission of both COP-vesicle types was shown to be dependent on the activated form of the small GTPases Sar1 or Arf, both proteins which insert an amphipathic helix into the membrane, but not on their ability to hydrolyze GTP (Barlowe et al., 1994, Beck et al., 2011, Adolf et al., 2013).

To dissect steps necessary for CCB formation and separation, it is important to employ a chemical defined reconstitution system. To date, such reconstitution studies were carried out using the whole or component-depleted cytosol. The few reconstitution experiments with defined recombinant proteins described were restricted by using truncated proteins. Therefore, an in vitro reconstitution system with defined full-length components was to be established. To this end, selected proteins involved in CCV biogenesis were expressed, purified and tested for functionality, and used in an assay to reconstitute CCVs. As a result, several combinations of these components revealed a minimal set of proteins necessary for the in vitro formation and scission of endocytic clathrin coated vesicles.

3.1 Expression and purification of proteins for CCV reconstitution

For my project to reconstitute endocytic CCVs with combinations of defined proteins, recombinant expression and purification of these components was to be established. Using the pFBDM/pUCDM vector system (Berger et al., 2004), the tetrameric AP-2, clathrin (heavy and light chain), the kinase AAK1 as well as dynamin-1/2 and a dynamin-2 mutant were expressed in insect cells. Importantly, with this system it is possible to express a multi-subunit protein encoded within one virus. Other advantages of using a baculovirus expression system in insect cells are a high yield of the expressed proteins. Likewise, eukaryotic proteins often undergo

more efficient folding in insect cells when compared with bacteria, and can undergo post-translational modifications similar to those in other eukaryotic systems.

To achieve high purity, all proteins and complexes were expressed as a TEV-cleavable One-Strep (OST-tag) fusion protein. Epsin-1 (GST-tag) and its ENTH-domain truncation (ΔENTH-epsin-1) can be functionally expressed in *E. coli* (Dannhauser and Ungewickell, 2012). In case of full length epsin-1, the GST-tag was fused to its C-terminal protein-interaction hub to avoid the presence of additional amino acids at the N-terminal membrane binding and curvature inducing ENTH-domain (Ford et al., 2002). For the truncated version of epsin-1 the ENTH-domain was replaced by a His_6-tag in order to allow recruiting this protein to membranes via a nickel chelating lipid.

All proteins were affinity purified to a high degree of purity using the appropriate affinity beads. However, initial clathrin purifications showed an overexpression of the light chain, resulting in stoichiometry of 19 light chains per heavy chain, rather than a 1:1 stoichiometry. To get a better expression level of the heavy chain, a new expression construct was generated harboring three copies of the CHC-gene. Theoretically, this should result in an increased mRNA level and therefore an increased expression level of only the heavy chain. Indeed, the new construct results in an about 1:1 stoichiometry of the clathrin complex.

The purification of the adaptor protein complex 2 did show an equimolar stoichiometry of all four subunits, however, endogenous insect cell clathrin was co-purified. Thus, for further purification, the complex was subsequently subjected to gel filtration using a Superdex 200 column. Here, the 650 kDa clathrin complex appears in the void volume of the column. AP-2 elutes as a peak in the retarded volume that corresponds to a molecular mass of about 291 kDa. Compared to the theoretical molecular mass of 281.5 kDa, the equimolar stoichiometry, found already in coomassie-stained SDS-gels, was confirmed.

After the initial affinity purification of epsin-1, the GST-tag was cleaved with thrombin and separated via gel filtration. From the literature it is known, that epsin (Mr = 60 kDa) in gel filtration and on SDS-gels behaves like a much bigger protein (about 245 kDa and 90 kDa, respectively). Hence, it was separated from the dimeric GST-tag which has a molecular mass close to the theoretical mass of full length epsin. The nature of this unusual behavior is based on epsin´s long poorly structured C-terminal part, responsible for protein-protein interactions, and not on oligomerization, as has been figured out in gel filtration, analytical ultracentrifugation and CD spectroscopy experiments (Kalthoff et al., 2002). In the same study, a stoke´s radius of 5.5 nm for recombinant full length epsin-1 and 4.8 nm for ΔENTH-epsin-1

was calculated, which would correspond to globular proteins with a molecular mass of about 250 kDa and 150 kDa, respectively.

3.2 Characterization of purified endocytic proteins

All proteins were tested for their activity in terms of membrane binding, protein-protein interaction and enzymatic activity, by comparison with data described in the literature. Membrane binding and protein-protein interactions were tested using liposomes as model donor membranes. Proteins bound to membranes were separated by sucrose gradient centrifugation and subsequently analyzed via immunoblotting. The enzymatic activity of AAK1 to phosphorylate the µ-subunit of AP-2 was tested via immunoblotting using antibodies raised against phosphorylated amino acid residues. To determine the nucleotide state of the large GTPase dynamin and its ability to hydrolyze GTP to GDP, a HPLC-based approach was applied.

From the literature it is known that AP-2 and epsin-1 are recruited to the plasma membrane via the phospholipid phosphatidylinositol-4,5-bisphosphate ($PI(4,5)P_2$). In case of epsin-1, the important feature necessary for its targeting to $PI(4,5)P_2$ containing membranes is its so-called N-terminal ENHT-domain. The second important feature is its membrane remodeling activity to induce positive curvature in membranes, which relies on the insertion of an amphipathic α-helix into the inner leaflet of the membrane. This helix, which becomes structured upon membrane binding, is referred as to helix zero or H_0. At high concentrations, epsin-1 alone is able to tubulate or even vesiculate $PI(4,5)P_2$ containing liposomes, a property, which is affected by concentration of $PI(4,5)P_2$ within the membrane. Binding and vesicle reconstitution experiments carried out here, however, were performed with much less epsin-1 and $PI(4,5)P_2$ (up to 40- and 10-times less, respectively) as compared to other studies (Ford et al., 2002, Yoon et al., 2010). Hence, epsin-1-driven tubulation or vesiculation was not observed under all assay conditions tested. In case of AP-2, $PI(4,5)P_2$ does play a fundamental role in membrane recruitment, however is not sufficient for a stable interaction with membranes. A model was put forward, in which AP-2 undergoes a large scale conformational change, initiated by $PI(4,5)P_2$- and stabilized by cargo-binding (Jackson et al., 2010). In the mechanism outlined there, both large AP-2 subunits seem to have a key role in initial membrane binding, whereas the binding sites within the µ-subunit drive the rearrangement from a closed to an open conformation. Only in this conformation, all four $PI(4,5)P_2$-binding sites and the two cargo-binding sites for the interaction with YxxΦ- and dileucine-motifs become coplanar, which

allows their simultaneous interaction with PI(4,5)P_2- and cargo-containing membranes (Jackson et al., 2010, Kelly et al., 2014).

In liposome-based recruitment assays, carried out in this study, AP-2 and epsin-1 showed binding characteristics as expected from the literature. Both proteins bound liposomes to a similar extent and the amount of recruited clathrin was comparable as well. However, when both clathrin adaptors were incubated simultaneously, the amount of each protein bound (AP-2, epsin and clathrin) increased threefold, arguing for a synergistic effect in terms of membrane binding and clathrin recruitment. This cooperative effect is also reflected by increasing amounts of invaginated structures that were observed on liposomes when AP-2 and epsin-1 were used as clathrin adaptors as compared to each adaptor alone (Figure 2-15). It has been shown that three adaptor interacting terminal domains will come in close proximity during the formation of a clathrin cage (Fotin et al., 2004) to provide enough binding sites for a cooperative clathrin recruitment. Additionally, a similar synergistic effect is known for AP-2 and AP180 (Hao et al., 1999). AP180 has a membrane binding domain (ANTH-domain) that is related to the ENTH-domain of epsin-1 but has a different mode of membrane interaction (Ford et al., 2001, Stahelin et al., 2003). AP-2 and AP180 together assemble many more clathrin into cages as compared to each adaptor alone, which indicates for a cooperativity in clathrin recruitment. Further cooperative effects in terms of clathrin binding were also reported between two clathrin-binding sides within epsin-1 (Drake et al., 2000) and AP-1 (Doray and Kornfeld, 2001).

In the very last step of CCV biogenesis, dynamin comes into play for the separation of a bud formed from the plasma membrane. Dynamins themselves do not possess a high affinity to nucleotides but have a high intrinsic GTP hydrolysis activity (Damke et al., 2001). Dynamins are interacting via their stalk-domain with each other, in order to assemble into a right-handed helical structure around the neck of a CCB. This assembly allows the dimerization of the G-domains from adjacent rings to trigger GTP-hydrolysis, when loaded with GTP. A subsequent conformational change is transmitted via the bundle signaling element (BSE) to the stalk-domain, resulting in constriction of the dynamin helix (Hinshaw and Schmid, 1995, Takei et al., 1995, Chappie et al., 2010, Faelber et al., 2012). For CCV reconstitutions discussed in the next chapter, it is of high importance to work with nucleotide free dynamin, to avoid any misleading results, for example when incubating with a non-hydrolysable GTP analogue (GTPγS, GMPPNP) or with GDP. For these experiments dynamin must be free of GTP. Due to the low affinity to nucleotides, it was not expected to purify dynamin loaded with GTP. Indeed, no signal for GTP or GDP was detected in HPLC- as well as in mass spectrometry analysis. For

purified dynamin-1 and dynamin-2, a specific activity of GTP hydrolysis of 3,75 U/mg and 2,75 U/mg was determined, dependent on the presence of liposomes. Without a membrane template, dynamin is still able to assemble into its typical helical fashion and to hydrolyze GTP, but only when subjected to a low ionic strength buffer (Hinshaw and Schmid, 1995, Warnock et al., 1996). Experiments carried out for this thesis were done in the presence of 150 mM potassium acetate. Therefore, no GTP was hydrolyzed in the absence of a membrane template, or when the dynamin-2 mutant K44A was incubated with membranes. This mutant cannot bind GTP (van der Bliek et al., 1993) but retains the ability to assemble on a membrane template (Sundborger et al., 2014).

3.3 AP-2µ phosphorylation

As already mentioned, AP-2 recruitment to the plasma membrane starts with the binding to $PI(4,5)P_2$ at the plasma membrane, which induces a membrane bound open conformation of AP-2. This conformation is, besides by interaction with cargos, further stabilized by a mono-phosphorylation of the AP-2µ subunit at threonine 156. This phosphorylation, mediated by the AAK1 kinase, enhances the affinity to YxxΦ-motifs but not to dileucine-motifs (Collins et al., 2002, Conner and Schmid, 2002, Honing et al., 2005, Ricotta et al., 2002). Point mutants were generated (AP-2µ T156D and T156E), mimicking the phosphorylated state of the µ-subunit. However, both mutants showed a decreased affinity to liposomes harboring $PI(4,5)P_2$ and the YxxΦ-motif of TGN38. For this reason, AP-2 was phosphorylated by incubating with AAK1, the respective kinase for AP-2µ phosphorylation. Besides the threonine phosphorylation site within AP-2µ, online protein databases (e.g. UniProt) annotate also additional serine phosphorylation sites throughout the AP-2 complex. Western blot analysis using antibodies detecting phosphorylated threonine, serine and tyrosine residues illustrated that AP-2, purified for this study, is not phosphorylated at any threonine or tyrosine residue during expression. In contrast, one of the two large subunits of AP-2, or both, and the µ-subunit are already phosphorylated at serine residues their host cells. There is no further threonine, serine or tyrosine phosphorylation upon the addition of ATP, which demonstrates that the AP-2 preparations are free of kinases able to phosphorylate AP-2 subunits. Note that purified endogenous AP-2 can be phosphorylated in vitro by a co-purified kinase (Keen et al., 1987, Fingerhut et al., 2001), later identified as AAK1 (Conner and Schmid, 2002). AAK1 exclusively phosphorylates the µ-subunit of AP-2 at threonine 156, when compared to kinase reactions using the phosphomimetic AP-2 variants, which cannot be phosphorylated at position 156 anymore. AAK1 itself is a serine/threonine-kinase (Conner and Schmid, 2002), thus,

tyrosine phosphorylation is not expected and also not observed. Unexpectedly, there was no increase in membrane bound AP-2, although about 70 - 80 % of the µ-subunits were phosphorylated.

Initial analysis of a role of AP-2 phosphorylation was done with endogenous AP-2 isolated from tissues. These preparations already exhibited AP-2 phosphorylation activity when ATP was added, indicating co-purified kinases (Pauloin et al., 1984). Functional analysis of these phosphorylated AP-2 complexes revealed an increased affinity to endocytic sorting motifs, as determined on liposomes by surface plasmon resonance. Phosphorylated AP-2 were also recruited to a higher extent to crude membranes from NRK cells, compared to untreated AP-2 (Fingerhut et al., 2001). However, these experiments do not rule out that factors other than the AP-2µ phosphorylation at position 156, like e.g. protein-protein interactions, are involved in the increased affinity to membranes. In subsequent work the same authors showed that the suggested phosphorylation of AP-2µ at position 156 is indeed responsible for increased affinity, using the bacterial expressed AP2-core (Honing et al., 2005) or immunopurified AP-2 (Ricotta et al., 2002). With this SPR-based approach, a 40-fold lower K_D for the phosphorylated AP2-core (72 nM) as compared to the non-phosphorylated core (2900 nm) was calculated for the binding to membranes harboring both $PI(4,5)P_2$ and the endocytic motif of TGN38 (Honing et al., 2005). In addition, in vivo studies identified the AP2µ-phosphorylation at position 156 as an important factor for the internalization of the transferrin receptor (Olusanya et al., 2001).

So, where may the discrepancy of the data obtained here to these findings may come from? One explanation could be bound in the fact that the SPR-based approach will detect any recruitment to the sensor chip. Hence, cannot distinguish between AP-2 recruitment due to its natural membrane binding sites, unspecific electrostatic interactions or the recruitment of protein aggregates to the sensor surface. The latter ones could be positively influenced by AP-2µ phosphorylation. In addition, an increased affinity to YxxΦ-motifs upon AP-2µ phosphorylation was only shown in the SPR-based approach mentioned above. Liposomal pull-down or flotation experiments with $PI(4,5)P_2$- and YxxΦ-motif-containing membranes are missing in addition to the SPR-based data. Another group analyzed the influence of the AP-2µ phosphorylation at position 156 in a far-western blot approach (Crump and Banting, 1999). Here, AP-2µ phosphorylation did also not result in an increased binding to the sorting signal of TGN38.

With regard to the expression host, post-translational modifications could also be responsible for the different findings. For the SPR-based analysis, which showed that AP-2µ phosphorylation increases the affinity to YxxΦ-motifs, the AP-2 core was phosphorylated via

AAK1 co-expression in *E. coli* (Honing et al., 2005). Therefore, other post-translational modifications are not expected. In contrast, the insect cell expression system, which was used for this thesis, is able to modify overexpressed proteins post-translationally, as initial analysis of the phosphorylation state of AP-2 has demonstrated. From the literature it is known that cytosolic AP-2 is more phosphorylated as compared to membrane bound AP-2 (Wilde and Brodsky, 1996). Thus, serine phosphorylation or other modifications could have a contradictory function and diminish or abolish the positive membrane binding effect of the threonine phosphorylation of AP-2µ at position 156. Further studies, in which the phosphorylated AP2-core, expressed and phosphorylated in *E. coli*, is directly compared with the full-length AP-2, expressed and purified form Sf9-cells and phosphorylated in vitro by AAK1, are necessary in order to learn whether AP-2 phosphorylation influences the affinity to YxxΦ-motifs or not.
Apart from this, phosphorylation and dephosphorylation events seem to represent an important regulatory mechanism, as they also influence the interactions of endocytic proteins during clathrin coated vesicle biogenesis (Wilde and Brodsky, 1996, Slepnev et al., 1998).

3.4 Reconstitution of clathrin-mediated endocytosis

Having all proteins at hand, described to be needed to generate endocytic clathrin coated vesicles, I firstly reproduced the results Dannhauser & Ungewickel published in 2012. They were able to generate CCV using the artificial clathrin adaptor ΔENTH-epsin-1, clathrin and dynamin-1 together with GTP. The presence of CCVs was analyzed using western blot and electron microscopy of thin sections of Epon-embedded samples. The data are nicely reproducible, showing a very similar result. Note that the efficiency of generating CCVs was very low in both cases, the published and the reproduced data. The data could also be reproduced with regard to using dynamin-2 instead of dynamin-1. This demonstrates that the components produced for this thesis are also functional in terms of vesicle generation. However, what is missing in the above publication is the use of the main endocytic clathrin adaptor AP-2 as well as of full-length epsin-1. In addition, they did not investigate whether epsin-1 will generate CCVs even in the absence of dynamin and GTP, as suggested from knock-down studies (Boucrot et al., 2012).
To fill this gap, AP-2 and epsin-1 were tested either individually or simultaneously for their ability to generate CCVs with the assay Dannhauser and Ungewickel had introduced in their publication. In the first place, Dannhauser and Ungewickel incubated the liposomes with ΔENTH-epsin-1 and pelleted the adaptor bound liposomes to get rid of small liposomes which could falsely be identified as CCV. Then, the pellet was resuspended and incubated with

clathrin, dynamin and GTP. Unfortunately, liposomes incubated with AP-2, epsin-1 or both adaptors simultaneously behaved either in the sedimentation behavior or in their ability to resuspend the pellet in such a way different that a comparison was not possible. Using the adaptors individually, the adaptor bound liposomes were not pelleted equally efficient at the same centrifugation conditions, and when both adaptors were used together, the pellet was not resuspendable. Thus, the efficiency of different adaptor combinations to generate clathrin coated vesicles could not be compared. To overcome these circumstances, the components were incubated as before while keeping unbound adaptors in the reaction. In this way, various protein compositions were tested for the formation of CCVs. Potentially vesicle-containing supernatants were centrifuged at 100 000 g and the pellets resuspended for negative-stained EM-analysis. In a first series of experiments, reasonable amounts of vesicle-like structures were generated when liposomes were incubated with AP-2 and/or epsin-1 and clathrin. AP-2 alone as clathrin adaptor was not able to generate vesicles. The presence or absence of dynamin and GTP did not influence vesicle formation, as similar amounts of vesicle-like structures could also be observed without them. These results argued for a potential scission activity of epsin-1 in CCV biogenesis. However, these results turned out not to be robust: In a second attempt, vesiculation seems to be dynamin- and GTP-dependent, while the overall amount of vesicle-like structures was strikingly decreased when compared with the first attempt. These opposing results could have been caused by the presence of vesicle sized liposomes in the liposomal donor membrane preparations. Such small liposomes may have been generated due to various conditions: (a) liposomes prepared by 10 freeze-thaw cycles may contain small liposomes with a diameter endocytic CCV usually have, (b) due to different lipid-mix stocks that were used for both experiments, liposome solutions could already have contained different amounts of small liposomes with CCV-like diameters right after the dried lipid film was resuspended in assay buffer and (c) while resuspending the vesicle fractions, coated donor membranes (liposomes) that were not pelleted in the first centrifugation step, could be sheared off and falsely be identified as CCV.

An alternative donor membrane source, suitable for this kind of experiments, are giant unilamellar vesicles (GUV). GUVs can be easily fractionated according to their sizes by low speed centrifugation steps. This minimizes remarkably the risk of having liposomes with a diameter typical for CCV. The amount of $PI(4,5)P_2$ was reduced to 1 % (w/w) (4-fold reduction) for a proper GUV electro-formation in order to prevent aggregation as compared to the liposomes used before. Titration experiments, carried out first, demonstrated a high affinity between AP-2 and epsin-1 as they cause aggregation of the GUVs. The interactions

between both proteins are between the α-appendage domain of AP-2 and the tripeptide DPW within the C-terminal unstructured part of epsin-1. As there are eight copies of the AP2-interacting tripeptide, epsin-1 can theoretically interact with more than one AP-2 complex (Rosenthal et al., 1999), thus, causing a high degree of aggregation even at low epsin concentrations. A 10-fold decrease of the epsin-1 amount (500 fmol), while keeping the amounts for the GUVs and AP-2 (5 nmol and 5 pmol, respectively), leads to the same aggregation behavior as compared to equimolar amounts of AP-2 and epsin-1. This was already observable by eye. Nevertheless, I tested both adaptors alone and together in the reconstitution assays using GUVs. In the first step of the assay, the GUVs were incubated with adaptor and clathrin to form buds and the coated GUVs were separated by centrifugation through a 5 % sucrose cushion. This step clearly separates the coated GUVs from almost any non-bound material in the supernatant, as confirmed by western blot analysis, allowing the detection of coat proteins by immunoblotting to analyze vesicle release. Then, the coated GUVs were incubated with dynamin-2 and GTP. Finally, the reaction was centrifuged to pellet the donor membranes and the supernatant was analyzed via immunoblotting for coat proteins (Figure 2-25). Indeed, the signal for clathrin is higher with GTP than without GTP, however the signals for the adaptors are the same. An even higher release of coat proteins was observable when dynamin-2 was excluded from the reaction. This unexpected result might be due to unspecific binding of proteins to the surface of the GUVs and their release during the scission step. However, this opens the question of why this was not observed in a reaction with dynamin-2. These discrepancies led us to conclude that this approach was not suitable to analyze the formation of CCVs in vitro.

Alternatively, the components were incubated at once and vesicle formation was analyzed by negative-stained electron micrographs of the donor membrane-cleared supernatant. This approach clearly demonstrated a dynamin- and GTP-hydrolysis-dependent mechanism of CCV-formation, which is in line with the literature. An involvement of epsin-1 in scission was not verified as suggested (Boucrot et al., 2012). However, the results revealed an important role of epsin in the formation of CCB and therefore vesicles. Most importantly, AP-2 alone turned out not to be able to form clathrin coated invaginations on membranes, rather clathrin aggregates were recruited to the membrane as it was shown on electron micrographs. This finding is in contrast to other findings (Kelly et al., 2014) where however, about 10-fold more $PI(4,5)P_2$ and TGN38-lipopeptide was used for the recruitment of AP-2 to PC/PE-derived liposomes. Under conditions used in my work, only when epsin with its ENTH-domain was present, buds and vesicles were observed. Furthermore, vesicle formation with the established

GUV-based approach, occurred with a much higher efficiency (28 vesicles per 10 µm^2) as compared to the approach Dannhauser and Ungewickell (2012) published for the formation of clathrin vesicles with ΔENTH-epsin-1 (about 3 vesicles per 10 µm^2). From the literature it is known that epsin is displaced to the rim of a growing bud (Saffarian et al., 2009, Sochacki et al., 2017) and that it can induce membrane curvature by the insertion of an α-helix into the leaflet (Ford et al., 2002). AP-2 itself is not able to induce membrane curvature, thus, epsin at the rim of a CCP possibly induces the curvature necessary for bud formation, which is subsequently stabilized by clathrin. This mechanism does also explain the finding that AP-2 alone as a clathrin adaptor is not able to generate CCV.

In the in vitro reconstitution of CCV, epsin-1 as clathrin adaptor is much more efficient in vesiculation as to a mix of epsin-1 and AP-2. This is most likely due to GUV aggregation. In the latter case, free membrane surface area is remarkably reduced and proteins are trapped within the aggregation interface. Therefore, a comparison in terms of vesicle amounts is not possible. The efficiency of vesicle formation could further be investigated employing immobilized GUVs to avoid aggregation. Resulting supernatants can then directly be analyzed for the presence of vesicles. Nevertheless, while incubating all components in solution, enough vesicles were generated to allow statistical analyses of their diameter. Vesicle size was not homogeneous, rather a broad Gaussian distribution was observed. CCVs generated with epsin-1 alone as adaptor resulted in vesicle structures between 30 nm and 90 nm with a peak at 50 nm. On the other hand, reconstitutions with epsin-1 plus AP-2 gave rise to vesicles shifted to 60 nm in average. These findings are in line with AP-2 knockdown experiments using small interfering RNA, in which a reduced vesicle size was observed (Miller et al., 2015).
EM-analysis revealed that clathrin assembles in cages of hexagons and pentagon (Heuser, 1980, Fotin et al., 2004). Thus, to vary the diameter of such a cage, it is necessary to vary the distribution of hexagons and pentagons. For bigger diameters, less pentagons are necessary than for smaller diameters. A clathrin assembly of only hexagons will end up as a flat lattice as has been found on the inner plasma membrane surface of fibroblasts (Heuser, 1980). The balance between hexagons and pentagons is very likely influenced by a cooperative recruitment of clathrin through the various contact sites of clathrin adaptor combinations. Although clathrin adaptors obviously play a certain role in defining the final vesicle size, other proteins involved in the biogenesis of CCV that can induce or sense curvature, like BAR-domain containing proteins, also present potent modulators to define vesicle dimensions. Hence, it is not clear what the main factors are that determine the size of CCV. However, these possibilities are not mutually exclusive, as membrane curvature inducing or sensing proteins are also adaptors for

the scaffolding protein clathrin, like epsins or amphiphysins. Two proteins, already linked to control the vesicle size, are the ubiquitously expressed clathrin assembly lymphoid myeloid leukaemia protein (CALM) (Miller et al., 2015) and its neuronal homologue AP180 (alternative names: F1-20, SNAP91) (Ye and Lafer, 1995).

In clathrin mediated endocytosis, CCP nucleation initiates through the recruitment of adaptor proteins and clathrin to the plasma membrane. While receptors, adaptors, clathrin and other regulatory proteins will continuously be recruited to the edge of the growing coat, the initial clathrin patch matures to an invaginated CCB that is finally separated from the membrane via the large GTPase dynamin (Cocucci et al., 2012, Robinson, 2015). For the last decades it was believed that curvature of a CCP constantly grows with clathrin polymerization (Kirchhausen, 2009, Saffarian et al., 2009). This model is known as the constant curvature model. However, a second model has increasingly come into focus over the last years, the constant area model. Here, clathrin grows as flat lattices up to a certain size before the lattice starts to remodel and becomes curved (Avinoam et al., 2015, Bucher et al., 2018). The area of the clathrin lattice is kept nearly constant during the conversion to a curved clathrin lattice. To change curvature during this remodeling step, the hexagonal flat clathrin lattice needs to be partially converted to pentagons to introduce curvature. Although the constant area model was already put forward at a time right after clathrin was linked to vesicle transport (Pearse, 1976, Heuser, 1980), it was initially rejected due to structural and energetic reasons (Kirchhausen, 2009, Saffarian et al., 2009). However, molecular simulations suggest that local conformational changes within the flat clathrin lattice are in fact able to induce the remodeling to a curved lattice (den Otter and Briels, 2011). However, the question remains as to how curvature is initiated in living cells. Two factors known to influence the curvature of clathrin lattices are the clathrin light chain (Wilbur et al., 2010) and an acidic pH (Heuser, 1989). Additionally, mutational analysis revealed a key role of adaptor proteins in controlling the curvature of the clathrin lattice. Without the C-terminal α-appendage domain of AP-2, flat clathrin lattices accumulate at the plasma membrane (Aguet et al., 2013). As the α-appendage domain is crucial for the recruitment of endocytic accessory proteins, this observation was suggested to be caused by the diminished recruitment of curvature-inducing accessory proteins to CCP. However, the exact mechanisms and regulators of generating curvature remain unclear. The data obtained in the course of this thesis suggest epsin to be such a regulator. The strongest evidence in support of this are observations on negative-stained electron micrographs of liposomes. When AP-2 and clathrin were added, no invaginated clathrin coated structures could be observed. However, when epsin-1 was added together with AP-2 and clathrin, or even without AP-2, such

invaginations were clearly visible. Thus, with regard to the constant area model, epsin may play an important role in the transition of flat clathrin lattices to invaginated clathrin coated structures by introducing curvature to the membrane and therefore overcome membrane tension, which has an antagonistic role in the generation of curved clathrin structures (Saleem et al., 2015, Bucher et al., 2018).

The experiments have shown that clathrin mediated endocytosis can be reconstituted in vitro. Similar to Dannhauser and Ungewickell (2012) the minimal requirements are a clathrin adaptor, clathrin, dynamin and the hydrolysis of GTP by dynamin to separate formed buds from the membrane. However, the main endocytic clathrin adaptor, AP-2, alone turns out not to be sufficient to generate clathrin coated vesicles. Rather the endocytic membrane remodeling protein epsin was necessary, and was also able to generate CCV even in the absence of AP-2. From this perspective it is of interest, how other curvature sensing and/or membrane remodeling proteins would influence in vitro reconstitutions of CCVs. Examples comprise like BAR-domain containing proteins, or the epsin-related proteins CALM and AP180 (ANTH-domain instead of ENTH-domain), abundant in CCV in amounts similar to AP-2 (Borner et al., 2012, Prasad and Lippoldt, 1988). The ANTH-domain of the huntingtin-interacting protein 1-related protein (Hip1r) homologue in yeast (Sla2) cannot tubulate GUVs, like the ENTH-domain of yeast epsin (Ent1), but influences the membrane bending activity of the ENTH-domain when co-assembled on membranes via direct interactions between the membrane-binding domains (Skruzny et al., 2015, Garcia-Alai et al., 2018). Moreover, in vivo studies in yeast have shown that the co-assembly of Sla2´s ANTH-domain with the ENTH-domain of Ent1 is critical for endocytosis (Skruzny et al., 2015). In contrast, extensive tubulation was observed when the mammalian CALM was incubated with liposomes (Miller et al., 2015). Recently, a synergistic effect on the vesicle release from supported bilayers with excess membrane reservoir (SUPER) templates for the BAR-domain containing protein amphiphysin and dynamin-2 was shown, whereas endophilin and sorting nexin-9 (SNX9) had an inhibitory effect on the release of vesicles (Pucadyil and Schmid, 2010).

The established approach, to reconstitute CCVs in a chemical defined environment, will provide a powerful tool for functional and mechanistic studies, to investigate the influence of proteins mentioned above and of other proteins involved in the biogenesis of CCVs. Finally, such reconstitutions will refine our mechanistic view of the formation of endocytic clathrin coated vesicles.

4 Materials and methods

4.1 Molecular biology

4.1.1 Plasmids

Table 4-1 List of plasmids.

Name	Insert	Creator
pCRBlunt-NdeI-Epsin1-KpnI	Epsin1	this thesis
pCRBlunt-NdeI-Epsin1-XhoI	Epsin1	this thesis
pCRBlunt-NdeI-ΔENTH-Epsin1-XhoI	ΔENTH-Epsin1	this thesis
pEGFP-N1-Dynamin1	Dynamin1	Addgene - Plasmid #34680
pEGFP-N1-Dynamin2	Dynamin2	AG Haucke - Leibnitz-Institut für Molekulare Pharmakologie (FMP) Berlin
pET29a-Epsin1-GST	Epsin1-GST	this thesis
pET29a-ΔENTH-Epsin1	ΔENTH-Epsin1	this thesis
pET32c-Epsin1	Epsin1	AG Ungewickel - Medizinische Hochschule Hannover
pET5a-AP2σ	AP2σ	AG Schepers - Karlsruher Institut für Technologie
pFASTBac-AP2α	AP2α	AG Schepers - Karlsruher Institut für Technologie
pFASTBac-AP2µ	AP2µ	AG Schepers - Karlsruher Institut für Technologie
pFBDM-AP2β	AP2β	this thesis
pFBDM-AP2	AP2	this thesis
pFBDM-AP2β/AP2µ	AP2β/AP2µ	this thesis
pFBDM-AP2β/AP2µT156D	AP2β/AP2µT156D	this thesis
pFBDM-AP2β/AP2µT156E	AP2β/AP2µT156E	this thesis
pFBDM-AP2σ/OST-AP2α	AP2σ/OST-AP2α	this thesis
pFBDM-x/OST-Dynamin1	OST-Dynamin1	this thesis
pFBDM-x/OST-Dynamin2	OST-Dynamin2	this thesis
pFBDM-x/OST-Dynamin2 K44A	OST-Dynamin2 K44A	this thesis

pFBDM-x/OST-Dynamin2 T65A	OST-Dynamin2 T65A	this thesis
pCR-XL-TOPO-AAK1	AAK1	Biocat GmbH, Heidelberg
pFBDM-x/AAK1-OST	AAK1	this thesis
pQE32-ΔENTH-Epsin1	Epsin1	AG Ungewickel - Medizinische Hochschule Hannover
pCMV-SPORT6-AP2β	AP2β	Source BioScience - I.M.A.G.E. ID: 7929959
pFBDM-CHC/CLC	Clathrin heavy and light chain	Sabine Finkenberger – AG Wieland
pUCDM-rCHC	Clathrin heavy chain	this thesis
pUCDM-rCHC / rCHC	Clathrin heavy chain	this thesis

4.1.2 Primer

All oligonucleotides were ordered from Biomers (Ulm).

Table 4-2 List of oligonucleotides.

Name	Sequence 5’ – 3’	Application
f_AP2_NotI_alpha2	TATAGCGGCCGCGAAAACCTGT	PCR
r_AP2_alpha2_XbaI	TATATCTAGAGAACTGTTCCGACAGCAATT	PCR
r_AP2_alpha2_XbaI_Stop	TATATCTAGATTAGAACTGTTCCGACAGCAATT	PCR
f_AP2_XmaI_beta1	TATACCCGGGATGACTGACTCCAAG	PCR
r_AP2_beta1_SphI	TATAGCATGCGTTTTCAAAATGCTG	PCR
r_AP2_beta1_SphI_Stop	TATAGCATGCTTAGTTTTTCAAAATGCTG	PCR
f_AP2_BssHII_mu	TATAGCGCGCATGATCGGAGG	PCR
r_AP2_mu_SalI	TATAGTCGACGCAGCGGGTTTC	PCR
r_AP2_mu_SalI_Stop	TATAGTCGACCTAGCAGCGGGTTTC	PCR
f_AP2_SmaI_sigma	TATACCCGGGATGATCCGATTCATTC	PCR
r_AP2_sigma_NcoI	TATACCATGGCTCCAGCGACTGC	PCR
r_AP2_sigma_NcoI_Stop	TATACCATGGTCACTCCAGCGACTGC	PCR

f_NotI_Dyn1	TATAGCGGCCGCATGGGCAACCG	PCR
r_Dyn1_XbaI	TATATCTAGATTAGAGGTCGAAGGGGGGCCTGG	PCR
f_NotI_Dyn2	TATAGCGGCCGCATGGGCAACCG	PCR
r_Dyn2_XbaI	TATATCTAGATTAGTCGAGCAGGGACGGCTCGG	PCR
f_NdeI_His-Epsin1_144-575	TATACATATGCACCATCACCATCACCATG	PCR
r_His-Epsin1_144-575_SalI	TATAGTCGACATTATAGGAGGAAGGGGTTAGTG	PCR
f_NdeI_Epsin1	TATACATATGTCGACATCATCGCTGCG	PCR
r_Epsin_KpnI	TATAGGTACCTAGGAGGAAGGGGTTAGTGTTG	PCR
r_Epsin-1_XhoI	TATACTCGAGTTATAGGAGGAAGGGG	PCR
f_NotI-rCLCa1	TTATTATTAGCGGCCGCATGGCTGAGTTGGATC	PCR
r_rCLCa1-XbaI	AAAAAATCTAGATCAATGCACCAGGGGCGC	PCR
f_XmaI_rCHC	TATACCCGGGATGGCCCAGATTC	PCR
f_BamHI_rCHC	TATAGGATCCATGGCCCAGATTCTG	PCR
r_rCHC_XhoI	TATACTCGAGTCACATGCTGTACCCAAAG	PCR
r_rCHC_XbaI	TATATCTAGACTCACATGCTGTACCCAAAGC	PCR
f_BssHII_rCHC	TATAGCGCGCATGGCCCAGATTC	PCR
r_cPCR_3xrCHC	AAGGTGACATCATCGGTCATGG	PCR
BssHII_AAK1	TATAGCGCGCATGAAGAAGTTTTTC	PCR
NotI_AAK1	TATAGCGGCCGCATGAAGAAGTTTTTC	PCR
AAK1_XbaI	TATATCTAGACTACAGGTCTATGAGCTGATC	PCR
AAK1_SalI	TATAGTCGACCAGGTCTATGAGCTGATC	PCR
AP2_alpha_wFP	CTTTGTCCCGGCTCCTTGG	Sequencing
AP2_alpha_wRP	GTGGACGCAGCACTGGTGC	Sequencing
sf_pFBDM MCS1	CAAATAAATAAGTATTTTAC	Sequencing

sr_pFBDM MCS1	GTTTTATTCTGTCTTTTTATTG	Sequencing
sf_pFBDM MCS2	CAAATAAATAAGTATTTTAC	Sequencing
sr_pFBDM MCS2	GTGTGGGAGGTTTTTTAAAG	Sequencing
AP2_beta_wFP	TCCACTTGTCACTTTGCTCTCTGG	Sequencing
AP2_beta_wRP	GCCGGACTTCCTCCAATGC	Sequencing
AP2_alpha_wFP2	GGACATCCCGTGTGGTACACC	Sequencing
pFBDM-AP2_FP	TTCCTCCCGATGTCATCTCTG	Sequencing
pFBDM-AP2_RP	TCCCCACGGTCATAGCAGC	Sequencing
Epsin-1_wFP	AGGCTGCAGATGGCAATAGAGG	Sequencing
Dyn1_wFP	GTCGCCAAGGAGGTGGACC	Sequencing
Dyn1_wRP	GAGCCATTCTCCTCGGTCTCG	Sequencing
Dyn2_wRP	GATGAAGGCACAGATGCCAGG	Sequencing
Dyn2_wFP	CTTGTTGATGATGGCCACATAGG	Sequencing
sPFBDM rev	GACGGTATGAATAATCCGGAATAT	Sequencing
S-Pr5 pFBDM BB1	CATCGTTTGTTCGCCCAGGA	Sequencing
Sec Primer rat CHC #1	ACCACCCACAGGAAACCAACC	Sequencing
Sec Primer rat CHC #2	TGCAGAGACAGGTCAAGTCCAG	Sequencing
Sec Primer rat CHC #3	GTGACCGCTTTGACTTCGTCC	Sequencing
Sec Primer rat CHC #4	AACCGCCTGGACAATTATGATGC	Sequencing
Sec Primer rat CHC #5	AGGCAGCCTTGGGACTAGAG	Sequencing
Sec Primer rat CHC #6	TTTGCCATGCCCTATTTCATCCAG	Sequencing
SecPrimer rCLC	AAGGCCTCGTCGTTCTCTATGCC	Sequencing
AAK1_wRP1	AAGTGGGATGCCAGAGTCC	Sequencing
AAK1_wRP2	ATCAGCTGTTGCTGAGCACC	Sequencing

AAK1_wFP1	GGTGTGCAAGAGGGAGATCC	Sequencing
AAK1_wFP2	AAACTACTCAAGAAAGAATGCCC	Sequencing
AAK1_Insert(BioCat)_RP	CAAGGGGTAGGAGAAAGGAGC	Sequencing
f_AP2_alpha2_131A	ATTTATGGGTCTGGCCCTGCACTGCAT	Mutagenesis
r_AP2_alpha2_131A	ATGCAGTGCAGGGCCAGACCCATAAAT	Mutagenesis
f_AP2_alpha2_677S	AGGGCCCCCTCCCTCCTCTGGCGGTGG	Mutagenesis
r_AP2_alpha2_667S	CCACCGCCAGAGGAGGGAGGGGGCCCT	Mutagenesis
f_AP2_mu_13E	AATCACAAGGGGGAGGTGCTTATCTCC	Mutagenesis
r_AP2_mu_13E	GGAGATAAGCACCTCCCCCTTGTGATT	Mutagenesis
f_Dyn2_K44A	CAGAGCGCCGGCGCGAGTTCGGTGCTC	Mutagenesis
r_Dyn2_K44A	GAGCACCGAACTCGCGCCGGCGCTCTG	Mutagenesis
f_Dyn2_T65A	ATCAGGAATTGTCGCCCGGAGGCCTCT	Mutagenesis
r_Dyn2_T65A	AGAGGCCTCCGGGCGACAATTCCTGAT	Mutagenesis
f_Dyn2_K142A	CCCAGGCATCACTGCGGTGCCAGTGGGG	Mutagenesis
r_Dyn2_K142A	CCCCACTGGCACCGCAGTGATGCCTGGG	Mutagenesis
f_AP2mu_T156E	ACCAGCCAGGTGGAGGGGCAAATTGGC	Mutagenesis
r_AP2mu_T156E	GCCAATTTGCCCCTCCACCTGGCTGGT	Mutagenesis
f_AP2mu_T156D	ACCAGCCAGGTGGACGGGCAAATTGGC	Mutagenesis
r_AP2mu_T156D	GCCAATTTGCCCGTCCACCTGGCTGGT	Mutagenesis
f_rCHC_SpeI_elimination	CAGGCCGCCAATACCAGTGGAAACTGG	Mutagenesis
r_rCHC_SpeI_elimination	CCAGTTTCCACTGGTATTGGCGGCCTG	Mutagenesis

4.1.3 DNA concentration determination

The spectrophotometer ND-1000 from NanoDrop (Wilminkton, USA) was used to determine the concentration of solubilized DNA. Two microliters of a DNA solution were applied to measure the absorption at 260 nm and calculate the final concentration.

4.1.4 DNA precipitation

For precipitation of DNA, first 0.1 volume of 3 M sodium acetate (pH 5.2) and second 2.5 volumes of ice-cold pure ethanol or 1 volume of ice-cold pure isopropanol were added to the DNA solution. The mixture was incubated for 1 hour at -20 °C or for 30 min at -80 °C to facilitate DNA precipitation. Then, the mixture was centrifuged 30 minutes at 16 000 g at 4 °C. Subsequently, the supernatant was discarded. The DNA pellet was washed with 0.5 ml of ice-cold 70 % ethanol to remove residual salts and centrifuged again for 10 min at conditions mentioned before. Again, the supernatant was discarded and the DNA pellet dried and resuspended in deionized water.

4.1.5 Agarose gel electrophoresis

Agarose gels were used for the electrophoretic separation of DNA. To prepare 1 % agarose gels, the appropriate amount of agarose was dissolved by heating in 1x TAE buffer. For in-gel staining, Clear G (Serva, Heidelberg) was added in a dilution of 1:25 000 just before pouring into the agarose gel preparation/running chamber (Peqlab, Erlangen). Prior to loading, the DNA samples were mixed with 0.2 volumes of 6x DNA loading dye (New England Biolabs, Ipswich, USA). All gels were run at 100 V in TAE buffer. After separation, the DNA fragments were visualized on a GelDoc System (Bio-Rad, Munich). The 1kb DNA ladder from New England Biolabs (Ipswich, USA) was used to determine the size of the DNA fragments.

Table 4-3 Buffers and solutions for agarose gel electrophoresis.

Buffers/Solutions	Composition	Concentration
TAE buffer	Tris-HCl pH 8.0	40 mM
	Acetic acid	20 mM
	EDTA	1 mM
1x DNA loading dye	Tris-HCl pH 8.0	3.3 mM
	EDTA	11 mM
	Ficoll-400	2.5 %
	SDS	0.017 %
	Bromophenol blue	0.015 %

4.1.6 Polymerase chain reaction (PCR)

The polymerase chain reaction was used for selective amplification of DNA using a programmable thermocycler. For further applications, the amplified fragment was either separated via agarose gel electrophoreses and extracted from the agarose gel using a gel extraction kit or purified using a PCR purification kit (both Qiagen, Hilden).

To introduce mutations, side-directed mutagenesis PCR was applied. Here, instead of two fragment-flanking primers, two complementary primers that carry single point mutations absent in the template DNA, were used to amplify the whole plasmid. After the reaction was finished, the methylated template DNA was digested with DpnI (10 U per reaction) for 1 hour at 37 °C. Subsequently, 5 µl of the reaction was used for the transformation in chemically competent *E. coli* DH5α or electrocompetent *E. coli* DH10b.

All amplifications were carried out using the *Pfu*Plus! DNA polymerase (Roboklon, Berlin) which exhibits a 3´- 5´ exonuclease activity to correct falsely incorporated nucleotides (proof-reading). The following components were mixed in 0.2 µl PCR tubes.

Table 4-4 Compositions of PCR- and side-directed-mutagenesis reactions.

Component	**Concentration**
Pfu polymerase	2.5 U
DNA template	20 ng
Primer forward	0.4 µM
Primer reverse	0.4 µM
Deoxynucleotides	0.3 mM each
Reaction buffer	1x
H_2O	add 50 µl

Table 4-5 Conditions used for PCR- and side-directed-mutagenesis reactions.

Step	**Temperature** [°C]	**Time** [sec]
Initial denaturation	95	120
Denaturation	95	30
Annealing	primer dependent	60
Extension	72	60/1 kb
Final extension	72	600
Storage	4	∞

4.1.7 Analytical & colony PCR

After transformation and selection via antibiotics, transformants were analyzed for the uptake of the correct plasmid by colony PCR. To this end, the components in Table 4-6 were mixed in an 0.2 ml PCR reaction tube. For multiple reactions, a master mix was prepared and aliquoted. All amplifications were carried out using the *Taq* DNA polymerase (Axon, Kaiserslautern).

Table 4-6 Compositions of analytical- and colony-PCR reactions.

Component	**Concentration**
Taq polymerase	2.5 U
DNA template	20 ng or colony
Primer forward	0.2 µM
Primer reverse	0.2 µM
Deoxynucleotides	0.2 mM each
Reaction buffer includes 15 mM $MgSO_4$	1x
$MgCl_2$	2 mM
H_2O	add 25 µl

For colony PCR, a single colony was transferred with a 10 µl pipette tip to the reaction mixture, before the amplification reaction (Table 4-7). The initial denaturation step at 95 °C was prolonged to 5 minutes to release the DNA template from the bacteria. Following the transfer to the PCR reaction, a backup of each colony on an agar plate containing the appropriate antibiotics was prepared and incubated overnight at 37 °C. This backup plate was used to

inoculate an overnight culture with bacteria carrying the correct plasmid-construct, as determined by PCR.

Table 4-7 Conditions used for analytical- and colony-PCR reactions.

Step	**Temperature** [°C]	**Time** [sec]
Initial denaturation	95	120-300
Denaturation	95	30
Annealing	primer dependent	60
Extension	72	60/1 kb
Final extension	72	600
Storage	4	∞

4.1.8 Plasmid isolation

For the isolation of plasmid DNA out of *E. coli*, the plasmid mini prep kit from Qiagen was used. Depending on the copy number of the plasmid, the yield was in the range of 0.8 to 7 µg plasmid DNA. Seven milliliters LB-medium with the respective selection antibiotics was inoculated with a single colony from an LB agar plate. After incubation overnight at 37 °C, the plasmid was isolated according to the manufacturers protocol.

4.1.9 Restriction digest of DNA

Isolated DNA was digested with sequence-specific restriction endonucleases purchased from New England Biolabs (Ipswich, USA). Digestion reactions were carried out according to the manufacturer´s guidelines for each enzyme. In case that two restriction enzymes required different buffer conditions, the reactions were carried out sequentially. After the first restriction digest, the DNA was purified with the QIAquick PCR purification kit from Qiagen to exchange the reaction buffer according to the requirements of the second restriction enzyme.

4.1.10 Dephosphorylation of DNA

Vector DNA was dephosphorylated at its 5´-ends to prevent re-ligation. The restriction enzymes were heat-inactivated according to the manufacturer´s guidelines after the restriction digest. Subsequently, 10 U of a calf intestine alkaline phosphatase (New England Biolabs, Ipswich, USA) were added to the reaction and incubated for 1 h at 37°C. The linearized vector DNA was purified by agarose gel electrophoresis and extracted from the agarose gel with a gel extraction kit from Qiagen.

4.1.11 Ligation of DNA

After restriction digestion, purified DNA fragments were mixed at vector:insert ratios of 1:3 or 1:5 in the presence of T4 DNA ligase (ThermoFisher Scientific, Waltham, USA) and the appropriate buffer. For sticky-end ligation the reaction was incubated for 30 minutes and for blunt-end ligation for 1 hour at room temperature. Alternatively, the ligation reaction was incubated overnight at 16 °C. Five microliters of each ligation reaction were transformed in chemically competent *E. coli* DH5α or electrocompetent *E. coli* DH10b.

4.1.12 DNA sequencing

For sequencing of DNA, 20 µl of DNA with a concentration ranging 30 ng/µl to 100 ng/µl were sent to the sequencing company GATC (Konstanz). Primers were chosen from their database. Alternatively, if no matching primer was available, 20 µl of a proprietary primer with a concentration of 10 pmol/µl was sent in addition.

4.1.13 Preparation of chemically competent cells

For the preparation of chemically competent *E. coli* cells, 250 ml TYM-medium were inoculated with 5 ml of an overnight culture and incubated at 37 °C. If possible, an antibiotic selection marker was added to the overnight culture. When reaching an OD_{600} of 0.5 – 0.6 the cells were harvested by centrifugation for 15 min at 2000 g and 4 °C. The cell pellet was resuspended in 50 ml of ice-cold TFB1 buffer and centrifuged as before. Finally, the pellet was resuspended in 15 ml ice-cold TFB2 buffer. 50 µl aliquots were snap-frozen in liquid nitrogen and stored at -80 °C. All buffers and media were autoclaved. Manganese chloride and magnesium chloride were dissolved separately and sterilized by passing through a filter with a pore size of 0.2 µm.

Table 4-8 Media and buffers for the preparation of chemically competent cells.

Medium/Buffers	Composition	Concentration
TYM medium	Tryptone/peptone	20 g/l
	Yeast extract	5 g/l
	NaCl	0.1 M
	$Mg(SO_4)$ * 7 H_2O	10 mM
TFB1 buffer	Potassium acetate	30 mM
pH 5 – 5.6 with acetic acid	KCl	0.1 M
	$CaCl_2$ * 2 H_2O	10 mM
	Glycerol (v/v)	15 %
	$MnCl_2$ * 4 H_2O	50 mM
TFB2 buffer	MOPS-NaOH pH 7.0	10 mM
	$CaCl_2$ * 2 H_2O	75 mM
	KCl	10 mM
	Glycerol (v/v)	15 %

4.1.14 Preparation of electrocompetent cells

Electrocompetent *E. coli* DH10b MultiBac^{Cre} cells were used for the generation of bacmids for insect cell expression. To this end, bacteria were streaked out on low salt LB-agar for blue-white screening. To further select for the presence of the bacmid (bMON14272) and the helper-plasmids (pMON7142 and pBADZ-Cre) necessary for Tn7 transposition or *cre-lox* site-specific recombination of DNA from the transfer vectors (pFBDM and pUCDM) into the baculoviral DNA, the agar medium was supplemented with 50 µg/ml kanamycin, 10 µg/ml tetracyclin and 25 µg/ml zeocin. A single blue colony was used to inoculate 500 ml low salt LB-medium including kanamycin, tetracycline and zeocin (concentrations as before) and incubated at 37 °C under agitation. At an OD_{600} of 0.25, 0.1 % L-arabinose was added to express the Cre-recombinase, allowing the recombinant integration of DNA into the baculoviral DNA. The culture was grown to an OD_{600} of 0.5 and harvest by centrifugation. Prior to cell harvest, the culture was cooled down on ice for 15 minutes and centrifuged at 4 000 rpm, 4 °C for 15 minutes (SLC 4000 rotor, Sorvall). The cell pellet was resuspended in 500 ml of ice-cold and sterilized 10 % glycerol. This washing step was repeated three times with decreasing volumes of ice-cold

and sterilized 10 % glycerol (250 ml, 10 ml and 1 ml). From the final suspension, 40 µl aliquots were flash frozen in liquid nitrogen and stored at -80 °C.

This protocol was also used to prepare other *E. coli* stains for electro-transformation using an appropriate antibiotic-mix and blue-white screening if applicable.

4.1.15 Growth media for bacteria

Table 4-9 Composition of growth media for bacteria.

Medium	Composition	Concentration
Lauria-Bertani (LB) broth	Tryptone	10 g/l
	Yeast extract	5 g/l
	NaCl	10 g/l
LB-agar	LB-medium	
	Agar	15 g/l
Low salt LB	Tryptone	10 g/l
	Yeast extract	5 g/l
	NaCl	5 g/l
Low salt LB-agar	LB-medium	
	Agar	15 g/l
SOC-medium Note: glucose and magnesium were sterile-filtered and added separately to the autoclaved medium	Tryptone	20 g/l
	Yeast extract	5 g/l
	NaCl	10 mM
	KCl	2.5 mM
	Glucose	20 mM
	$MgSO_4$	10 mM
	$MgCl_2$	10 mM

4.1.16 Bacterial strains

Table 4-10 Bacterial strains.

Strain	Application	Manufacturer
E. coli DH10b	sub-cloning	Invitrogen
E. coli DH5α	sub-cloning	Invitrogen
E. coli DH10b MultiBac	bacmid production	I. Berger (Zürich)
E. coli BL21(DE3) pLysS	expression	Invitrogen

4.1.17 Transformation of chemically competent *E. coli* cells

For each transformation, 50 µl chemically competent *E. coli* cells were thawed on ice and incubated for 30 minutes with 10 ng purified plasmid DNA or 5 µl of a ligation/mutation reaction on ice. The mixture was subjected to a heat shock at 42 °C for 45 seconds and immediately cooled down for 5 minutes on ice before 250 µl pre-heated (37 °C) SOC-medium was added. Subsequently, the bacteria were incubated for 50 minutes at 37 °C for regeneration purposes and the development of antibiotic resistances encoded on the plasmid. In case purified plasmid DNA was transformed, 20 µl and 50 µl were streaked out on LB-agar including the respective antibiotic selection markers and incubated at 37 °C overnight. If a ligation or mutation reaction was transformed, the bacteria were centrifuged at room temperature for 3 minutes at 10.000 g. The pellet was resuspended in 100 µl SOC-medium and streaked out.

4.1.18 Transformation of electrocompetent *E. coli* cells

40 µl electrocompetent cells were thawed on ice, transferred to a pre-cooled 2 mm electroporation cuvette, and incubated for 15 minutes with 10 ng purified plasmid DNA, 10 ng bacmid DNA, or 5 µl of a ligation/mutation reaction on ice. The electroporation was carried out at 2.5 kV, 200 Ω, and 25 µF. One milliliter SOC-medium was added and the cells incubated in 2 ml reaction tubes for 1 – 2 hours at 37 °C under agitation. In case purified plasmid DNA was being transformed, 50 µl and 100 µl were streaked out on LB-agar including the respective antibiotic selection markers an incubated at 37 °C overnight. If a ligation or mutation reaction was transformed, the bacteria were centrifuged for 3 minutes at room temperature and 10 000 g. The pellet was resuspended in 100 µl SOC-medium and streaked out.

4.1.19 Blue-white screening

Blue-white screens can be used to identify bacteria transformed with a vector containing a ligated insert (white colonies). Re-ligated vector DNA can be identified as blue colonies. This method relies on the α-complementation that produces a functional β-galactosidase. The enzyme hydrolyses the chromogenic substrate Bluo-gal to produce insoluble blue pigments. Because β-galactosidase occurs in *E. coli*, only lacZΔM15 deletion mutants can be used for blue-white screening. To identify recombinant bacteria, transformed cells were streaked out on LB-agar containing 40 µg/ml Bluo-gal, 100 µg/ml IPTG, and appropriate antibiotics and incubated at 37 °C. Blue colonies (non-recombinant) could be distinguished from recombinant colonies (white) after one or two days.

4.1.20 Protein expression in *E. coli*

For protein expression, chemically competent *E. coli* BL21(DE3) pLysS cells were transformed with an expression vector and selected via its respective antibiotic resistances. A single colony was used to inoculate 100 ml overnight culture incubated at 37 °C under agitation, to serve as inoculum for the large-scale expression culture. Next, the overnight culture was used to inoculate the expression culture to reach an OD_{600} of 0.05 – 0.1. At an OD_{600} between 0.6 – 0.7, IPTG was added to a final concentration of 1 mM to induce protein expression. After induction, proteins were expressed for 4 hours at 37 °C under agitation and the cells harvested by centrifugation at 2000 rpm for 20 minutes at room temperature. The first pellet was washed once with PBS and centrifuged again in a 50 ml reaction tube. The final pellet was snap-frozen in liquid nitrogen and stored at -80 °C.

Alternatively, an auto-induction medium was used (Table 4-11). To this end, a one-liter expression culture was inoculated with 2 ml of a glycerol stock and incubated overnight at 37 °C under agitation. The bacteria were harvested as explained above.

Table 4-11 Composition of PBS and the auto-induction medium (AIM) for protein expression in *E. coli*.

Medium/Buffer	Composition	Concentration
PBS pH 7.4 Phosphate buffered saline	Na_2HPO_4	4,3 mM
	KH_2PO_4	1.5 mM
	NaCl	137 mM
	KCl	2.7 mM
AIM medium	tryptone/peptone	10 g/l
	yeast extract	5 g/l
	Na_2HPO_4	25 mM
	KH_2PO_4	25 mM
	NH_4Cl	50 mM
	Na_2SO_4	5 mM
	$MgSO_4$	2 mM
	glycerol	0,5 %
	glucose	0,5 g/l
	lactose	2 g/l

4.1.21 Bacmid generation and isolation

For demanding proteins, a baculovirus expression system was used that allows the expression of proteins as well as of multi protein complexes encoded by a single virus (Berger et al., 2004). Genes of interest were assembled into a transfer vector (pFBDM or pUCDM) essentially as described before (Berger et al., 2004). Detailed cloning strategies for proteins and protein complexes used in this thesis are described in the results section. The assembled transfer vectors were transformed into *E. coli* DH10 MultiBac^{Cre} by electroporation to incorporate genes into the baculoviral genome for insect cell expression. After regeneration at 37 °C for 4 hours in 1 ml SOC-medium, 150 µl were steaked out on LB-agar plates. The residual 850 µl were centrifuged for 3 minutes at room temperature and 10 000 g. The pellet was resuspended in SOC-medium and streaked out. Agar plates were incubated overnight at 37 °C. For the transformation of pFBDM vectors, agar plates for blue-white screening containing 100 µg/ml ampicillin, 50 µg/ml kanamycin, 10 µg/ml tetracycline, and 7 µg/ml gentamycin were used. For the transformation of pUCDM vectors, agar plates including 100 µg/ml ampicillin, 50 µg/ml kanamycin and 25 µg/ml chloramphenicol were used. In case that genes from both transfer vectors needed to be integrated into the bacmid, the pUCDM vector was transformed

first as described before. Then, *E. coli* DH10 MultiBac^{Cre} cells harboring the bacmid including an integrated pUCDM derivative were streaked on LB-agar plates for blue-white screening containing 25 µg/ml chloramphenicol, 50 µg/ml kanamycin, 100 µg/ml ampicillin and 10 µg/ml tetracycline and incubated overnight at 37 °C. Subsequently, one blue colony was used to prepare electrocompetent DH10 MultiBac^{Cre} cells including the pUCDM derivative within the bacmid. Finally, the pFBDM vector was transformed into these cells as described above and subjected to blue-white screening.

Bacmid DNA was isolated via alkaline lysis using the buffers S1 – S3 of the NucleoSpin Plasmid kit from Macherey Nagel. Five milliliters LB-medium including the respective antibiotics were inoculated with a single colony and incubated overnight at 37 °C. When blue-white screens were done, a white colony was taken for the overnight culture. 1.5 ml of the overnight culture was centrifuged and the pellet resuspended in 300 µl S1-buffer. For lysis, 300 µl S2-buffer were added, incubated for 1 – 2 minutes at room temperature and immediately neutralized with 300 µl S3-buffer. Precipitated material was removed by centrifugation. The supernatant (900 µl) was transferred to a fresh 1.5 ml reaction tube. Bacmid DNA was precipitated by adding 700 µl isopropanol. The resulting bacmid DNA pellet was once washed with ice-cold 70 % ethanol and dried at 30 °C.

4.2 Biochemical methods

4.2.1 Sodium dodecyl sulfate polyacrylamide gel electrophoresis (SDS-PAGE)

Analytical separation of proteins was performed by discontinuous SDS-PAGE (Laemmli, 1970), using 10 % separation gels, overlaid with a 4 % stacking gel. Protein samples were mixed with SDS sample buffer and denatured at 95 °C for 3 minutes. Subsequently, samples were chilled on ice for 2 minutes, centrifuged, and loaded into the wells of the acrylamide gel. All SDS-PAGEs were performed in Mini Protean III gel electrophoresis chambers (Bio-Rad, Munich) at a constant voltage between 150 V and 200 V. The Precision Plus Protein Standard All Blue was purchased from Bio-Rad (Munich). This standard consists of highly purified recombinant proteins of the sizes 250, 150, 100, 75, 50, 37, 25, 20, 15, and 10 kDa and was used to assess the apparent molecular weight of proteins.

Table 4-12 Composition of the SDS sample buffer and electrophoresis buffer.

Buffer	Composition	Concentration 1x	Amount 4x (20ml)
SDS sample buffer	Tris-HCl pH 6.8	63 mM	610 mg
	Glycerol	10 %	8 ml
	SDS	2 %	1.6 g
	Bromophenol blue	0,01 %	8 mg
	β-mercaptoethanol	5 %	4 ml
Electrophoresis buffer	Tris	25 mM	
	Glycine	250 mM	
	SDS (w/v)	0.1 %	

Table 4-13 Composition of 10 % acrylamide gel used for discontinuous SDS-PAGE. The outlined volumes are sufficient to prepare one gel.

Composition	Separation Gel 10 %	Stacking Gel 4 %
Tris-HCl 1.5M, pH 8.8	1.25 ml	---
Tris-HCl 0.5 M, pH 6.8	---	0,625 ml
H_2O	2.02 ml	1.5 ml
Acrylamide 30 % acrylamide/bisacrylamide (37.5:1)	1.65 ml	0.325 ml
APS 10 %	50 µl	25 µl
SDS 10 %	50 µl	25 µl
TEMED	5 µl	5 µl

4.2.2 Western blot

Western blot was used to transfer proteins resolved by SDS-PAGE onto a PVDF (Immobilon-FL, Millipore, Eschborn) membrane for their specific detection with antibodies. To this end, the wet blot system Mini Trans-Blot Cell (Bio-Rad, Munich) was used. The gel and the filter papers for chromatography (thickness of 0.7 mm, Macherey-Nagel, Düren) were equilibrated in transfer buffer and the PVDF membrane was activated with 100 % methanol. The blot sandwich was assembled as follows, from cathode to the anode (clear side and black side of the gel holder cassette, respectively). A fiber pad was first placed on the clear side of the gel holder cassette and overlaid with two sheets of the equilibrated filter paper, the PVDF membrane, the gel, two sheets of equilibrated filter paper, and finally a second fiber pad. Air bubbles were removed and the cassette closed. Proteins were transferred onto the membrane at 100 V for 1 hour or overnight at 30 V, both at 4 °C.

Table 4-14 Transfer buffer for Western Blot.

Buffer	Composition	Concentration
Transfer buffer	Tris	48 mM
	Glycine	39 mM
	SDS	1.3 mM
	Methanol (v/v)	20 %

4.2.3 Immunodetection of proteins on a PVDF membrane

Proteins transferred to the PVDF membrane were specifically detected with antibodies. In a first step unspecific binding of the antibodies to the membrane was blocked by incubating the membrane for 30 minutes in 5 % (w/v) milk powder dissolved in PBS-T (PBS plus 0,05 % Tween 20, for the composition of PBS refer to Table 4-11). Then, the milk powder solution was discarded and the membrane was washed three times with PBS-T for 5 minutes. Next, the membrane was incubated with primary antibody either for 2 hours at room temperature or overnight at 4 °C. Subsequently, the membrane was washed again three times with PBS-T for 5 minutes and incubated with the secondary antibody for 30 minutes at room temperature. At last, the membrane was washed three times with PBS-T as before, and the epitope-bound antibody was visualized and documented with a Li-Cor Odyssey Imaging system (Li-Cor Biosciences, Newton, USA).

All secondary antibodies suitable to work with the Li-Cor system were purchased from Invitrogen (Karlsruhe). Dilutions (1:10 000) were prepared in PBS-T supplemented with 1 % bovine serum albumin (w/v) and stored at -20 °C.

4.2.4 Antibodies

Table 4-15 Antibodies.

Antibody	Source	Dilution	Origin
Epsin-1 (clone B-12)	mouse	1:100	Santa Cruz
AP2-2µ1 (clone K-13)	goat	1:200	Santa Cruz
Dynamin I/II (clone N-19)	goat	1:100	Santa Cruz
AAK1 (#15354-1-AP)	rabbit	1:200	Proteintech
Clathrin heavy chain (#43820)	mouse	1:2000	BD Transduction

4.2.5 Coomassie brilliant blue staining

Proteins resolved by SDS-PAGE were visualized within the gel by Coomassie staining. The gel was placed into the staining solution and heated in a microwave for 30 seconds. The staining solution must not boil. After incubation for 15 minutes on a shaker, the staining solution was discarded and destaining solution was added. Again, the solution was heated in the microwave and incubated for 30 minutes on a shaker. After this, fresh destaining solution was added, but not heated, and the gel further incubated until it was completely destained.

Table 4-16 Solutions for the staining of SDS-gels with Coomassie.

Solutions	Composition	Concentration
Staining solution (v/v)	Coomassie R250	2.5 g/l
	Acetic acid	10 %
	Ethanol	40 %
Destaining solution (v/v)	Acetic acid	5 %
	Ethanol	20 %

4.2.6 Determination of protein concentration

The concentration of proteins was determined with the Bradford assay (Bradford, 1976). Up to 8 µl of a protein solution were incubated with 1 ml of fivefold diluted Bradford reagent (Bio-Rad, Munich) for 10 minutes at room temperature. The absorption was measured at 595 nm and the concentration calculated with the help of BSA standard solutions.

4.2.7 Purification of OST-tagged proteins

Two pellets of a 500 ml Sf9 insect cell expression culture or one pellet originating from 2 liters of bacterial expression culture were thawed at 37 °C with 15 ml purification buffer, supplemented with protease inhibitor cocktail (Roche, Basel, Switzerland). Insect cells were lysed by sonification, *E. coli* by passing them through a microfluidizer four times (Microfluidics, Newton, USA) at 12 k psi. Cell debris were removed via centrifugation at 100 000 g for one hour at 4 °C. The cleared supernatant was incubated with 3 ml (1 column volume (CV)) Strep-Tactin Sepharose beads (IBA Lifesciences, Göttingen) equilibrated in purification buffer for 2 hours at 4 °C on a rotary wheel. For the purification of clathrin, 3 ml Strep-Tactin Sepharose beads were used for one pellet originated from a 500 ml insect cell expression. After the proteins had bound, the beads were pelleted at 2000 rpm for 5 minutes at 4 °C and transferred to a gravity flow column (Bio-Rad, Munich). The supernatant was discarded. To remove unbound proteins, 3 CVs of purification buffer were applied to the column to remove unbound proteins. Finally, bound proteins were eluted in 1 ml fractions. Protein containing fractions were pooled and subjected to a PD-10 desalting column (GE Healthcare, Chalfont St Giles, UK) for the exchange of purification buffer with storage buffer. Proteins were aliquoted, snap-frozen and stored at -80 °C

For multiple use, beads were regenerated after each purification and stored according to the manufacturer's protocol.

Table 4-17 Buffers used for the purification of Strep-tagged proteins.

Medium/Buffers	Composition	Concentration
Purification buffer	HEPES/KOH pH 8.0	25 mM
	Potassium acetate	300 mM
	1-Thioglycerol (v/v)	0.05 %
Elution buffer	HEPES/KOH pH 8.0	25 mM
	Potassium acetate	300 mM
	1-Thioglycerol	0.05 %
	Desthiobiotin	2.5 mM
Storage buffer	HEPES/KOH pH 8.0	25 mM
	Potassium acetate	300 mM
	1-Thioglycerol	0.05 %
	Glycerol (w/w)	10 %

4.2.8 Purification of GST-tagged proteins

The purification of GST-tagged proteins was essentially performed as described for OST-tagged proteins (chapter 4.2.7) but using Glutathione Sepharose 4 Fast Flow beads (GE Healthcare, Chalfont St Giles, UK) instead of Strep-Tactin Sepharose.

Table 4-18 Buffers used for the purification of GST-tagged proteins.

Medium/Buffers	Composition	Concentration
Purification buffer	HEPES/KOH pH 8.0	25 mM
	Potassium acetate	300 mM
	1-Thioglycerol (v/v)	0.05 %
Elution buffer	HEPES/KOH pH 8.0	25 mM
	Potassium acetate	300 mM
	1-Thioglycerol	0.05 %
	Reduced glutathione	10 mM
Storage buffer	HEPES/KOH pH 8.0	25 mM
	Potassium acetate	300 mM
	1-Thioglycerol	0.05 %
	Glycerol (w/w)	10 %

4.2.9 Purification of His-tagged proteins

The purification of His-tagged proteins was essentially achieved as described for OST-tagged proteins (chapter 4.2.7) but using Ni Sepharose 4 Fast Flow beads (GE Healthcare, Chalfont St Giles, UK) instead of Strep-Tactin Sepharose. Bound proteins were eluted from the column with increasing amounts of imidazole, as is described for each His-tagged protein in the result part.

Table 4-19 Buffers used for the purification of His-tagged proteins.

Medium/Buffers	Composition	Concentration
Purification buffer	HEPES/KOH pH 8.0	25 mM
	Potassium acetate	300 mM
	Imidazole	25 mM
	1-Thioglycerol (v/v)	0.05 %
Elution buffer	HEPES/KOH pH 8.0	25 mM
	Potassium acetate	300 mM
	1-Thioglycerol	0.05 %
	Imidazole	40 – 500 mM
Storage buffer	HEPES/KOH pH 8.0	25 mM
	Potassium acetate	300 mM
	1-Thioglycerol	0.05 %
	Glycerol (w/w)	10 %

4.2.10 Chloroform-methanol precipitation

The method was used to concentrate proteins of a diluted solution. It was performed before the proteins were subjected as samples to SDS-PAGE. This fast and quantitative method is based on a defined mixture of chloroform, methanol and water. To 100 µl of sample, 400 µl methanol, 200 µl chloroform, and 200 µl H_2O were added successively. After each addition of a solvent or water the sample was mixed by vortexing. For a faster phase separation, the mixture was centrifuged in a table top centrifuge for 2 minutes at maximum speed and room temperature. The proteins appear as white precipitate at the interphase. The upper phase was carefully removed without disturbing the precipitated proteins. Subsequently, 300 µl methanol was added, the sample vigorously vortexed and centrifuged again for 5 minutes as before. Now, the

precipitated proteins form a white pellet at the bottom of the tube. Finally, the supernatant was discarded and the pellet dried using a vacuum concentrator (RVC 2-18, Chris, Osterode). For SDS-PAGE analysis, the pellet was dissolved in 1x SDS sample buffer and incubated at 95 °C for 3 minutes.

4.2.11 Size exclusion chromatography (SEC)

Affinity purified proteins were further purified by size exclusion chromatography (SEC). To this end, an appropriate column was connected to an ÄKTAprime plus system (GE Healthcare, Chalfont St Giles, UK) and equilibrated with storage buffer (25 mM HEPES pH 8.0, 300 mM KOAc, 0.05 % 1-Thioglycerol, and 10 % glycerol). Chromatography conditions according to the manufacturer's protocols were chosen, if not otherwise stated in the result part. The calibration standard for SEC was purchased from Bio-Rad (Munich). It contains the five proteins thyroglobulin (670 kDa, bovine), γ-globulin (158 kDa, bovine), ovalbumin (44 kDa, chicken), myoglobulin (17 kDa, horse), and vitamin B12 (1.35 kDa).

4.2.12 Reversed-phase high-performance liquid chromatography (HPLC)

Reversed-phase chromatography was used to control the nucleotide state of dynamin and to determine its GTP-hydrolysis rate. Before loading onto an equilibrated HiChrom Ultrasphere 5 ODS column (MZ Analysetechnik, Mainz), 150 µl (15 - 20 µM) of each dynamin isoform were heated up to 95 °C for 1 min. The precipitated material was pellet by centrifugation. Standard GDP and GTP solution (10 nmol each) eluted after 4.7 minutes and 6 minutes, respectively. A model 1525 HPLC system (Waters, Eschborn) was used for the analytical runs at a flow rate of 1 ml/min. The nucleotides were detected via absorbance at a wavelength of 254 nm.

Table 4-20 Buffer used for reversed-phase HPLC.

Buffer	Composition	Concentration
HPLC buffer	KH_2PO_4/K_2HPO_4 pH 6.5	100 mM
	Tetra butyl ammonium bromide	10 mM
	Acetonitrile (v/v)	7.5 %

4.2.13 GTP-hydrolysis assay

To analyze if recombinant dynamin is able to hydrolyze GTP to GDP, 1 µM dynamin was incubated in the presence of 2 mM GTP with or without 0.1 mM liposomes (100 nm) at 37 °C

for 30 minutes. At various time points samples were taken, diluted 1:15 with assay buffer including 5 mM EDTA, and snap-frozen in liquid nitrogen to stop the reaction. Then, the thawed samples were prepared for reversed-phase chromatography as described for the determination of the nucleotide state of dynamin (chapter 4.2.12).

4.2.14 Synthesis of TGN38-lipopeptide

Since the stable recruitment of the endocytic adapter protein complex 2 (AP-2) to the plasma membrane depends in addition to $PI(4,5)P_2$ also on binding to a cargo molecule, a lipopeptide was synthesized mimicking an endocytic cargo which was incorporated into the lipid mixtures for liposome and GUV preparations. To this end, a short peptide (Figure 2-11) resembling the cytoplasmic part of the *trans*-Golgi network integral membrane protein TGN38 was linked to a maleimide group containing lipid (MPB-PE (16:0), Avanti Polar Lipids, Alabaster, USA) essentially as described before (Nickel and Wieland, 2001). The peptide was synthesized with an N-terminal cysteine. At its C-terminus, the peptide harbors the sorting signal (YQRL) which is recognized as the cargo binding motif YxxΦ by AP-2.

The synthesis was set up by transferring an appropriate volume of the activated lipid, dissolved in chloroform, to a glass vial or another chloroform-resistant tube. Chloroform was evaporated using a gentle stream of nitrogen. To start the reaction, a 10 % molar excess of the peptide dissolved in 1 ml DMF was added. Therefore, the cysteine-containing TGN38 peptide was analyzed for potential oxidation of the N-terminal thiol group by employing the Ellman´s reagent (ThermoFisher Scientific, Waltham, USA) according to the manufacturer`s instructions prior to each synthesis. The reaction was overlaid with argon and incubated overnight at room temperature on a rotating wheel. On the next day, free maleimide groups were quenched by adding 20 µl β-mercaptoethanol before the solvent was evaporated with the help of a vacuum concentrator (RVC 2-18, Chris, Osterode). The dried samples can be stored at -80 °C.

The lipopeptide was purified by reversed phase chromatography. Accordingly, a 1 ml (CV) SEP-Pak C18 cartridge (Waters, Eschborn) was treated with 2 CVs 100 % acetonitrile (AN) followed by 30 CVs of 30 % AN/0.1 % trifluoroacetic acid (TFA) for equilibration. The dried sample was dissolved in 30 % AN/0.1 % TFA and loaded onto the column. Bound proteins were eluted from the column in 2 ml fractions using increasing concentrations of AN acidified with 0.1 % TFA as before, 2 CVs 30 % AN, 2 CVs 40 % AN, 2 CVs 60 % AN, 2 CVs 80 % AN, 4 CVs 90 % AN and 2 CVs 100 % AN. The vast majority of lipopeptide eluted typically at 80 % AN. All fractions were dried in a vacuum concentrator, overlaid with argon, and stored at -80 °C.

The dried fractions were dissolved in 100 µl 95 % methanol/0.1 % TFA. Ten microliters of each fraction were analyzed together with 40 nmol of the activated lipid, 40 nmol of the TGN38 peptide, and 3 µl of the reaction mixture (after incubation) by thin layer chromatography (TLC). A mixture of butanol, pyridine, acetic acid, and water (9.7 : 7.5 : 1.5 : 6; v:v:v:v) was used as the solvent system together with a standard silica 60 glass plate (20 x 20 cm) (Merck, Darmstadt). Silica plates were developed for at least 3 hours. After separation, the silica plate was kept for 1 hour in a fume hood to remove remaining solvent by evaporation. The used lipid and peptide can be visualized by ninhydrin staining. Fractions with a similar purity were pooled and dried again. The pool was overlaid with argon and stored at -80 °C.

4.2.15 Phosphate determination

The concentration of the synthesized TGN38-lipopeptide pool was determined via its phosphate content, according to (Rouser et al., 1970).

The pooled lipopeptide was dissolved in 95 % methanol/0.1 % trifluoroacetic acid (TFA). A solution of 0.4 mM potassium dihydrogen phosphate was used to prepare standards in the range of 0 – 40 nmol phosphate. All reactions were performed in glass tubes. For the standard reactions, desired amounts were transferred to glass tubes and adjusted to 500 µl with H_2O. Volumes between 10 µl – 25 µl of the dissolved lipopeptide were transferred to glass tubes and dried. To release the phosphate, 150 µl perchloric acid was added to each reaction and only the lipid reactions were incubated for 40 minutes at 180 °C. After cooling, 500 µl H_2O was added to the lipid reactions to adjust their volumes to that of the standard reactions. Then, equal volumes of 1.25 % ammonium molybdate and 5 % ascorbic acid were mixed and 400 µl of this mixture added to each reaction. Subsequently, all reactions were incubated for 5 minutes at 100 °C. Finally, the absorption at 797 nm was measured to calculate the concentration of the lipopeptide pool. Aliquots containing the desired lipopeptide amounts were prepared, dried, and stored at -80 °C overlaid with argon.

4.2.16 Determination of ADP-concentration

The fluorometric ADP Assay Kit from abcam (Cambridge, UK) was used to estimate the degree of phosphorylated AP-2µ upon incubation with AAK1 and ATP. To this end, AP-2, AAK1 (each 1 µM) and, 2 mM ATP were incubated in assay buffer for 30 minutes in a final assay volume of 50 µl. AP-2 with a mutated µ-subunit (T156E) was used in a control reaction. After the incubation time, 5 µl of a 100 mM EDTA solution was added to stop the reaction. Twenty

and thirty microliters of each phosphorylation reaction were finally used to determine the ADP concentration according to the manufacturer's protocol.

4.2.17 Electron microscopy

Samples for negative stain electron microscopy were prepared according to Table 4-21. A drop of each solution or sample was placed on Parafilm. Carbon coated copper grids were glow-discharged shortly before the sample adsorption step. In the final contrasting step with uranyl acetate, methyl cellulose as an embedding reagent was included to preserve putative ultrastructures. A regular methyl cellulose film was achieved by collecting and drying the grids with drying-loops (diameter of 4 mm and a wire diameter of 0.3 mm). For Epon-embedding, 2 % glutaraldehyde was added to the sample. Subsequently, the sample was incubated for 10 minutes at room temperature and pelleted for 30 minutes at 100 000 g. The further processing of samples for Epon-embedding and sample imaging with an EM-900 transmission electron microscope (Zeiss, Oberkochen) were performed by Andrea Hellwig from the Bading group at the Interdisciplinary Center for Neurosciences (INZ) at the University of Heidelberg.

Table 4-21 Protocol for negative stain electron microscopy.

Step	**Time** [min]	**Solution**
Sample adsorption	15	
Fixation	10	1 % glutaraldehyde in buffer
Washing	1	buffer
Contrast enhancing	5	0.05 % tannic acid in H_2O
Washing	1	H_2O
Contrasting	10	0.4 % uranyl acetate 1.8 % methyl cellulose

4.2.18 Preparation of liposomes

All lipids used for the preparation of liposomes were purchase from Avanti Polar Lipids (Alabaster, USA) and stored at -20 °C overlaid with Argon to prevent oxidation. The lyophilized phosphatidylinositol-4,5-bisphosphate ($PI(4,5)P_2$) and the lipopeptides were

reconstituted in a mixture of chloroform, methanol, and water (20:9:1), all other lyophilized lipids were reconstituted in chloroform. The lipids were mixed in a 2 ml Eppendorf tube. To prevent precipitation of $PI(4,5)P_2$, the appropriate volume of a mixture of chloroform, methanol and water (20:9:1), that is needed to adjust the lipid mix to the desired concentration, was added to the Eppendorf tube first. Liposomes with different amounts of $PI(4,5)P_2$ or the TGN38-lipopeptide were prepared by substituting PC with equivalent amounts of $PI(4,5)P_2$ or TGN38-lipopeptide. For fluorescence microscopy and fluorescence measurements, PE-lissamine rhodamine B was added. The lipid mixture was aliquoted and dried using a vacuum concentrator (RVC 2-18, Chris, Osterode). Dried lipid films were overlaid with argon and stored at -80 °C until use. Liposomes were resuspended to the desired concentration in an appropriate volume, vortexed until homogeneity, and subjected to freeze-thaw cycles to make them unilamellar. To this end, the homogeneous liposome suspension was immersed for 5 minutes into liquid nitrogen and immediately thawed at 37 °C for 5 minutes. These steps were repeated ten times.

Table 4-22 Lipid composition of plasma membrane (PM)-like (Malsam et al., 2012) and BPLE-derived liposomes. All lipids were ordered from Avanti Polar Lipids (Alabaster, USA).

Lipid	**Order number**		**PM-like** [mol%]	**BPLE-derived** (w/w)
Phosphatidylcholine	840055	**PC**	16 – 36	---
Phosphatidylethanolamine	840026	**PE**	20	---
PE-Rhodamine	810150	**PE-R**	1	1
Phosphatidylserine	840032	**PS**	15	---
Phosphatidylinositol	840042	**PI**	3	---
Cholesterol	700000	**Chol**	25	20
Brain Polar Lipid Extract	141101	**BPLE**	---	59 – 69
Phosphatidylinositol-4,5-bisphosphate	840046	**PIP_2**	0 – 10	0 – 10
TGN38-Lipopeptide		**TGN38**	0 – 10	0 – 10
Ni^{2+}-NTA-DGS	790404	**Ni^{2+}-NTA-DGS**	0 – 5	0 – 5

4.2.19 Float-up analysis

Float-up experiments were done to determine the amount of proteins bound to liposomes. Following incubation, one to five percent of each reaction mixture were used as the input sample. A solution of 65 % sucrose (w/w) was added to the residual reaction mixture to a final

concentration of 40 % sucrose and the sample mixed thoroughly. Then, this solution was transferred to a 0.7 ml SW60 tube and carefully overlaid with 200 µl of 30 % sucrose (w/w) and finally 50 µl assay buffer. All sucrose solutions were prepared in the respective assay buffer. The gradients were centrifuged for 1 hour at 50 000 rpm at 4 °C in a SW60 swinging bucket rotor (Beckmann Coulter, Brea, USA) to isolate liposomes coated with proteins from the reaction mixture. One hundred microliter from the top of the gradient were taken to collect the protein coated liposomes (top fraction). Indicated amounts (result part) of the inputs and the top fractions were resolved on a 10 % SDS-gel and analyzed by Coomassie staining or immunoblotting.

4.2.20 Fluorescence microscopy

GUVs were visualized by rhodamine fluorescence on a Nikon Eclipse Ti-S inverted fluorescence microscope equipped with a G-2A filter cube (Em: 510 – 560 nm; Ex: 590 nm cut-on). The microscopy chamber µ-Slide 18 Well from ibidi (Martinsried, Munich) was used for all measurements. Prior sample application, wells were treated with 2 % BSA to block unspecific binding of GUVs to the surface of the microscopy chamber. After blocking, the wells were washed twice with assay buffer with an osmolarity similar to that of the GUV solution. Finally, 0.2 – 0.5 µl of the GUV solution was placed onto the bottom of the well, that is filled with assay buffer.

4.2.21 Preparation of GUVs

Giant unilamellar vesicles (GUVs) were essentially prepared as described earlier (Malsam et al., 2012). To this end, 5 µmol dried lipids (PM-like mix (Table 4-22) supplemented with 1 mol% PI(4,5)P_2 and TGN38-lipopeptide, each) were dissolved in 690 µl reconstitution buffer (25 mM HEPES/KOH pH 7.4, 150 mM KOAc, 1 mM DTT, 100 µM EDTA) containing 1.1 % octyl-β-D-glucopyranoside (OG). Successively, 2 µl of a 25 % OG solution in reconstitution buffer was added until the lipid solution became clear and subsequently adjusted to 700 µl with reconstitution buffer. Two volumes (1.4 ml) of reconstitution buffer was rapidly added and vortexed to dilute the detergent, that allow the formation of small unilamellar vesicles (SUVs). At this point it is important to take an aliquot as input, that is used to determine the concentration of generated GUVs. Therefore, 16 µl were diluted 1:50 in H_2O containing 1 % Triton X to solubilize the liposomes. Generated SUVs were subsequently desalted using a PD-10 desalting column (GE Healthcare, Chalfont St Giles, UK) equilibrated with 25 ml desalting buffer (1 mM HEPES/KOH pH 7.4, 20 mM trehalose, 1 % glycerol (v/v), 1 mM DTT, 100 µM EDTA)

according to the manufacturer's spin protocol. The sample was applied to the desalting column and centrifuged for 2 minutes at 2000 g. Recovered SUVs were snap-frozen in liquid nitrogen as 500 µl aliquots and stored at -80 °C until use.

The SUVs needs to be desalted once more to remove residual detergent and salts prior to GUV preparation. To this end, an SUV aliquot was thawed and applied to a PD midiTrap G-25 desalting column (GE Healthcare) equilibrated with desalting buffer. After the sample had entered the packed bed completely, 550 µl desalting buffer were added. SUVs were eluted with 1.4 ml desalting buffer into a 1.5 ml low binding reaction tube (Biozym Scientific, Hessisch Oldenburg). The eluate was centrifuged in a TLA-55 rotor (Beckmann Coulter, Brea, USA) at 55000 rpm for 2 hours at 4 °C. Next, the pellet was resuspended in a total volume of 20 µl and spread as a uniform layer with a diameter of about 10 mm onto the surface of a 25 x 25 mm (0.05 mm thick) platinum foil (Alfa Aesar, Haverhill, USA). The platinum foil was attached to a glass support with double-sided adhesive tape. Subsequently, the liposome film was dried for 1 hour in a vacuum (50 mbar). An O-ring (20 x 2 mm) was placed onto the platinum foil, surrounding the dried lipid film to seal the chamber. The electroformation chamber was filled with 550 µl swelling buffer (1 mM HEPES/KOH pH 8, 272 mM sucrose, 1 mM DTT) and covered with a second platinum foil. GUVs were generated overnight at 10 Hz and 1 V at 4 °C. The next day, GUVs were detached from the bottom by gentle pipetting, transferred to a 1.5 low binding reaction tube and stored at 4 °C. GUVs were used up within the next three days.

Platinum foil preparation:

Before usage, all platinum foils were cleaned by applying 2 M NaOH for 2 hours followed by 4 % hydrofluoric acid for 10 minutes. The foils were thoroughly washed after each incubation step. An adhesive copper tape was applied to each foil to connect the assembled electroformation chamber to the power supply. The bottom platinum foil was covered with a Teflon tape, excluding a circular area with a diameter of about 10 mm. This space is used for the application of the concentrated SUV solution. Prior lipid application, both platinum foils were subjected to plasma cleaning for 2 minutes.

4.2.22 Vesicle formation assay with liposomes

Vesicle reconstitution experiments with the truncated epsin-1 construct ΔENTH-epsin-1 were essentially done as described previously (Dannhauser and Ungewickell, 2012) and in case of AP-2 and/or epsin-1 with minor differences. All reactions were performed with low-binding reaction tubes and pipette tips.

BPLE-derived liposomes (0.5 mg/ml) were first incubated with ΔENTH-epsin-1 (1.8 µM) in a final volume of 100 µl for 30 minutes at 25 °C in assay buffer (25 mM HEPES/KOH pH 7.5, 150 mM KOAc, 3 mM $MgCl_2$). To remove unbound proteins, the liposomes were pelleted for 10 minutes at 800 g and then resuspended in assay buffer containing clathrin (0.4 µM) and dynamin-1 (0.3 µM) in a final volume of 100 µl. After pre-incubation with dynamin and clathrin on ice for 30 minutes, the assay volume was quadrupled and GTP added to a final concentration of 2 mM. Vesicles were generated by incubating the reaction for 30 minutes at 37 °C. Then, the larger liposomes were pelleted (10 min at 10 000 g (low speed pellet (LSP)) and the supernatant was centrifuged at 100 000 g for 30 min (high speed pellet (HSP). The pellets were analyzed by Coomassie staining following SDS-PAGE, western blot, and electron microscopy. When AP-2 and/epsin-1 were used as clathrin adaptors, reactions were not centrifuged at 800 g after the incubation step of liposomes with adaptors. The concentration for AP-2 and epsin-1 was 1 µM. The concentrations for dynamin, clathrin and GTP were not altered.

4.2.23 Vesicle formation assay with GUVs

For reconstitution experiments it is important to control the osmolarity. Therefore, it was necessary to dialyze all proteins against assay buffer (25 mM HEPES/KOH pH 7.5, 150 mM KOAc). AP-2 and clathrin were diluted with assay buffer to 1.2 mM, epsin-1 to 2.2 mM and Dynamin to 1.5 mM, each in 100 µl – 200 µl. After two hours, the dialysis buffer was exchanged with fresh one and the dialyzes continued overnight. It is important to adjust the osmolarity of the dialysis buffer to that of the GUV solution with glycerol before the dialysis is started. All protein dilutions were centrifuged the next day for 10 minutes at 16 000 g to get rid of precipitated material. The concentration of each protein dilution was determined by comparing their adsorption at 280 nm with the absorption at the start of the dialysis using the spectrophotometer ND-1000 from NanoDrop.

Before each set of experiment, the GUVs were separated from aggregates, multilamellar GUVs and small liposomes with sizes corresponding to diameters typical for endocytic clathrin coated vesicles by differential centrifugation. To this end, 150 µl of the GUV solution was diluted 1:10 in assay buffer containing 100 µM EDTA and first centrifuged at 100 g to pellet aggregates and multilamellar GUVs. Subsequently, the supernatant was centrifuged at 5000 g to pellet the GUVs, small liposomes stay in the supernatant. The supernatant from the last centrifugation step was discarded almost completely. Finally, the GUV pellet was resuspended in 20 µl – 25 µl of assay buffer and the concentration determined by comparing the rhodamine fluorescence of

a 1:50 dilution (including 1 % Triton X) with that of an input, taken during GUV preparation (refer to chapter 4.2.21).

If not otherwise stated, 10 nmol GUVs were pre-incubated with 10 pmol AP-2 and/or epsin-1 for 10 minutes at 25 °C in assay buffer, before 10 pmol clathrin were added. The reaction was further incubated at 25 °C for 30 minutes in a final assay volume of 40 µl. Then, 10 pmol dynamin-2, 2 mM GTP and 3 mM $MgCl_2$ were added and the reaction with a final volume of 55 µl further incubated for 30 minutes at 37 °C. After pelleting the donor membranes at 10 000 g for 10 minutes, the cleared supernatant was analyzed by electron microscopy or subjected to float-up analysis.

The scale of the reactions was tripled when GUV-derived vesicles were subjected to float-up analysis. To this end, the supernatant cleared of donor membranes was adjusted 50 % sucrose (w/w) and split. Both fractions were overlaid with 200 µl of 45 % sucrose (w/w) and 50 µl assay buffer in a 0.7 ml SW60 tube and the gradients were centrifuged for one hour at 40 000 rpm in an SW60 swinging bucket rotor. All sucrose solutions were prepared in assay buffer. One hundred microliter from the top of each gradient were taken to collect the floated material (top fraction). Duplicates were combined and subjected to chloroform-methanol-precipitation. The whole pellet and 1.3 µl from the reaction mixture (input) were loaded on a 10 % SDS-gel and analyzed by immunoblotting. All reactions were performed with low-binding reaction tubes and pipette tips.

4.3 Cell biology methods

4.3.1 Insect cell cultivation

Sf9 cells were used for the expression of proteins in a suspension culture. The cells were cultivated either adherent as a monolayer in 10 – 75 cm^2 cell culture flasks or as suspension culture, both in Sf-900 II SFM medium (Invitrogen, Karlsruhe) at 27 °C and at ambient humidity in the presence of 5 % CO_2. The doubling time under these conditions is about 22 – 24 hours. The cell density of a suspension culture was kept between 1 x 10^6 cells/ml and 8 x 10^6 cells/ml.

4.3.2 Freezing and thawing of insect cells

Sf9 insect cells were frozen in 1ml aliquots of 1 x 10^7 cells in a mixture of 0.6 ml Sf-900 II SFM medium, 0.3 ml FCS, and 0.2 ml DMSO. Cells were first kept for 1 hour at -20 °C, followed by storage for 24 hours at -80 °C in cryo-tubes (ThermoFisher Scientific, Waltham, USA). Finally, the frozen cells were transferred to liquid nitrogen for long-term storage.

To initiate an Sf9 insect cell culture from a frozen stock, one aliquot (1 x 10^7 cells) was thawed at 37 °C and immediately spun down for 3 minutes at 1500 rpm at 4 °C to get rid of the DMSO. The cell pellet was resuspended in 22 ml of fresh Sf-900 II SFM medium (Invitrogen, Karlsruhe) supplemented with 10 % fetal calf serum and seed into a 75 cm^2 cell culture flask. The cells from 4 confluent monolayer cultures (75 cm^2) were detached and combined in a 250 ml Erlenmeyer flask in a final volume of 50 ml insect cell medium.

4.3.3 Cell counting

Cells were diluted to approximately 10^6 cells/ml with PBS and applied to a Neubauer chamber. Trypan blue (0.1 %) was added to distinguish between dead (blue) and living (unstained) cells. The average of living cells from 4 large squares was used to calculate the cell density per ml, according to the manufacturer's protocol.

4.3.4 Transfection of Sf9 insect cells and test expression of P1 virus

Isolated bacmid DNA was used to transfect Sf9 insect cells for the preparation of recombinant infectious baculovirus. 3 ml of an insect cell suspension with a density of 0.25 x 10^6 cells/ml were seeded in 6-well plates. Bacmid DNA was resuspended in 20 µl sterile H_2O and diluted with 200 µl SF900 II SFM medium. Separately, 15 µl Extreme Gene HP DNA transfection reagent (Roche, Basel, Switzerland) was diluted with 100 µl SF900 II SFM medium. 112 µl transfection reagent dilution was added to the diluted bacmid DNA and mixed. After the insect

cells had attached to the well (after about 10 min), 156 µl of the final mixture was pipetted to each well in a dropwise manner. Each transfection was done in duplicate. The plates were wrapped in parafilm to prevent evaporation of the medium and incubated for approximately 60 hours at 27 °C. The baculovirus-containing supernatants of the duplicates were combined and stored at 4 °C in the dark. This virus is referred to as the P1 virus. For a test expression, 2 ml fresh SF900 II SFM medium was added to each well. After incubation for further 48 hours at 27 °C, Sf9 cells were detached, pelleted in a table top centrifuge for 2 minutes at maximum speed and room temperature, and resuspended in 200 µl 1x SDS sample buffer to control protein expression by SDS-gel electrophoresis.

4.3.5 Baculovirus amplification

For baculovirus amplification, 25 ml of an uninfected Sf9 cell suspension with a density of 0.8 x 10^6 cells/ml was infected with 0.3 ml, 0.6 ml, 1 ml, and 3 ml of the P1 virus stock in 250 ml Erlenmeyer flasks and incubated for three days at 27 °C shaking with 80 rpm. Following incubation, 1 ml of the infected Sf9 cell suspension was centrifuged in a table top centrifuge for 2 minutes at maximum speed and room temperature and the pellet resuspended in 80 µl 1x SDS sample buffer to control protein expression in SDS-gel electrophoresis. To harvest the amplified baculovirus, the cell suspension was centrifuged in a 50 ml reaction tube for 5 minutes at 2000 rpm, 4 °C. The virus-containing supernatant was transferred to a fresh 50 ml reaction tube and stored at 4 °C in the dark. This virus, referred to as the P2 virus, was used for large scale protein expressions.

4.3.6 Large scale protein expression in insect cells

Large scale expression (500 ml Sf9 cell suspension) was carried out in 2 liter roller bottles at a cell density of 2 x 10^6 cells/ml. To this end, suitable amounts of the P2 virus stock necessary to infect the large-scale expression culture were determined by test expressions. To this end, 25 ml of an uninfected Sf9 cell suspension with a density of 2 x 10^6 cells/ml was infected with 0.15 ml, 0.3 ml, 0.6 ml, and 1 ml of the P2 virus stock in 250 ml Erlenmeyer flasks and incubated for three days at 27 °C shaking with 80 rpm. After incubation, 1 ml of the infected Sf9 cell suspension was centrifuged in a table top centrifuge for 2 minutes at maximum speed and room temperature and the pellet resuspended in 200 µl 1x SDS sample buffer to control protein expression in SDS-gel electrophoresis. The condition with the best expression level was used to infect the large-scale expression. After three days of incubation at 27 °C under agitation, 1 ml of the infected Sf9 cell suspension was centrifuged in a table top centrifuge for 2 minutes

at maximum speed and room temperature and the pellet resuspended in 200 µl 1x SDS sample buffer to control protein expression in SDS-gel electrophoresis. Sf9 cells were harvested by centrifugation at 2000 rpm for 5 minutes, washed once with-ice cold PBS, centrifuged again, and the pellet snap-frozen in liquid nitrogen. Until use, the pellets were stored at -80 °C.
If BIIC-stocks were used to infect large scale protein expression cultures, the incubation time at 27 °C was prolonged to 4 days.

4.3.7 Preparation and test expression with baculovirus-infected insect cell (BIIC) stocks

For long term storage of baculoviruses, baculovirus-infected insect cell (BIIC) stocks were prepared. To this end, 200 ml of a Sf9 insect cell suspension at a density of 1.0 x 10^6 cells/ml was infected with 10 ml of a P2 virus stock, that was previously used to successfully infect the large-scale expressions and incubated at 27 °C under agitation. The cells were harvested at 500 rpm for 10 minutes after one day of incubation. Then, the cells were resuspended in a mixture of 12 ml Sf-900 II SFM II medium, 6 ml FCS, and 2 ml DMSO. One milliliter aliquots were prepared and successively cooled down first for 20 minutes at 4 °C, then 2 hours at -20 °C, and lastly for two days at -80 °C. Finally, the aliquots were transferred to liquid nitrogen for long-term storage.
The amount of BIIC-stock necessary to infect a large-scale expression to achieve a high yield of protein expression was determined by test expressions. To this end, 25 ml of an insect cell suspension at a density of 2 x 10^6 cells/ml were infected with 25 µl, 50 µl, 75 µl, 100 µl, and 125 µl and incubated for 4 days at 27 °C under agitation. Following incubation, 1 ml of each test expression was centrifuged in a table top centrifuge for 2 minutes at maximum speed and room temperature and the pellet resuspended in 200 µl 1x SDS sample buffer to control protein expression in SDS-gel electrophoresis.

5 Literature

ADOLF, F., HERRMANN, A., HELLWIG, A., BECK, R., BRUGGER, B. & WIELAND, F. T. 2013. Scission of COPI and COPII vesicles is independent of GTP hydrolysis. *Traffic,* 14**,** 922-32.

ADOLF, F., RHIEL, M., RECKMANN, I. & WIELAND, F. T. 2016. Sec24C/D-isoform-specific sorting of the preassembled ER-Golgi Q-SNARE complex. *Mol Biol Cell,* 27**,** 2697-707.

AGUET, F., ANTONESCU, C. N., METTLEN, M., SCHMID, S. L. & DANUSER, G. 2013. Advances in analysis of low signal-to-noise images link dynamin and AP2 to the functions of an endocytic checkpoint. *Dev Cell,* 26**,** 279-91.

AGUILAR, R. C., BOEHM, M., GORSHKOVA, I., CROUCH, R. J., TOMITA, K., SAITO, T., OHNO, H. & BONIFACINO, J. S. 2001. Signal-binding specificity of the mu4 subunit of the adaptor protein complex AP-4. *J Biol Chem,* 276**,** 13145-52.

AHLE, S. & UNGEWICKELL, E. 1990. Auxilin, a newly identified clathrin-associated protein in coated vesicles from bovine brain. *J Cell Biol,* 111**,** 19-29.

ANDERSON, R. G. 1998. The caveolae membrane system. *Annu Rev Biochem,* 67**,** 199-225.

ANTONNY, B., BERAUD-DUFOUR, S., CHARDIN, P. & CHABRE, M. 1997. N-terminal hydrophobic residues of the G-protein ADP-ribosylation factor-1 insert into membrane phospholipids upon GDP to GTP exchange. *Biochemistry,* 36**,** 4675-84.

ANTONNY, B., BURD, C., DE CAMILLI, P., CHEN, E., DAUMKE, O., FAELBER, K., FORD, M., FROLOV, V. A., FROST, A., HINSHAW, J. E., KIRCHHAUSEN, T., KOZLOV, M. M., LENZ, M., LOW, H. H., MCMAHON, H., MERRIFIELD, C., POLLARD, T. D., ROBINSON, P. J., ROUX, A. & SCHMID, S. 2016. Membrane fission by dynamin: what we know and what we need to know. *EMBO J,* 35**,** 2270-2284.

ANTONNY, B., MADDEN, D., HAMAMOTO, S., ORCI, L. & SCHEKMAN, R. 2001. Dynamics of the COPII coat with GTP and stable analogues. *Nat Cell Biol,* 3**,** 531-7.

AVINOAM, O., SCHORB, M., BEESE, C. J., BRIGGS, J. A. & KAKSONEN, M. 2015. ENDOCYTOSIS. Endocytic sites mature by continuous bending and remodeling of the clathrin coat. *Science,* 348**,** 1369-72.

BALL, C. L., HUNT, S. P. & ROBINSON, M. S. 1995. Expression and localization of alpha-adaptin isoforms. *J Cell Sci,* 108 (Pt 8)**,** 2865-75.

BANNYKH, S. I., ROWE, T. & BALCH, W. E. 1996. The organization of endoplasmic reticulum export complexes. *J Cell Biol,* 135**,** 19-35.

BARLOWE, C. 1995. COPII: a membrane coat that forms endoplasmic reticulum-derived vesicles. *FEBS Lett,* 369**,** 93-6.

BARLOWE, C. 2003. Signals for COPII-dependent export from the ER: what's the ticket out? *Trends Cell Biol,* 13**,** 295-300.

BARLOWE, C., ORCI, L., YEUNG, T., HOSOBUCHI, M., HAMAMOTO, S., SALAMA, N., REXACH, M. F., RAVAZZOLA, M., AMHERDT, M. & SCHEKMAN, R. 1994. COPII: a membrane coat formed by Sec proteins that drive vesicle budding from the endoplasmic reticulum. *Cell,* 77**,** 895-907.

BARLOWE, C. & SCHEKMAN, R. 1993. SEC12 encodes a guanine-nucleotide-exchange factor essential for transport vesicle budding from the ER. *Nature,* 365**,** 347-9.

BECK, R., PRINZ, S., DIESTELKOTTER-BACHERT, P., ROHLING, S., ADOLF, F., HOEHNER, K., WELSCH, S., RONCHI, P., BRUGGER, B., BRIGGS, J. A. & WIELAND, F. 2011. Coatomer and dimeric ADP ribosylation factor 1 promote distinct steps in membrane scission. *J Cell Biol,* 194**,** 765-77.

BECK, R., SUN, Z., ADOLF, F., RUTZ, C., BASSLER, J., WILD, K., SINNING, I., HURT, E., BRUGGER, B., BETHUNE, J. & WIELAND, F. 2008. Membrane curvature induced by Arf1-GTP is essential for vesicle formation. *Proc Natl Acad Sci U S A,* 105**,** 11731-6.

BELDEN, W. J. & BARLOWE, C. 2001. Role of Erv29p in collecting soluble secretory proteins into ER-derived transport vesicles. *Science,* 294**,** 1528-31.

BERGER, I., FITZGERALD, D. J. & RICHMOND, T. J. 2004. Baculovirus expression system for heterologous multiprotein complexes. *Nat Biotechnol,* 22**,** 1583-7.

BETHUNE, J., KOL, M., HOFFMANN, J., RECKMANN, I., BRUGGER, B. & WIELAND, F. 2006. Coatomer, the coat protein of COPI transport vesicles, discriminates endoplasmic reticulum residents from p24 proteins. *Mol Cell Biol,* 26**,** 8011-21.

BI, X., CORPINA, R. A. & GOLDBERG, J. 2002. Structure of the Sec23/24-Sar1 pre-budding complex of the COPII vesicle coat. *Nature,* 419**,** 271-7.

BI, X., MANCIAS, J. D. & GOLDBERG, J. 2007. Insights into COPII coat nucleation from the structure of Sec23.Sar1 complexed with the active fragment of Sec31. *Dev Cell,* 13**,** 635-45.

BLAGITKO, N., SCHULZ, U., SCHINZEL, A. A., ROPERS, H. H. & KALSCHEUER, V. M. 1999. gamma2-COP, a novel imprinted gene on chromosome 7q32, defines a new imprinting cluster in the human genome. *Hum Mol Genet,* 8**,** 2387-96.

BOEHM, M., AGUILAR, R. C. & BONIFACINO, J. S. 2001. Functional and physical interactions of the adaptor protein complex AP-4 with ADP-ribosylation factors (ARFs). *EMBO J,* 20**,** 6265-76.

BOEHM, M. & BONIFACINO, J. S. 2001. Adaptins: the final recount. *Mol Biol Cell,* 12**,** 2907-20.

BONIFACINO, J. S. & GLICK, B. S. 2004. The mechanisms of vesicle budding and fusion. *Cell,* 116**,** 153-66.

BORNER, G. H., ANTROBUS, R., HIRST, J., BHUMBRA, G. S., KOZIK, P., JACKSON, L. P., SAHLENDER, D. A. & ROBINSON, M. S. 2012. Multivariate proteomic profiling identifies novel accessory proteins of coated vesicles. *J Cell Biol,* 197**,** 141-60.

BOUCROT, E., FERREIRA, A. P., ALMEIDA-SOUZA, L., DEBARD, S., VALLIS, Y., HOWARD, G., BERTOT, L., SAUVONNET, N. & MCMAHON, H. T. 2015. Endophilin marks and controls a clathrin-independent endocytic pathway. *Nature,* 517**,** 460-5.

BOUCROT, E., PICK, A., CAMDERE, G., LISKA, N., EVERGREN, E., MCMAHON, H. T. & KOZLOV, M. M. 2012. Membrane fission is promoted by insertion of amphipathic helices and is restricted by crescent BAR domains. *Cell,* 149**,** 124-36.

BOUCROT, E., SAFFARIAN, S., ZHANG, R. & KIRCHHAUSEN, T. 2010. Roles of AP-2 in clathrin-mediated endocytosis. *PLoS One,* 5**,** e10597.

BRADFORD, M. M. 1976. A rapid and sensitive method for the quantitation of microgram quantities of protein utilizing the principle of protein-dye binding. *Anal Biochem,* 72**,** 248-54.

BREMSER, M., NICKEL, W., SCHWEIKERT, M., RAVAZZOLA, M., AMHERDT, M., HUGHES, C. A., SOLLNER, T. H., ROTHMAN, J. E. & WIELAND, F. T. 1999. Coupling of coat assembly and vesicle budding to packaging of putative cargo receptors. *Cell,* 96**,** 495-506.

BUCHER, D., FREY, F., SOCHACKI, K. A., KUMMER, S., BERGEEST, J. P., GODINEZ, W. J., KRAUSSLICH, H. G., ROHR, K., TARASKA, J. W., SCHWARZ, U. S. & BOULANT, S. 2018. Clathrin-adaptor ratio and membrane tension regulate the flat-to-curved transition of the clathrin coat during endocytosis. *Nat Commun,* 9**,** 1109.

BUDNIK, A. & STEPHENS, D. J. 2009. ER exit sites--localization and control of COPII vesicle formation. *FEBS Lett,* 583**,** 3796-803.

BURGOS, P. V., MARDONES, G. A., ROJAS, A. L., DASILVA, L. L., PRABHU, Y., HURLEY, J. H. & BONIFACINO, J. S. 2010. Sorting of the Alzheimer's disease amyloid precursor protein mediated by the AP-4 complex. *Dev Cell,* 18**,** 425-36.

CABRERA, M., MUNIZ, M., HIDALGO, J., VEGA, L., MARTIN, M. E. & VELASCO, A. 2003. The retrieval function of the KDEL receptor requires PKA phosphorylation of its C-terminus. *Mol Biol Cell,* 14**,** 4114-25.

CAMLEY, B. A. & BROWN, F. L. 2011. Beyond the creeping viscous flow limit for lipid bilayer membranes: theory of single-particle microrheology, domain flicker spectroscopy, and long-time tails. *Phys Rev E Stat Nonlin Soft Matter Phys,* 84**,** 021904.

CANTLEY, L. C. 2002. The phosphoinositide 3-kinase pathway. *Science,* 296**,** 1655-7.

CAO, H., GARCIA, F. & MCNIVEN, M. A. 1998. Differential distribution of dynamin isoforms in mammalian cells. *Mol Biol Cell,* 9**,** 2595-609.

CHAPPIE, J. S., ACHARYA, S., LEONARD, M., SCHMID, S. L. & DYDA, F. 2010. G domain dimerization controls dynamin's assembly-stimulated GTPase activity. *Nature,* 465**,** 435-40.

CHAPPIE, J. S., MEARS, J. A., FANG, S., LEONARD, M., SCHMID, S. L., MILLIGAN, R. A., HINSHAW, J. E. & DYDA, F. 2011. A pseudoatomic model of the dynamin polymer identifies a hydrolysis-dependent powerstroke. *Cell,* 147**,** 209-22.

CHEN, H., FRE, S., SLEPNEV, V. I., CAPUA, M. R., TAKEI, K., BUTLER, M. H., DI FIORE, P. P. & DE CAMILLI, P. 1998. Epsin is an EH-domain-binding protein implicated in clathrin-mediated endocytosis. *Nature,* 394**,** 793-7.

CHEN, M. S., OBAR, R. A., SCHROEDER, C. C., AUSTIN, T. W., POODRY, C. A., WADSWORTH, S. C. & VALLEE, R. B. 1991. Multiple forms of dynamin are encoded by shibire, a Drosophila gene involved in endocytosis. *Nature,* 351**,** 583-6.

COCUCCI, E., AGUET, F., BOULANT, S. & KIRCHHAUSEN, T. 2012. The first five seconds in the life of a clathrin-coated pit. *Cell,* 150**,** 495-507.

COCUCCI, E., GAUDIN, R. & KIRCHHAUSEN, T. 2014. Dynamin recruitment and membrane scission at the neck of a clathrin-coated pit. *Mol Biol Cell,* 25**,** 3595-609.

COLLINS, B. M., MCCOY, A. J., KENT, H. M., EVANS, P. R. & OWEN, D. J. 2002. Molecular architecture and functional model of the endocytic AP2 complex. *Cell,* 109**,** 523-35.

CONNER, S. D. & SCHMID, S. L. 2002. Identification of an adaptor-associated kinase, AAK1, as a regulator of clathrin-mediated endocytosis. *J Cell Biol,* 156**,** 921-9.

COOK, T., MESA, K. & URRUTIA, R. 1996. Three dynamin-encoding genes are differentially expressed in developing rat brain. *J Neurochem,* 67**,** 927-31.

COOK, T. A., URRUTIA, R. & MCNIVEN, M. A. 1994. Identification of dynamin 2, an isoform ubiquitously expressed in rat tissues. *Proc Natl Acad Sci U S A,* 91**,** 644-8.

CRUMP, C. M. & BANTING, G. 1999. Phosphorylation of the medium chain subunit of the AP-2 adaptor complex does not influence its interaction with the tyrosine based internalisation motif of TGN38. *FEBS Lett,* 444**,** 195-200.

CZECH, M. P. 2003. Dynamics of phosphoinositides in membrane retrieval and insertion. *Annu Rev Physiol,* 65**,** 791-815.

DAMKE, H., BABA, T., WARNOCK, D. E. & SCHMID, S. L. 1994. Induction of mutant dynamin specifically blocks endocytic coated vesicle formation. *J Cell Biol,* 127**,** 915-34.

DAMKE, H., BINNS, D. D., UEDA, H., SCHMID, S. L. & BABA, T. 2001. Dynamin GTPase domain mutants block endocytic vesicle formation at morphologically distinct stages. *Mol Biol Cell,* 12**,** 2578-89.

DANNHAUSER, P. N. & UNGEWICKELL, E. J. 2012. Reconstitution of clathrin-coated bud and vesicle formation with minimal components. *Nat Cell Biol,* 14**,** 634-9.

DAUMKE, O., ROUX, A. & HAUCKE, V. 2014. BAR domain scaffolds in dynamin-mediated membrane fission. *Cell,* 156**,** 882-92.

DAWSON, J. C., LEGG, J. A. & MACHESKY, L. M. 2006. Bar domain proteins: a role in tubulation, scission and actin assembly in clathrin-mediated endocytosis. *Trends Cell Biol,* 16**,** 493-8.

DE MATTEIS, M. A. & LUINI, A. 2008. Exiting the Golgi complex. *Nat Rev Mol Cell Biol,* 9**,** 273-84.

DEAN, N. & PELHAM, H. R. 1990. Recycling of proteins from the Golgi compartment to the ER in yeast. *J Cell Biol,* 111**,** 369-77.

DELL'ANGELICA, E. C., MULLINS, C. & BONIFACINO, J. S. 1999. AP-4, a novel protein complex related to clathrin adaptors. *J Biol Chem,* 274**,** 7278-85.

DELL'ANGELICA, E. C., OHNO, H., OOI, C. E., RABINOVICH, E., ROCHE, K. W. & BONIFACINO, J. S. 1997. AP-3: an adaptor-like protein complex with ubiquitous expression. *EMBO J,* 16**,** 917-28.

DEN OTTER, W. K. & BRIELS, W. J. 2011. The generation of curved clathrin coats from flat plaques. *Traffic,* 12**,** 1407-16.

DI PAOLO, G. & DE CAMILLI, P. 2006. Phosphoinositides in cell regulation and membrane dynamics. *Nature,* 443**,** 651-7.

DODONOVA, S. O., ADERHOLD, P., KOPP, J., GANEVA, I., ROHLING, S., HAGEN, W. J. H., SINNING, I., WIELAND, F. & BRIGGS, J. A. G. 2017. 9A structure of the COPI coat reveals that the Arf1 GTPase occupies two contrasting molecular environments. *Elife,* 6.

DODONOVA, S. O., DIESTELKOETTER-BACHERT, P., VON APPEN, A., HAGEN, W. J., BECK, R., BECK, M., WIELAND, F. & BRIGGS, J. A. 2015. VESICULAR TRANSPORT. A structure of the COPI coat and the role of coat proteins in membrane vesicle assembly. *Science,* 349**,** 195-8.

DOMINGUEZ, M., DEJGAARD, K., FULLEKRUG, J., DAHAN, S., FAZEL, A., PACCAUD, J. P., THOMAS, D. Y., BERGERON, J. J. & NILSSON, T. 1998. gp25L/emp24/p24 protein family members of the cis-Golgi network bind both COP I and II coatomer. *J Cell Biol,* 140**,** 751-65.

DONALDSON, J. G., FINAZZI, D. & KLAUSNER, R. D. 1992. Brefeldin A inhibits Golgi membrane-catalysed exchange of guanine nucleotide onto ARF protein. *Nature,* 360**,** 350-2.

DONALDSON, J. G. & HONDA, A. 2005. Localization and function of Arf family GTPases. *Biochem Soc Trans,* 33**,** 639-42.

DONALDSON, J. G. & JACKSON, C. L. 2011. ARF family G proteins and their regulators: roles in membrane transport, development and disease. *Nat Rev Mol Cell Biol,* 12**,** 362-75.

DORAY, B. & KORNFELD, S. 2001. Gamma subunit of the AP-1 adaptor complex binds clathrin: implications for cooperative binding in coated vesicle assembly. *Mol Biol Cell,* 12**,** 1925-35.

DORAY, B., LEE, I., KNISELY, J., BU, G. & KORNFELD, S. 2007. The gamma/sigma1 and alpha/sigma2 hemicomplexes of clathrin adaptors AP-1 and AP-2 harbor the dileucine recognition site. *Mol Biol Cell,* 18**,** 1887-96.

DRAB, M., VERKADE, P., ELGER, M., KASPER, M., LOHN, M., LAUTERBACH, B., MENNE, J., LINDSCHAU, C., MENDE, F., LUFT, F. C., SCHEDL, A., HALLER, H. & KURZCHALIA, T. V. 2001. Loss of caveolae, vascular dysfunction, and pulmonary defects in caveolin-1 gene-disrupted mice. *Science,* 293**,** 2449-52.

DRAKE, M. T., DOWNS, M. A. & TRAUB, L. M. 2000. Epsin binds to clathrin by associating directly with the clathrin-terminal domain. Evidence for cooperative binding through two discrete sites. *J Biol Chem,* 275**,** 6479-89.

DUDEN, R., GRIFFITHS, G., FRANK, R., ARGOS, P. & KREIS, T. E. 1991. Beta-COP, a 110 kd protein associated with non-clathrin-coated vesicles and the Golgi complex, shows homology to beta-adaptin. *Cell,* 64**,** 649-65.

EUGSTER, A., FRIGERIO, G., DALE, M. & DUDEN, R. 2004. The alpha- and beta'-COP WD40 domains mediate cargo-selective interactions with distinct di-lysine motifs. *Mol Biol Cell,* 15**,** 1011-23.

FAELBER, K., HELD, M., GAO, S., POSOR, Y., HAUCKE, V., NOE, F. & DAUMKE, O. 2012. Structural insights into dynamin-mediated membrane fission. *Structure,* 20**,** 1621-8.

FALKENBURGER, B. H., JENSEN, J. B., DICKSON, E. J., SUH, B. C. & HILLE, B. 2010. Phosphoinositides: lipid regulators of membrane proteins. *J Physiol,* 588**,** 3179-85.

FINGERHUT, A., VON FIGURA, K. & HONING, S. 2001. Binding of AP2 to sorting signals is modulated by AP2 phosphorylation. *J Biol Chem,* 276**,** 5476-82.

FLANNAGAN, R. S., JAUMOUILLE, V. & GRINSTEIN, S. 2012. The cell biology of phagocytosis. *Annu Rev Pathol,* 7**,** 61-98.

FOLSCH, H., OHNO, H., BONIFACINO, J. S. & MELLMAN, I. 1999. A novel clathrin adaptor complex mediates basolateral targeting in polarized epithelial cells. *Cell,* 99**,** 189-98.

FORD, M. G., MILLS, I. G., PETER, B. J., VALLIS, Y., PRAEFCKE, G. J., EVANS, P. R. & MCMAHON, H. T. 2002. Curvature of clathrin-coated pits driven by epsin. *Nature,* 419**,** 361-6.

FORD, M. G., PEARSE, B. M., HIGGINS, M. K., VALLIS, Y., OWEN, D. J., GIBSON, A., HOPKINS, C. R., EVANS, P. R. & MCMAHON, H. T. 2001. Simultaneous binding of PtdIns(4,5)P2 and clathrin by AP180 in the nucleation of clathrin lattices on membranes. *Science,* 291**,** 1051-5.

FOTIN, A., CHENG, Y., SLIZ, P., GRIGORIEFF, N., HARRISON, S. C., KIRCHHAUSEN, T. & WALZ, T. 2004. Molecular model for a complete clathrin lattice from electron cryomicroscopy. *Nature,* 432**,** 573-9.

FRANCO, M., CHARDIN, P., CHABRE, M. & PARIS, S. 1996. Myristoylation-facilitated binding of the G protein ARF1GDP to membrane phospholipids is required for its activation by a soluble nucleotide exchange factor. *J Biol Chem,* 271**,** 1573-8.

FUTATSUMORI, M., KASAI, K., TAKATSU, H., SHIN, H. W. & NAKAYAMA, K. 2000. Identification and characterization of novel isoforms of COP I subunits. *J Biochem,* 128**,** 793-801.

GAIDAROV, I. & KEEN, J. H. 1999. Phosphoinositide-AP-2 interactions required for targeting to plasma membrane clathrin-coated pits. *J Cell Biol,* 146**,** 755-64.

GAMBIN, Y., ARIOTTI, N., MCMAHON, K. A., BASTIANI, M., SIERECKI, E., KOVTUN, O., POLINKOVSKY, M. E., MAGENAU, A., JUNG, W., OKANO, S., ZHOU, Y., LENEVA, N., MUREEV, S., JOHNSTON, W., GAUS, K., HANCOCK, J. F., COLLINS, B. M., ALEXANDROV, K. & PARTON, R. G. 2013. Single-molecule analysis reveals self assembly and nanoscale segregation of two distinct cavin subcomplexes on caveolae. *Elife,* 3**,** e01434.

GARCIA-ALAI, M. M., HEIDEMANN, J., SKRUZNY, M., GIERAS, A., MERTENS, H. D. T., SVERGUN, D. I., KAKSONEN, M., UETRECHT, C. & MEIJERS, R. 2018. Epsin and Sla2 form assemblies through phospholipid interfaces. *Nat Commun,* 9**,** 328.

GILBERT, A., PACCAUD, J. P. & CARPENTIER, J. L. 1997. Direct measurement of clathrin-coated vesicle formation using a cell-free assay. *J Cell Sci,* 110 (Pt 24)**,** 3105-15.

GLEBOV, O. O., BRIGHT, N. A. & NICHOLS, B. J. 2006. Flotillin-1 defines a clathrin-independent endocytic pathway in mammalian cells. *Nat Cell Biol,* 8**,** 46-54.

GLICK, B. S. & LUINI, A. 2011. Models for Golgi traffic: a critical assessment. *Cold Spring Harb Perspect Biol,* 3**,** a005215.

GOMMEL, D. U., MEMON, A. R., HEISS, A., LOTTSPEICH, F., PFANNSTIEL, J., LECHNER, J., REINHARD, C., HELMS, J. B., NICKEL, W. & WIELAND, F. T. 2001. Recruitment to Golgi membranes of ADP-ribosylation factor 1 is mediated by the cytoplasmic domain of p23. *EMBO J,* 20**,** 6751-60.

GRIGLIATTI, T. A., HALL, L., ROSENBLUTH, R. & SUZUKI, D. T. 1973. Temperature-sensitive mutations in Drosophila melanogaster. XIV. A selection of immobile adults. *Mol Gen Genet,* 120**,** 107-14.

GUO, Y., SIRKIS, D. W. & SCHEKMAN, R. 2014. Protein sorting at the trans-Golgi network. *Annu Rev Cell Dev Biol,* 30**,** 169-206.

HAIGLER, H. T., MCKANNA, J. A. & COHEN, S. 1979. Rapid stimulation of pinocytosis in human carcinoma cells A-431 by epidermal growth factor. *J Cell Biol,* 83**,** 82-90.

HAO, W., LUO, Z., ZHENG, L., PRASAD, K. & LAFER, E. M. 1999. AP180 and AP-2 interact directly in a complex that cooperatively assembles clathrin. *J Biol Chem,* 274**,** 22785-94.

HARA-KUGE, S., KUGE, O., ORCI, L., AMHERDT, M., RAVAZZOLA, M., WIELAND, F. T. & ROTHMAN, J. E. 1994. En bloc incorporation of coatomer subunits during the assembly of COP-coated vesicles. *J Cell Biol,* 124**,** 883-92.

HENLEY, J. R., KRUEGER, E. W., OSWALD, B. J. & MCNIVEN, M. A. 1998. Dynamin-mediated internalization of caveolae. *J Cell Biol,* 141**,** 85-99.

HENNE, W. M., BOUCROT, E., MEINECKE, M., EVERGREN, E., VALLIS, Y., MITTAL, R. & MCMAHON, H. T. 2010. FCHo proteins are nucleators of clathrin-mediated endocytosis. *Science,* 328**,** 1281-4.

HERSKOVITS, J. S., BURGESS, C. C., OBAR, R. A. & VALLEE, R. B. 1993. Effects of mutant rat dynamin on endocytosis. *J Cell Biol,* 122**,** 565-78.

HEUSER, J. 1980. Three-dimensional visualization of coated vesicle formation in fibroblasts. *J Cell Biol,* 84**,** 560-83.

HEUSER, J. 1989. Effects of cytoplasmic acidification on clathrin lattice morphology. *J Cell Biol,* 108**,** 401-11.

HEWLETT, L. J., PRESCOTT, A. R. & WATTS, C. 1994. The coated pit and macropinocytic pathways serve distinct endosome populations. *J Cell Biol,* 124**,** 689-703.

HINSHAW, J. E. & SCHMID, S. L. 1995. Dynamin self-assembles into rings suggesting a mechanism for coated vesicle budding. *Nature,* 374**,** 190-2.

HIRST, J., BARLOW, L. D., FRANCISCO, G. C., SAHLENDER, D. A., SEAMAN, M. N., DACKS, J. B. & ROBINSON, M. S. 2011. The fifth adaptor protein complex. *PLoS Biol,* 9**,** e1001170.

HIRST, J., BORNER, G. H., EDGAR, J., HEIN, M. Y., MANN, M., BUCHHOLZ, F., ANTROBUS, R. & ROBINSON, M. S. 2013. Interaction between AP-5 and the hereditary spastic paraplegia proteins SPG11 and SPG15. *Mol Biol Cell,* 24**,** 2558-69.

HIRST, J., MOTLEY, A., HARASAKI, K., PEAK CHEW, S. Y. & ROBINSON, M. S. 2003. EpsinR: an ENTH domain-containing protein that interacts with AP-1. *Mol Biol Cell,* 14**,** 625-41.

HIRST, J., SCHLACHT, A., NORCOTT, J. P., TRAYNOR, D., BLOOMFIELD, G., ANTROBUS, R., KAY, R. R., DACKS, J. B. & ROBINSON, M. S. 2014. Characterization of TSET, an ancient and widespread membrane trafficking complex. *Elife,* 3**,** e02866.

HOLZMANN, K., POLTL, A. & SAUERMANN, G. 1998. A novel spliced transcript of human CLAPS2 encoding a protein alternative to clathrin adaptor protein AP17. *Gene,* 220**,** 39-44.

HONDA, A., NOGAMI, M., YOKOZEKI, T., YAMAZAKI, M., NAKAMURA, H., WATANABE, H., KAWAMOTO, K., NAKAYAMA, K., MORRIS, A. J., FROHMAN, M. A. & KANAHO, Y. 1999. Phosphatidylinositol 4-phosphate 5-kinase alpha is a downstream effector of the small G protein ARF6 in membrane ruffle formation. *Cell,* 99**,** 521-32.

HONING, S., RICOTTA, D., KRAUSS, M., SPATE, K., SPOLAORE, B., MOTLEY, A., ROBINSON, M., ROBINSON, C., HAUCKE, V. & OWEN, D. J. 2005. Phosphatidylinositol-(4,5)-bisphosphate regulates sorting signal recognition by the clathrin-associated adaptor complex AP2. *Mol Cell,* 18**,** 519-31.

HUANG, F., KHVOROVA, A., MARSHALL, W. & SORKIN, A. 2004. Analysis of clathrin-mediated endocytosis of epidermal growth factor receptor by RNA interference. *J Biol Chem,* 279**,** 16657-61.

HUANG, M., WEISSMAN, J. T., BERAUD-DUFOUR, S., LUAN, P., WANG, C., CHEN, W., ARIDOR, M., WILSON, I. A. & BALCH, W. E. 2001. Crystal structure of Sar1-GDP at 1.7 A resolution and the role of the NH2 terminus in ER export. *J Cell Biol,* 155**,** 937-48.

JACKSON, L. P., KELLY, B. T., MCCOY, A. J., GAFFRY, T., JAMES, L. C., COLLINS, B. M., HONING, S., EVANS, P. R. & OWEN, D. J. 2010. A large-scale conformational change couples membrane recruitment to cargo binding in the AP2 clathrin adaptor complex. *Cell,* 141**,** 1220-9.

JACKSON, M. R., NILSSON, T. & PETERSON, P. A. 1990. Identification of a consensus motif for retention of transmembrane proteins in the endoplasmic reticulum. *EMBO J,* 9**,** 3153-62.

JANVIER, K., KATO, Y., BOEHM, M., ROSE, J. R., MARTINA, J. A., KIM, B. Y., VENKATESAN, S. & BONIFACINO, J. S. 2003. Recognition of dileucine-based sorting signals from HIV-1 Nef and LIMP-II by the AP-1 gamma-sigma1 and AP-3 delta-sigma3 hemicomplexes. *J Cell Biol,* 163**,** 1281-90.

JONES, S. M., HOWELL, K. E., HENLEY, J. R., CAO, H. & MCNIVEN, M. A. 1998. Role of dynamin in the formation of transport vesicles from the trans-Golgi network. *Science,* 279**,** 573-7.

KALTHOFF, C., ALVES, J., URBANKE, C., KNORR, R. & UNGEWICKELL, E. J. 2002. Unusual structural organization of the endocytic proteins AP180 and epsin 1. *J Biol Chem,* 277**,** 8209-16.

KANASEKI, T. & KADOTA, K. 1969. The "vesicle in a basket". A morphological study of the coated vesicle isolated from the nerve endings of the guinea pig brain, with special reference to the mechanism of membrane movements. *J Cell Biol,* 42**,** 202-20.

KAPPELER, F., KLOPFENSTEIN, D. R., FOGUET, M., PACCAUD, J. P. & HAURI, H. P. 1997. The recycling of ERGIC-53 in the early secretory pathway. ERGIC-53 carries a cytosolic endoplasmic reticulum-exit determinant interacting with COPII. *J Biol Chem,* 272**,** 31801-8.

KATSO, R., OKKENHAUG, K., AHMADI, K., WHITE, S., TIMMS, J. & WATERFIELD, M. D. 2001. Cellular function of phosphoinositide 3-kinases: implications for development, homeostasis, and cancer. *Annu Rev Cell Dev Biol,* 17**,** 615-75.

KEEN, J. H. 1987. Clathrin assembly proteins: affinity purification and a model for coat assembly. *J Cell Biol,* 105**,** 1989-98.

KEEN, J. H., CHESTNUT, M. H. & BECK, K. A. 1987. The clathrin coat assembly polypeptide complex. Autophosphorylation and assembly activities. *J Biol Chem,* 262**,** 3864-71.

KEEN, J. H., WILLINGHAM, M. C. & PASTAN, I. H. 1979. Clathrin-coated vesicles: isolation, dissociation and factor-dependent reassociation of clathrin baskets. *Cell,* 16**,** 303-12.

KELLY, B. T., GRAHAM, S. C., LISKA, N., DANNHAUSER, P. N., HONING, S., UNGEWICKELL, E. J. & OWEN, D. J. 2014. Clathrin adaptors. AP2 controls clathrin polymerization with a membrane-activated switch. *Science,* 345**,** 459-63.

KIRCHHAUSEN, T. 2009. Imaging endocytic clathrin structures in living cells. *Trends Cell Biol,* 19**,** 596-605.

KIRCHHAUSEN, T., HARRISON, S. C., CHOW, E. P., MATTALIANO, R. J., RAMACHANDRAN, K. L., SMART, J. & BROSIUS, J. 1987. Clathrin heavy chain: molecular cloning and complete primary structure. *Proc Natl Acad Sci U S A,* 84**,** 8805-9.

KIRKHAM, M., FUJITA, A., CHADDA, R., NIXON, S. J., KURZCHALIA, T. V., SHARMA, D. K., PAGANO, R. E., HANCOCK, J. F., MAYOR, S. & PARTON, R. G. 2005. Ultrastructural identification of uncoated caveolin-independent early endocytic vehicles. *J Cell Biol,* 168**,** 465-76.

KIRKHAM, M. & PARTON, R. G. 2005. Clathrin-independent endocytosis: new insights into caveolae and non-caveolar lipid raft carriers. *Biochim Biophys Acta,* 1746**,** 349-63.

KNUEHL, C., CHEN, C. Y., MANALO, V., HWANG, P. K., OTA, N. & BRODSKY, F. M. 2006. Novel binding sites on clathrin and adaptors regulate distinct aspects of coat assembly. *Traffic,* 7**,** 1688-700.

KO, G., PARADISE, S., CHEN, H., GRAHAM, M., VECCHI, M., BIANCHI, F., CREMONA, O., DI FIORE, P. P. & DE CAMILLI, P. 2010. Selective high-level expression of epsin 3 in gastric parietal cells, where it is localized at endocytic sites of apical canaliculi. *Proc Natl Acad Sci U S A,* 107**,** 21511-6.

KOSAKA, T. & IKEDA, K. 1983. Possible temperature-dependent blockage of synaptic vesicle recycling induced by a single gene mutation in Drosophila. *J Neurobiol,* 14**,** 207-25.

KOVTUN, O., TILLU, V. A., ARIOTTI, N., PARTON, R. G. & COLLINS, B. M. 2015. Cavin family proteins and the assembly of caveolae. *J Cell Sci,* 128**,** 1269-78.

KOVTUN, O., TILLU, V. A., JUNG, W., LENEVA, N., ARIOTTI, N., CHAUDHARY, N., MANDYAM, R. A., FERGUSON, C., MORGAN, G. P., JOHNSTON, W. A., HARROP, S. J., ALEXANDROV, K., PARTON, R. G. & COLLINS, B. M. 2014. Structural insights into the organization of the cavin membrane coat complex. *Dev Cell,* 31**,** 405-19.

KRAUSS, M., JIA, J. Y., ROUX, A., BECK, R., WIELAND, F. T., DE CAMILLI, P. & HAUCKE, V. 2008. Arf1-GTP-induced tubule formation suggests a function of Arf family proteins in curvature acquisition at sites of vesicle budding. *J Biol Chem,* 283**,** 27717-23.

KRAUSS, M., KINUTA, M., WENK, M. R., DE CAMILLI, P., TAKEI, K. & HAUCKE, V. 2003. ARF6 stimulates clathrin/AP-2 recruitment to synaptic membranes by activating phosphatidylinositol phosphate kinase type Igamma. *J Cell Biol,* 162**,** 113-24.

KUEHN, M. J., HERRMANN, J. M. & SCHEKMAN, R. 1998. COPII-cargo interactions direct protein sorting into ER-derived transport vesicles. *Nature,* 391**,** 187-90.

KUGE, O., HARA-KUGE, S., ORCI, L., RAVAZZOLA, M., AMHERDT, M., TANIGAWA, G., WIELAND, F. T. & ROTHMAN, J. E. 1993. zeta-COP, a subunit of coatomer, is required for COP-coated vesicle assembly. *J Cell Biol,* 123**,** 1727-34.

KURIHARA, T., HAMAMOTO, S., GIMENO, R. E., KAISER, C. A., SCHEKMAN, R. & YOSHIHISA, T. 2000. Sec24p and Iss1p function interchangeably in transport vesicle formation from the endoplasmic reticulum in Saccharomyces cerevisiae. *Mol Biol Cell,* 11**,** 983-98.

KUTATELADZE, T. G. 2010. Translation of the phosphoinositide code by PI effectors. *Nat Chem Biol,* 6**,** 507-13.

LAEMMLI, U. K. 1970. Cleavage of structural proteins during the assembly of the head of bacteriophage T4. *Nature,* 227**,** 680-5.

LAMAZE, C., DUJEANCOURT, A., BABA, T., LO, C. G., BENMERAH, A. & DAUTRY-VARSAT, A. 2001. Interleukin 2 receptors and detergent-resistant membrane domains define a clathrin-independent endocytic pathway. *Mol Cell,* 7**,** 661-71.

LEE, M. C., ORCI, L., HAMAMOTO, S., FUTAI, E., RAVAZZOLA, M. & SCHEKMAN, R. 2005. Sar1p N-terminal helix initiates membrane curvature and completes the fission of a COPII vesicle. *Cell,* 122**,** 605-17.

LEMMON, S. K. & TRAUB, L. M. 2000. Sorting in the endosomal system in yeast and animal cells. *Curr Opin Cell Biol,* 12**,** 457-66.

LEMMON, S. K. & TRAUB, L. M. 2012. Getting in touch with the clathrin terminal domain. *Traffic,* 13**,** 511-9.

LEWIN, D. A., SHEFF, D., OOI, C. E., WHITNEY, J. A., YAMAMOTO, E., CHICIONE, L. M., WEBSTER, P., BONIFACINO, J. S. & MELLMAN, I. 1998. Cloning, expression, and localization of a novel gamma-adaptin-like molecule. *FEBS Lett,* 435**,** 263-8.

LEWIS, M. J. & PELHAM, H. R. 1990. A human homologue of the yeast HDEL receptor. *Nature,* 348**,** 162-3.

LEWIS, M. J. & PELHAM, H. R. 1992. Sequence of a second human KDEL receptor. *J Mol Biol,* 226**,** 913-6.

LEWIS, W. H. 1931. Pinocytosis. *Bull John Hopkins Hosp,* 49**,** 17-27.

LI, W., PUERTOLLANO, R., BONIFACINO, J. S., OVERBEEK, P. A. & EVERETT, E. T. 2010. Disruption of the murine Ap2beta1 gene causes nonsyndromic cleft palate. *Cleft Palate Craniofac J,* 47**,** 566-73.

LIM, J. P. & GLEESON, P. A. 2011. Macropinocytosis: an endocytic pathway for internalising large gulps. *Immunol Cell Biol,* 89**,** 836-43.

LIN, H. C., MOORE, M. S., SANAN, D. A. & ANDERSON, R. G. 1991. Reconstitution of clathrin-coated pit budding from plasma membranes. *J Cell Biol,* 114**,** 881-91.

LIPFERT, J., KERSSEMAKERS, J. W., JAGER, T. & DEKKER, N. H. 2010. Magnetic torque tweezers: measuring torsional stiffness in DNA and RecA-DNA filaments. *Nat Methods,* 7**,** 977-80.

LIPPINCOTT-SCHWARTZ, J., ROBERTS, T. H. & HIRSCHBERG, K. 2000. Secretory protein trafficking and organelle dynamics in living cells. *Annu Rev Cell Dev Biol,* 16**,** 557-89.

LIU, L., BROWN, D., MCKEE, M., LEBRASSEUR, N. K., YANG, D., ALBRECHT, K. H., RAVID, K. & PILCH, P. F. 2008. Deletion of Cavin/PTRF causes global loss of caveolae, dyslipidemia, and glucose intolerance. *Cell Metab,* 8**,** 310-7.

LIU, S. H., TOWLER, M. C., CHEN, E., CHEN, C. Y., SONG, W., APODACA, G. & BRODSKY, F. M. 2001. A novel clathrin homolog that co-distributes with cytoskeletal components functions in the trans-Golgi network. *EMBO J,* 20**,** 272-84.

LOTTEAU, V., TEYTON, L., PELERAUX, A., NILSSON, T., KARLSSON, L., SCHMID, S. L., QUARANTA, V. & PETERSON, P. A. 1990. Intracellular transport of class II MHC molecules directed by invariant chain. *Nature,* 348**,** 600-5.

LUDWIG, A., HOWARD, G., MENDOZA-TOPAZ, C., DEERINCK, T., MACKEY, M., SANDIN, S., ELLISMAN, M. H. & NICHOLS, B. J. 2013. Molecular composition and ultrastructure of the caveolar coat complex. *PLoS Biol,* 11**,** e1001640.

MAIER, O., KNOBLICH, M. & WESTERMANN, P. 1996. Dynamin II binds to the trans-Golgi network. *Biochem Biophys Res Commun,* 223**,** 229-33.

MALKUS, P., JIANG, F. & SCHEKMAN, R. 2002. Concentrative sorting of secretory cargo proteins into COPII-coated vesicles. *J Cell Biol,* 159**,** 915-21.

MALSAM, J., PARISOTTO, D., BHARAT, T. A., SCHEUTZOW, A., KRAUSE, J. M., BRIGGS, J. A. & SOLLNER, T. H. 2012. Complexin arrests a pool of docked vesicles for fast Ca2+-dependent release. *EMBO J,* 31**,** 3270-81.

MANCIAS, J. D. & GOLDBERG, J. 2007. The transport signal on Sec22 for packaging into COPII-coated vesicles is a conformational epitope. *Mol Cell,* 26**,** 403-14.

MANCIAS, J. D. & GOLDBERG, J. 2008. Structural basis of cargo membrane protein discrimination by the human COPII coat machinery. *EMBO J,* 27**,** 2918-28.

MARDONES, G. A., BURGOS, P. V., LIN, Y., KLOER, D. P., MAGADAN, J. G., HURLEY, J. H. & BONIFACINO, J. S. 2013. Structural basis for the recognition of tyrosine-based sorting signals by the mu3A subunit of the AP-3 adaptor complex. *J Biol Chem,* 288**,** 9563-71.

MARGETA-MITROVIC, M., JAN, Y. N. & JAN, L. Y. 2000. A trafficking checkpoint controls GABA(B) receptor heterodimerization. *Neuron,* 27**,** 97-106.

MARKS, B., STOWELL, M. H., VALLIS, Y., MILLS, I. G., GIBSON, A., HOPKINS, C. R. & MCMAHON, H. T. 2001. GTPase activity of dynamin and resulting conformation change are essential for endocytosis. *Nature,* 410**,** 231-5.

MATSUOKA, K., SCHEKMAN, R., ORCI, L. & HEUSER, J. E. 2001. Surface structure of the COPII-coated vesicle. *Proc Natl Acad Sci U S A,* 98**,** 13705-9.

MATTERA, R., BOEHM, M., CHAUDHURI, R., PRABHU, Y. & BONIFACINO, J. S. 2011. Conservation and diversification of dileucine signal recognition by adaptor protein (AP) complex variants. *J Biol Chem,* 286**,** 2022-30.

MATTILA, J. P., SHNYROVA, A. V., SUNDBORGER, A. C., HORTELANO, E. R., FUHRMANS, M., NEUMANN, S., MULLER, M., HINSHAW, J. E., SCHMID, S. L. & FROLOV, V. A. 2015. A hemi-fission intermediate links two mechanistically distinct stages of membrane fission. *Nature,* 524**,** 109-113.

MAYOR, S. & PAGANO, R. E. 2007. Pathways of clathrin-independent endocytosis. *Nat Rev Mol Cell Biol,* 8**,** 603-12.

MAYOR, S., PARTON, R. G. & DONALDSON, J. G. 2014. Clathrin-independent pathways of endocytosis. *Cold Spring Harb Perspect Biol,* 6.

MCMAHON, H. T. & BOUCROT, E. 2011. Molecular mechanism and physiological functions of clathrin-mediated endocytosis. *Nat Rev Mol Cell Biol,* 12**,** 517-33.

MEINECKE, M., BOUCROT, E., CAMDERE, G., HON, W. C., MITTAL, R. & MCMAHON, H. T. 2013. Cooperative recruitment of dynamin and BIN/amphiphysin/Rvs (BAR) domain-containing proteins leads to GTP-dependent membrane scission. *J Biol Chem,* 288**,** 6651-61.

MERRIFIELD, C. J., QUALMANN, B., KESSELS, M. M. & ALMERS, W. 2004. Neural Wiskott Aldrich Syndrome Protein (N-WASP) and the Arp2/3 complex are recruited to sites of clathrin-mediated endocytosis in cultured fibroblasts. *Eur J Cell Biol,* 83**,** 13-8.

METSCHNIKOFF, E. 1884. Über die Beziehung der Phagocyten zu Milzbrandbacillen. *Arch. Pathol. Anat.,* 97.

MICHELSEN, K., SCHMID, V., METZ, J., HEUSSER, K., LIEBEL, U., SCHWEDE, T., SPANG, A. & SCHWAPPACH, B. 2007. Novel cargo-binding site in the beta and delta subunits of coatomer. *J Cell Biol,* 179**,** 209-17.

MICHELSEN, K., YUAN, H. & SCHWAPPACH, B. 2005. Hide and run. Arginine-based endoplasmic-reticulum-sorting motifs in the assembly of heteromultimeric membrane proteins. *EMBO Rep,* 6**,** 717-22.

MILLER, E. A., BEILHARZ, T. H., MALKUS, P. N., LEE, M. C., HAMAMOTO, S., ORCI, L. & SCHEKMAN, R. 2003. Multiple cargo binding sites on the COPII subunit Sec24p ensure capture of diverse membrane proteins into transport vesicles. *Cell,* 114**,** 497-509.

MILLER, S. E., MATHIASEN, S., BRIGHT, N. A., PIERRE, F., KELLY, B. T., KLADT, N., SCHAUSS, A., MERRIFIELD, C. J., STAMOU, D., HONING, S. & OWEN, D. J. 2015. CALM regulates clathrin-

coated vesicle size and maturation by directly sensing and driving membrane curvature. *Dev Cell,* 33**,** 163-75.

MILOSEVIC, I., GIOVEDI, S., LOU, X., RAIMONDI, A., COLLESI, C., SHEN, H., PARADISE, S., O'TOOLE, E., FERGUSON, S., CREMONA, O. & DE CAMILLI, P. 2011. Recruitment of endophilin to clathrin-coated pit necks is required for efficient vesicle uncoating after fission. *Neuron,* 72**,** 587-601.

MIWAKO, I., SCHROTER, T. & SCHMID, S. L. 2003. Clathrin- and dynamin-dependent coated vesicle formation from isolated plasma membranes. *Traffic,* 4**,** 376-89.

MOELLEKEN, J., MALSAM, J., BETTS, M. J., MOVAFEGHI, A., RECKMANN, I., MEISSNER, I., HELLWIG, A., RUSSELL, R. B., SOLLNER, T., BRUGGER, B. & WIELAND, F. T. 2007. Differential localization of coatomer complex isoforms within the Golgi apparatus. *Proc Natl Acad Sci U S A,* 104**,** 4425-30.

MOREN, B., SHAH, C., HOWES, M. T., SCHIEBER, N. L., MCMAHON, H. T., PARTON, R. G., DAUMKE, O. & LUNDMARK, R. 2012. EHD2 regulates caveolar dynamics via ATP-driven targeting and oligomerization. *Mol Biol Cell,* 23**,** 1316-29.

MORLOT, S., GALLI, V., KLEIN, M., CHIARUTTINI, N., MANZI, J., HUMBERT, F., DINIS, L., LENZ, M., CAPPELLO, G. & ROUX, A. 2012. Membrane shape at the edge of the dynamin helix sets location and duration of the fission reaction. *Cell,* 151**,** 619-29.

MOSSESSOVA, E., BICKFORD, L. C. & GOLDBERG, J. 2003. SNARE selectivity of the COPII coat. *Cell,* 114**,** 483-95.

MOTLEY, A., BRIGHT, N. A., SEAMAN, M. N. & ROBINSON, M. S. 2003. Clathrin-mediated endocytosis in AP-2-depleted cells. *J Cell Biol,* 162**,** 909-18.

MUNRO, S. & PELHAM, H. R. 1987. A C-terminal signal prevents secretion of luminal ER proteins. *Cell,* 48**,** 899-907.

NAKANO, A. & MURAMATSU, M. 1989. A novel GTP-binding protein, Sar1p, is involved in transport from the endoplasmic reticulum to the Golgi apparatus. *J Cell Biol,* 109**,** 2677-91.

NAKATA, T., TAKEMURA, R. & HIROKAWA, N. 1993. A novel member of the dynamin family of GTP-binding proteins is expressed specifically in the testis. *J Cell Sci,* 105 (Pt 1)**,** 1-5.

NEWMAN, L. S., MCKEEVER, M. O., OKANO, H. J. & DARNELL, R. B. 1995. Beta-NAP, a cerebellar degeneration antigen, is a neuron-specific vesicle coat protein. *Cell,* 82**,** 773-83.

NICKEL, W. & WIELAND, F. T. 2001. Receptor-dependent formation of COPI-coated vesicles from chemically defined donor liposomes. *Methods Enzymol,* 329**,** 388-404.

NICOZIANI, P., VILHARDT, F., LLORENTE, A., HILOUT, L., COURTOY, P. J., SANDVIG, K. & VAN DEURS, B. 2000. Role for dynamin in late endosome dynamics and trafficking of the cation-independent mannose 6-phosphate receptor. *Mol Biol Cell,* 11**,** 481-95.

NILSSON, T., JACKSON, M. & PETERSON, P. A. 1989. Short cytoplasmic sequences serve as retention signals for transmembrane proteins in the endoplasmic reticulum. *Cell,* 58**,** 707-18.

NISHIMURA, N. & BALCH, W. E. 1997. A di-acidic signal required for selective export from the endoplasmic reticulum. *Science,* 277**,** 556-8.

NORBURY, C. C., CHAMBERS, B. J., PRESCOTT, A. R., LJUNGGREN, H. G. & WATTS, C. 1997. Constitutive macropinocytosis allows TAP-dependent major histocompatibility complex class I presentation of exogenous soluble antigen by bone marrow-derived dendritic cells. *Eur J Immunol,* 27**,** 280-8.

O'KELLY, I., BUTLER, M. H., ZILBERBERG, N. & GOLDSTEIN, S. A. 2002. Forward transport. 14-3-3 binding overcomes retention in endoplasmic reticulum by dibasic signals. *Cell,* 111**,** 577-88.

ODORIZZI, G., BABST, M. & EMR, S. D. 2000. Phosphoinositide signaling and the regulation of membrane trafficking in yeast. *Trends Biochem Sci,* 25**,** 229-35.

OHNO, H., AGUILAR, R. C., YEH, D., TAURA, D., SAITO, T. & BONIFACINO, J. S. 1998a. The medium subunits of adaptor complexes recognize distinct but overlapping sets of tyrosine-based sorting signals. *J Biol Chem,* 273**,** 25915-21.

OHNO, H., POY, G. & BONIFACINO, J. S. 1998b. Cloning of the gene encoding the murine clathrin-associated adaptor medium chain mu 2: gene organization, alternative splicing and chromosomal assignment. *Gene,* 210**,** 187-93.

OHNO, H., STEWART, J., FOURNIER, M. C., BOSSHART, H., RHEE, I., MIYATAKE, S., SAITO, T., GALLUSSER, A., KIRCHHAUSEN, T. & BONIFACINO, J. S. 1995. Interaction of tyrosine-based sorting signals with clathrin-associated proteins. *Science,* 269**,** 1872-5.

OHNO, H., TOMEMORI, T., NAKATSU, F., OKAZAKI, Y., AGUILAR, R. C., FOELSCH, H., MELLMAN, I., SAITO, T., SHIRASAWA, T. & BONIFACINO, J. S. 1999. Mu1B, a novel adaptor medium chain expressed in polarized epithelial cells. *FEBS Lett,* 449**,** 215-20.

OKADA, R., YAMAUCHI, Y., HONGU, T., FUNAKOSHI, Y., OHBAYASHI, N., HASEGAWA, H. & KANAHO, Y. 2015. Activation of the Small G Protein Arf6 by Dynamin2 through Guanine Nucleotide Exchange Factors in Endocytosis. *Sci Rep,* 5**,** 14919.

OLUSANYA, O., ANDREWS, P. D., SWEDLOW, J. R. & SMYTHE, E. 2001. Phosphorylation of threonine 156 of the mu2 subunit of the AP2 complex is essential for endocytosis in vitro and in vivo. *Curr Biol,* 11**,** 896-900.

OOI, C. E., DELL'ANGELICA, E. C. & BONIFACINO, J. S. 1998. ADP-Ribosylation factor 1 (ARF1) regulates recruitment of the AP-3 adaptor complex to membranes. *J Cell Biol,* 142**,** 391-402.

ORCI, L., GLICK, B. S. & ROTHMAN, J. E. 1986. A new type of coated vesicular carrier that appears not to contain clathrin: its possible role in protein transport within the Golgi stack. *Cell,* 46**,** 171-84.

ORCI, L., RAVAZZOLA, M., MEDA, P., HOLCOMB, C., MOORE, H. P., HICKE, L. & SCHEKMAN, R. 1991. Mammalian Sec23p homologue is restricted to the endoplasmic reticulum transitional cytoplasm. *Proc Natl Acad Sci U S A,* 88**,** 8611-5.

OTTE, S. & BARLOWE, C. 2002. The Erv41p-Erv46p complex: multiple export signals are required in trans for COPII-dependent transport from the ER. *EMBO J,* 21**,** 6095-104.

OTTE, S. & BARLOWE, C. 2004. Sorting signals can direct receptor-mediated export of soluble proteins into COPII vesicles. *Nat Cell Biol,* 6**,** 1189-94.

PAGANO, A., LETOURNEUR, F., GARCIA-ESTEFANIA, D., CARPENTIER, J. L., ORCI, L. & PACCAUD, J. P. 1999. Sec24 proteins and sorting at the endoplasmic reticulum. *J Biol Chem,* 274**,** 7833-40.

PALADE, G. E. 1953. Fine structure of blood capillaries. *J Appl Phys,* 24**,** 1424.

PALEOTTI, O., MACIA, E., LUTON, F., KLEIN, S., PARTISANI, M., CHARDIN, P., KIRCHHAUSEN, T. & FRANCO, M. 2005. The small G-protein Arf6GTP recruits the AP-2 adaptor complex to membranes. *J Biol Chem,* 280**,** 21661-6.

PALMER, S. E., SMACZYNSKA-DE, R., II, MARKLEW, C. J., ALLWOOD, E. G., MISHRA, R., JOHNSON, S., GOLDBERG, M. W. & AYSCOUGH, K. R. 2015. A dynamin-actin interaction is required for vesicle scission during endocytosis in yeast. *Curr Biol,* 25**,** 868-78.

PARK, S. Y. & GUO, X. 2014. Adaptor protein complexes and intracellular transport. *Biosci Rep,* 34.

PASCHAL, B. M., SHPETNER, H. S. & VALLEE, R. B. 1987. MAP 1C is a microtubule-activated ATPase which translocates microtubules in vitro and has dynein-like properties. *J Cell Biol,* 105**,** 1273-82.

PAULOIN, A., LOEB, J. & JOLLES, P. 1984. Protein kinase(s) in bovine brain coated vesicles. *Biochim Biophys Acta,* 799**,** 238-45.

PEARSE, B. M. 1975. Coated vesicles from pig brain: purification and biochemical characterization. *J Mol Biol,* 97**,** 93-8.

PEARSE, B. M. 1976. Clathrin: a unique protein associated with intracellular transfer of membrane by coated vesicles. *Proc Natl Acad Sci U S A,* 73**,** 1255-9.

PEARSE, B. M. & ROBINSON, M. S. 1984. Purification and properties of 100-kd proteins from coated vesicles and their reconstitution with clathrin. *EMBO J,* 3**,** 1951-7.

PELHAM, H. R. 1988. Evidence that luminal ER proteins are sorted from secreted proteins in a post-ER compartment. *EMBO J,* 7**,** 913-8.

PELHAM, H. R. & ROTHMAN, J. E. 2000. The debate about transport in the Golgi--two sides of the same coin? *Cell,* 102**,** 713-9.

PEVSNER, J., VOLKNANDT, W., WONG, B. R. & SCHELLER, R. H. 1994. Two rat homologs of clathrin-associated adaptor proteins. *Gene,* 146**,** 279-83.

PEYROCHE, A., ANTONNY, B., ROBINEAU, S., ACKER, J., CHERFILS, J. & JACKSON, C. L. 1999. Brefeldin A acts to stabilize an abortive ARF-GDP-Sec7 domain protein complex: involvement of specific residues of the Sec7 domain. *Mol Cell,* 3**,** 275-85.

POLO, S., SIGISMUND, S., FARETTA, M., GUIDI, M., CAPUA, M. R., BOSSI, G., CHEN, H., DE CAMILLI, P. & DI FIORE, P. P. 2002. A single motif responsible for ubiquitin recognition and monoubiquitination in endocytic proteins. *Nature,* 416**,** 451-5.

POPOFF, V., ADOLF, F., BRUGGER, B. & WIELAND, F. 2011. COPI budding within the Golgi stack. *Cold Spring Harb Perspect Biol,* 3**,** a005231.

POSOR, Y., EICHHORN-GRUENIG, M., PUCHKOV, D., SCHONEBERG, J., ULLRICH, A., LAMPE, A., MULLER, R., ZARBAKHSH, S., GULLUNI, F., HIRSCH, E., KRAUSS, M., SCHULTZ, C., SCHMORANZER, J., NOE, F. & HAUCKE, V. 2013. Spatiotemporal control of endocytosis by phosphatidylinositol-3,4-bisphosphate. *Nature,* 499**,** 233-7.

PRASAD, K., BAROUCH, W., GREENE, L. & EISENBERG, E. 1993. A protein cofactor is required for uncoating of clathrin baskets by uncoating ATPase. *J Biol Chem,* 268**,** 23758-61.

PRASAD, K. & LIPPOLDT, R. E. 1988. Molecular characterization of the AP180 coated vesicle assembly protein. *Biochemistry,* 27**,** 6098-104.

PUCADYIL, T. J. & SCHMID, S. L. 2010. Supported bilayers with excess membrane reservoir: a template for reconstituting membrane budding and fission. *Biophys J,* 99**,** 517-25.

RACOOSIN, E. L. & SWANSON, J. A. 1989. Macrophage colony-stimulating factor (rM-CSF) stimulates pinocytosis in bone marrow-derived macrophages. *J Exp Med,* 170**,** 1635-48.

RADHAKRISHNA, H. & DONALDSON, J. G. 1997. ADP-ribosylation factor 6 regulates a novel plasma membrane recycling pathway. *J Cell Biol,* 139**,** 49-61.

RAMACHANDRAN, R., PUCADYIL, T. J., LIU, Y. W., ACHARYA, S., LEONARD, M., LUKIYANCHUK, V. & SCHMID, S. L. 2009. Membrane insertion of the pleckstrin homology domain variable loop 1 is critical for dynamin-catalyzed vesicle scission. *Mol Biol Cell,* 20**,** 4630-9.

RANDAZZO, P. A. & KAHN, R. A. 1994. GTP hydrolysis by ADP-ribosylation factor is dependent on both an ADP-ribosylation factor GTPase-activating protein and acid phospholipids. *J Biol Chem,* 269**,** 10758-63.

RAPOPORT, I., BOLL, W., YU, A., BOCKING, T. & KIRCHHAUSEN, T. 2008. A motif in the clathrin heavy chain required for the Hsc70/auxilin uncoating reaction. *Mol Biol Cell,* 19**,** 405-13.

RAYKHEL, I., ALANEN, H., SALO, K., JURVANSUU, J., NGUYEN, V. D., LATVA-RANTA, M. & RUDDOCK, L. 2007. A molecular specificity code for the three mammalian KDEL receptors. *J Cell Biol,* 179**,** 1193-204.

REIDER, A., BARKER, S. L., MISHRA, S. K., IM, Y. J., MALDONADO-BAEZ, L., HURLEY, J. H., TRAUB, L. M. & WENDLAND, B. 2009. Syp1 is a conserved endocytic adaptor that contains domains involved in cargo selection and membrane tubulation. *EMBO J,* 28**,** 3103-16.

REINHARD, C., HARTER, C., BREMSER, M., BRUGGER, B., SOHN, K., HELMS, J. B. & WIELAND, F. 1999. Receptor-induced polymerization of coatomer. *Proc Natl Acad Sci U S A,* 96**,** 1224-8.

REN, X., FARIAS, G. G., CANAGARAJAH, B. J., BONIFACINO, J. S. & HURLEY, J. H. 2013. Structural basis for recruitment and activation of the AP-1 clathrin adaptor complex by Arf1. *Cell,* 152**,** 755-67.

REUBOLD, T. F., FAELBER, K., PLATTNER, N., POSOR, Y., KETEL, K., CURTH, U., SCHLEGEL, J., ANAND, R., MANSTEIN, D. J., NOE, F., HAUCKE, V., DAUMKE, O. & ESCHENBURG, S. 2015. Crystal structure of the dynamin tetramer. *Nature,* 525**,** 404-8.

RICOTTA, D., CONNER, S. D., SCHMID, S. L., VON FIGURA, K. & HONING, S. 2002. Phosphorylation of the AP2 mu subunit by AAK1 mediates high affinity binding to membrane protein sorting signals. *J Cell Biol,* 156**,** 791-5.

ROBERG, K. J., CROTWELL, M., ESPENSHADE, P., GIMENO, R. & KAISER, C. A. 1999. LST1 is a SEC24 homologue used for selective export of the plasma membrane ATPase from the endoplasmic reticulum. *J Cell Biol,* 145**,** 659-72.

ROBINSON, M. S. 2015. Forty Years of Clathrin-coated Vesicles. *Traffic,* 16**,** 1210-38.

ROHDE, G., WENZEL, D. & HAUCKE, V. 2002. A phosphatidylinositol (4,5)-bisphosphate binding site within mu2-adaptin regulates clathrin-mediated endocytosis. *J Cell Biol,* 158**,** 209-14.

ROMER, W., PONTANI, L. L., SORRE, B., RENTERO, C., BERLAND, L., CHAMBON, V., LAMAZE, C., BASSEREAU, P., SYKES, C., GAUS, K. & JOHANNES, L. 2010. Actin dynamics drive membrane reorganization and scission in clathrin-independent endocytosis. *Cell,* 140**,** 540-53.

ROSENTHAL, J. A., CHEN, H., SLEPNEV, V. I., PELLEGRINI, L., SALCINI, A. E., DI FIORE, P. P. & DE CAMILLI, P. 1999. The epsins define a family of proteins that interact with components of the clathrin coat and contain a new protein module. *J Biol Chem,* 274**,** 33959-65.

ROSS, B. H., LIN, Y., CORALES, E. A., BURGOS, P. V. & MARDONES, G. A. 2014. Structural and functional characterization of cargo-binding sites on the mu4-subunit of adaptor protein complex 4. *PLoS One,* 9**,** e88147.

ROTH, T. F. & PORTER, K. R. 1964. Yolk Protein Uptake in the Oocyte of the Mosquito Aedes Aegypti. L. *J Cell Biol,* 20**,** 313-32.

ROTHBERG, K. G., HEUSER, J. E., DONZELL, W. C., YING, Y. S., GLENNEY, J. R. & ANDERSON, R. G. 1992. Caveolin, a protein component of caveolae membrane coats. *Cell,* 68**,** 673-82.

ROUSER, G., FKEISCHER, S. & YAMAMOTO, A. 1970. Two dimensional then layer chromatographic separation of polar lipids and determination of phospholipids by phosphorus analysis of spots. *Lipids,* 5**,** 494-6.

ROUX, A., UYHAZI, K., FROST, A. & DE CAMILLI, P. 2006. GTP-dependent twisting of dynamin implicates constriction and tension in membrane fission. *Nature,* 441**,** 528-31.

SAFFARIAN, S., COCUCCI, E. & KIRCHHAUSEN, T. 2009. Distinct dynamics of endocytic clathrin-coated pits and coated plaques. *PLoS Biol,* 7**,** e1000191.

SALEEM, M., MORLOT, S., HOHENDAHL, A., MANZI, J., LENZ, M. & ROUX, A. 2015. A balance between membrane elasticity and polymerization energy sets the shape of spherical clathrin coats. *Nat Commun,* 6**,** 6249.

SANDVIG, K., PUST, S., SKOTLAND, T. & VAN DEURS, B. 2011. Clathrin-independent endocytosis: mechanisms and function. *Curr Opin Cell Biol,* 23**,** 413-20.

SARKES, D. & RAMEH, L. E. 2010. A novel HPLC-based approach makes possible the spatial characterization of cellular PtdIns5P and other phosphoinositides. *Biochem J,* 428**,** 375-84.

SATO, K. & NAKANO, A. 2002. Emp47p and its close homolog Emp46p have a tyrosine-containing endoplasmic reticulum exit signal and function in glycoprotein secretion in Saccharomyces cerevisiae. *Mol Biol Cell,* 13**,** 2518-32.

SATO, K. & NAKANO, A. 2007. Mechanisms of COPII vesicle formation and protein sorting. *FEBS Lett,* 581**,** 2076-82.

SATO, M., SATO, K. & NAKANO, A. 1996. Endoplasmic reticulum localization of Sec12p is achieved by two mechanisms: Rer1p-dependent retrieval that requires the transmembrane domain and Rer1p-independent retention that involves the cytoplasmic domain. *J Cell Biol,* 134**,** 279-93.

SCAIFE, R. & MARGOLIS, R. L. 1990. Biochemical and immunochemical analysis of rat brain dynamin interaction with microtubules and organelles in vivo and in vitro. *J Cell Biol,* 111**,** 3023-33.

SCHERER, P. E., OKAMOTO, T., CHUN, M., NISHIMOTO, I., LODISH, H. F. & LISANTI, M. P. 1996. Identification, sequence, and expression of caveolin-2 defines a caveolin gene family. *Proc Natl Acad Sci U S A,* 93**,** 131-5.

SCHLOSSMAN, D. M., SCHMID, S. L., BRAELL, W. A. & ROTHMAN, J. E. 1984. An enzyme that removes clathrin coats: purification of an uncoating ATPase. *J Cell Biol,* 99**,** 723-33.

SCHMID, E. M. & MCMAHON, H. T. 2007. Integrating molecular and network biology to decode endocytosis. *Nature,* 448**,** 883-8.

SCHNEIDER, C. A., RASBAND, W. S. & ELICEIRI, K. W. 2012. NIH Image to ImageJ: 25 years of image analysis. *Nat Methods,* 9**,** 671-5.

SCHUTZE, M. P., PETERSON, P. A. & JACKSON, M. R. 1994. An N-terminal double-arginine motif maintains type II membrane proteins in the endoplasmic reticulum. *EMBO J,* 13**,** 1696-705.

SCHWEIZER, A., FRANSEN, J. A., BACHI, T., GINSEL, L. & HAURI, H. P. 1988. Identification, by a monoclonal antibody, of a 53-kD protein associated with a tubulo-vesicular compartment at the cis-side of the Golgi apparatus. *J Cell Biol,* 107**,** 1643-53.

SEMENZA, J. C., HARDWICK, K. G., DEAN, N. & PELHAM, H. R. 1990. ERD2, a yeast gene required for the receptor-mediated retrieval of luminal ER proteins from the secretory pathway. *Cell,* 61**,** 1349-57.

SEN, A., MADHIVANAN, K., MUKHERJEE, D. & AGUILAR, R. C. 2012. The epsin protein family: coordinators of endocytosis and signaling. *Biomol Concepts,* 3**,** 117-126.

SENJU, Y., ITOH, Y., TAKANO, K., HAMADA, S. & SUETSUGU, S. 2011. Essential role of PACSIN2/syndapin-II in caveolae membrane sculpting. *J Cell Sci,* 124**,** 2032-40.

SERAFINI, T., STENBECK, G., BRECHT, A., LOTTSPEICH, F., ORCI, L., ROTHMAN, J. E. & WIELAND, F. T. 1991. A coat subunit of Golgi-derived non-clathrin-coated vesicles with homology to the clathrin-coated vesicle coat protein beta-adaptin. *Nature,* 349**,** 215-20.

SHEMESH, T., LUINI, A., MALHOTRA, V., BURGER, K. N. & KOZLOV, M. M. 2003. Prefission constriction of Golgi tubular carriers driven by local lipid metabolism: a theoretical model. *Biophys J,* 85**,** 3813-27.

SHNYROVA, A. V., BASHKIROV, P. V., AKIMOV, S. A., PUCADYIL, T. J., ZIMMERBERG, J., SCHMID, S. L. & FROLOV, V. A. 2013. Geometric catalysis of membrane fission driven by flexible dynamin rings. *Science,* 339**,** 1433-6.

SHPETNER, H. S. & VALLEE, R. B. 1989. Identification of dynamin, a novel mechanochemical enzyme that mediates interactions between microtubules. *Cell,* 59**,** 421-32.

SKRUZNY, M., DESFOSSES, A., PRINZ, S., DODONOVA, S. O., GIERAS, A., UETRECHT, C., JAKOBI, A. J., ABELLA, M., HAGEN, W. J., SCHULZ, J., MEIJERS, R., RYBIN, V., BRIGGS, J. A., SACHSE, C. & KAKSONEN, M. 2015. An organized co-assembly of clathrin adaptors is essential for endocytosis. *Dev Cell,* 33**,** 150-62.

SLEPNEV, V. I., OCHOA, G. C., BUTLER, M. H., GRABS, D. & DE CAMILLI, P. 1998. Role of phosphorylation in regulation of the assembly of endocytic coat complexes. *Science,* 281**,** 821-4.

SOCHACKI, K. A., DICKEY, A. M., STRUB, M. P. & TARASKA, J. W. 2017. Endocytic proteins are partitioned at the edge of the clathrin lattice in mammalian cells. *Nat Cell Biol,* 19**,** 352-361.

SOUSA, R. & LAFER, E. M. 2015. The role of molecular chaperones in clathrin mediated vesicular trafficking. *Front Mol Biosci,* 2**,** 26.

SPRADLING, K. D., MCDANIEL, A. E., LOHI, J. & PILCHER, B. K. 2001. Epsin 3 is a novel extracellular matrix-induced transcript specific to wounded epithelia. *J Biol Chem,* 276**,** 29257-67.

STAHELIN, R. V., LONG, F., PETER, B. J., MURRAY, D., DE CAMILLI, P., MCMAHON, H. T. & CHO, W. 2003. Contrasting membrane interaction mechanisms of AP180 N-terminal homology (ANTH) and epsin N-terminal homology (ENTH) domains. *J Biol Chem,* 278**,** 28993-9.

STAMNES, M. A. & ROTHMAN, J. E. 1993. The binding of AP-1 clathrin adaptor particles to Golgi membranes requires ADP-ribosylation factor, a small GTP-binding protein. *Cell,* 73**,** 999-1005.

STENBECK, G., HARTER, C., BRECHT, A., HERRMANN, D., LOTTSPEICH, F., ORCI, L. & WIELAND, F. T. 1993. beta'-COP, a novel subunit of coatomer. *EMBO J,* 12**,** 2841-5.

STIMPSON, H. E., TORET, C. P., CHENG, A. T., PAULY, B. S. & DRUBIN, D. G. 2009. Early-arriving Syp1p and Ede1p function in endocytic site placement and formation in budding yeast. *Mol Biol Cell,* 20**,** 4640-51.

STOEBER, M., STOECK, I. K., HANNI, C., BLECK, C. K., BALISTRERI, G. & HELENIUS, A. 2012. Oligomers of the ATPase EHD2 confine caveolae to the plasma membrane through association with actin. *EMBO J,* 31**,** 2350-64.

STOWELL, M. H., MARKS, B., WIGGE, P. & MCMAHON, H. T. 1999. Nucleotide-dependent conformational changes in dynamin: evidence for a mechanochemical molecular spring. *Nat Cell Biol,* 1**,** 27-32.

SUN, Z., ANDERL, F., FROHLICH, K., ZHAO, L., HANKE, S., BRUGGER, B., WIELAND, F. & BETHUNE, J. 2007. Multiple and stepwise interactions between coatomer and ADP-ribosylation factor-1 (Arf1)-GTP. *Traffic,* 8**,** 582-93.

SUNDBORGER, A. C., FANG, S., HEYMANN, J. A., RAY, P., CHAPPIE, J. S. & HINSHAW, J. E. 2014. A dynamin mutant defines a superconstricted prefission state. *Cell Rep,* 8**,** 734-42.

SWEITZER, S. M. & HINSHAW, J. E. 1998. Dynamin undergoes a GTP-dependent conformational change causing vesiculation. *Cell,* 93**,** 1021-9.

TAKEI, K., MCPHERSON, P. S., SCHMID, S. L. & DE CAMILLI, P. 1995. Tubular membrane invaginations coated by dynamin rings are induced by GTP-gamma S in nerve terminals. *Nature,* 374**,** 186-90.

TAYLOR, M. J., LAMPE, M. & MERRIFIELD, C. J. 2012. A feedback loop between dynamin and actin recruitment during clathrin-mediated endocytosis. *PLoS Biol,* 10**,** e1001302.

TEBAR, F., SORKINA, T., SORKIN, A., ERICSSON, M. & KIRCHHAUSEN, T. 1996. Eps15 is a component of clathrin-coated pits and vesicles and is located at the rim of coated pits. *J Biol Chem,* 271**,** 28727-30.

TER HAAR, E., MUSACCHIO, A., HARRISON, S. C. & KIRCHHAUSEN, T. 1998. Atomic structure of clathrin: a beta propeller terminal domain joins an alpha zigzag linker. *Cell,* 95**,** 563-73.

TOWLER, M. C., GLEESON, P. A., HOSHINO, S., RAHKILA, P., MANALO, V., OHKOSHI, N., ORDAHL, C., PARTON, R. G. & BRODSKY, F. M. 2004. Clathrin isoform CHC22, a component of neuromuscular and myotendinous junctions, binds sorting nexin 5 and has increased expression during myogenesis and muscle regeneration. *Mol Biol Cell,* 15**,** 3181-95.

TRAUB, L. M. 2009. Tickets to ride: selecting cargo for clathrin-regulated internalization. *Nat Rev Mol Cell Biol,* 10**,** 583-96.

TRAUB, L. M., OSTROM, J. A. & KORNFELD, S. 1993. Biochemical dissection of AP-1 recruitment onto Golgi membranes. *J Cell Biol,* 123**,** 561-73.

TUMA, P. L. & COLLINS, C. A. 1994. Activation of dynamin GTPase is a result of positive cooperativity. *J Biol Chem,* 269**,** 30842-7.

UNANUE, E. R., UNGEWICKELL, E. & BRANTON, D. 1981. The binding of clathrin triskelions to membranes from coated vesicles. *Cell,* 26**,** 439-46.

VAN DER BLIEK, A. M. & MEYEROWITZ, E. M. 1991. Dynamin-like protein encoded by the Drosophila shibire gene associated with vesicular traffic. *Nature,* 351**,** 411-4.

VAN DER BLIEK, A. M., REDELMEIER, T. E., DAMKE, H., TISDALE, E. J., MEYEROWITZ, E. M. & SCHMID, S. L. 1993. Mutations in human dynamin block an intermediate stage in coated vesicle formation. *J Cell Biol,* 122**,** 553-63.

VIGERS, G. P., CROWTHER, R. A. & PEARSE, B. M. 1986. Three-dimensional structure of clathrin cages in ice. *EMBO J,* 5**,** 529-34.

VOTSMEIER, C. & GALLWITZ, D. 2001. An acidic sequence of a putative yeast Golgi membrane protein binds COPII and facilitates ER export. *EMBO J,* 20**,** 6742-50.

WAKEHAM, D. E., ABI-RACHED, L., TOWLER, M. C., WILBUR, J. D., PARHAM, P. & BRODSKY, F. M. 2005. Clathrin heavy and light chain isoforms originated by independent mechanisms of gene duplication during chordate evolution. *Proc Natl Acad Sci U S A,* 102**,** 7209-14.

WANG, Y. J., WANG, J., SUN, H. Q., MARTINEZ, M., SUN, Y. X., MACIA, E., KIRCHHAUSEN, T., ALBANESI, J. P., ROTH, M. G. & YIN, H. L. 2003. Phosphatidylinositol 4 phosphate regulates targeting of clathrin adaptor AP-1 complexes to the Golgi. *Cell,* 114**,** 299-310.

WARNOCK, D. E., HINSHAW, J. E. & SCHMID, S. L. 1996. Dynamin self-assembly stimulates its GTPase activity. *J Biol Chem,* 271**,** 22310-4.

WATERS, M. G., SERAFINI, T. & ROTHMAN, J. E. 1991. 'Coatomer': a cytosolic protein complex containing subunits of non-clathrin-coated Golgi transport vesicles. *Nature,* 349**,** 248-51.

WATT, S. A., KIMBER, W. A., FLEMING, I. N., LESLIE, N. R., DOWNES, C. P. & LUCOCQ, J. M. 2004. Detection of novel intracellular agonist responsive pools of phosphatidylinositol 3,4-bisphosphate using the TAPP1 pleckstrin homology domain in immunoelectron microscopy. *Biochem J,* 377**,** 653-63.

WAY, M. & PARTON, R. G. 1995. M-caveolin, a muscle-specific caveolin-related protein. *FEBS Lett,* 376**,** 108-12.

WEGMANN, D., HESS, P., BAIER, C., WIELAND, F. T. & REINHARD, C. 2004. Novel isotypic gamma/zeta subunits reveal three coatomer complexes in mammals. *Mol Cell Biol,* 24**,** 1070-80.

WENDELER, M. W., PACCAUD, J. P. & HAURI, H. P. 2007. Role of Sec24 isoforms in selective export of membrane proteins from the endoplasmic reticulum. *EMBO Rep,* 8**,** 258-64.

WILBUR, J. D., HWANG, P. K., YBE, J. A., LANE, M., SELLERS, B. D., JACOBSON, M. P., FLETTERICK, R. J. & BRODSKY, F. M. 2010. Conformation switching of clathrin light chain regulates clathrin lattice assembly. *Dev Cell,* 18**,** 841-8.

WILDE, A. & BRODSKY, F. M. 1996. In vivo phosphorylation of adaptors regulates their interaction with clathrin. *J Cell Biol,* 135**,** 635-45.

WILLOX, A. K. & ROYLE, S. J. 2012. Functional analysis of interaction sites on the N-terminal domain of clathrin heavy chain. *Traffic,* 13**,** 70-81.

WILSON, D. W., LEWIS, M. J. & PELHAM, H. R. 1993. pH-dependent binding of KDEL to its receptor in vitro. *J Biol Chem,* 268**,** 7465-8.

XING, Y., BOCKING, T., WOLF, M., GRIGORIEFF, N., KIRCHHAUSEN, T. & HARRISON, S. C. 2010. Structure of clathrin coat with bound Hsc70 and auxilin: mechanism of Hsc70-facilitated disassembly. *EMBO J,* 29**,** 655-65.

YANG, J. S., GAD, H., LEE, S. Y., MIRONOV, A., ZHANG, L., BEZNOUSSENKO, G. V., VALENTE, C., TURACCHIO, G., BONSRA, A. N., DU, G., BALDANZI, G., GRAZIANI, A., BOURGOIN, S., FROHMAN, M. A., LUINI, A. & HSU, V. W. 2008. A role for phosphatidic acid in COPI vesicle fission yields insights into Golgi maintenance. *Nat Cell Biol,* 10**,** 1146-53.

YANG, J. S., LEE, S. Y., SPANO, S., GAD, H., ZHANG, L., NIE, Z., BONAZZI, M., CORDA, D., LUINI, A. & HSU, V. W. 2005. A role for BARS at the fission step of COPI vesicle formation from Golgi membrane. *EMBO J,* 24**,** 4133-43.

YAP, C. C., MURATE, M., KISHIGAMI, S., MUTO, Y., KISHIDA, H., HASHIKAWA, T. & YANO, R. 2003. Adaptor protein complex-4 (AP-4) is expressed in the central nervous system neurons and interacts with glutamate receptor delta2. *Mol Cell Neurosci,* 24**,** 283-95.

YASUDA, R., NOJI, H., KINOSITA, K., JR. & YOSHIDA, M. 1998. F1-ATPase is a highly efficient molecular motor that rotates with discrete 120 degree steps. *Cell,* 93**,** 1117-24.

YBE, J. A., BRODSKY, F. M., HOFMANN, K., LIN, K., LIU, S. H., CHEN, L., EARNEST, T. N., FLETTERICK, R. J. & HWANG, P. K. 1999. Clathrin self-assembly is mediated by a tandemly repeated superhelix. *Nature,* 399**,** 371-5.

YBE, J. A., PEREZ-MILLER, S., NIU, Q., COATES, D. A., DRAZER, M. W. & CLEGG, M. E. 2007. Light chain C-terminal region reinforces the stability of clathrin heavy chain trimers. *Traffic,* 8**,** 1101-10.

YE, W. & LAFER, E. M. 1995. Bacterially expressed F1-20/AP-3 assembles clathrin into cages with a narrow size distribution: implications for the regulation of quantal size during neurotransmission. *J Neurosci Res,* 41**,** 15-26.

YOON, Y., TONG, J., LEE, P. J., ALBANESE, A., BHARDWAJ, N., KALLBERG, M., DIGMAN, M. A., LU, H., GRATTON, E., SHIN, Y. K. & CHO, W. 2010. Molecular basis of the potent membrane-remodeling activity of the epsin 1 N-terminal homology domain. *J Biol Chem,* 285**,** 531-40.

YOSHIHISA, T., BARLOWE, C. & SCHEKMAN, R. 1993. Requirement for a GTPase-activating protein in vesicle budding from the endoplasmic reticulum. *Science,* 259**,** 1466-8.

ZERANGUE, N., SCHWAPPACH, B., JAN, Y. N. & JAN, L. Y. 1999. A new ER trafficking signal regulates the subunit stoichiometry of plasma membrane K(ATP) channels. *Neuron,* 22**,** 537-48.

ZHAO, L., HELMS, J. B., BRUNNER, J. & WIELAND, F. T. 1999. GTP-dependent binding of ADP-ribosylation factor to coatomer in close proximity to the binding site for dilysine retrieval motifs and p23. *J Biol Chem,* 274**,** 14198-203.

ZHAO, X., LASELL, T. K. & MELANCON, P. 2002. Localization of large ADP-ribosylation factor-guanine nucleotide exchange factors to different Golgi compartments: evidence for distinct functions in protein traffic. *Mol Biol Cell,* 13**,** 119-33.

6 Acknowledgement

At the end of my thesis I would like to thank all who has contributed to bringing this work to an end. It has been a period of intense learning for me, not only in the scientific field, but also on a personal level.

First and foremost I am grateful to my supervisor Prof. Dr. Felix Wieland for giving me the opportunity to work on an fascinating and challenging project in his lab, his constant discussion readiness, and for his support over the past years.

I am grateful to Prof. Dr. Thomas Söllner for being my second referee and also to Prof. Dr. Michael Brunner and Prof. Dr. Sabine Strahl for kindly agreeing to be on my defense committee.

I would also like to thank Prof. Dr. Thomas Söllner and Prof. Dr. Michael Brunner for being part of my thesis advisory committee, their helpful discussions and support they provided during my thesis.

I would like to thank the DFG GRK 1188 and Prof. Dr. Felix Wieland for funding.

I am deeply grateful to all members of the Wieland lab, past and present, I had the pleasure to work with. Thank you for the great working atmosphere, all the discussions, and the fun outside the lab. I would particularly like to thank my colleague Manuel Rhiel who has become a good friend over the last years.

Special thanks to Andrea Hellwig, Jörg Malsam and Dirk Flemming. My thesis would not have come to a successful completion without their continuous support.

I would also like to thank my whole family for their unconditional support, not only over the last years.

Last, I am most grateful to my beloved girlfriend and our wonderful son.